PRODUCTION, CHARACTERISATION AND USE OF FLUORESCENT MARKERS IN THE STUDY OF PLANT NUCLEAR ENVELOPE DYNAMICS

Sarah L. Irons

A thesis submitted in partial fulfilment of the
requirements of Oxford Brookes University
for the degree of Doctor of Philosophy

February 2004

ABSTRACT

The nuclear envelope (NE) is one of the least studied membranes in plant cells. Genes encoding NE protein homologues are absent from currently available sequenced plant genomes. To produce a specific marker for the plant NE and in view of previous positive results with heterologously expressed proteins in plant cells, mammalian NE proteins were considered in order to find a marker for the plant NE. Green fluorescent protein (GFP) was chosen to label the protein of interest as it provides a non-invasive method of monitoring protein location and movement *in vivo*.

The lamin B receptor (LBR) is the most extensively studied of the mammalian inner NE (INE) proteins. It is an INE protein that binds lamin B, chromatin and chromatin-associated proteins. A LBR-GFP_5 construct was produced and placed in a plant expression vector. Transient expression of the LBR-GFP_5 protein in tobacco leaf epidermal cells showed labelling of the NE, with minimal labelling of the endoplasmic reticulum (ER). The construct was used to produce stably transformed tobacco plants and tobacco BY-2 cells. NE labelling was observed in the majority of tissues stably expressing the protein, with NE location confirmed by electron microscopy. In BY-2 cells the construct showed NE location during interphase, with co-localisation with an ER marker, sporamin signal peptide YFP-HDEL (spYFP-HDEL) during mitosis. Similar labelling of the ER with NE proteins is seen in mammalian cells during division. This, in combination with the targeting and retention of LBR-GFP_5 at the plant NE suggests a conservation of mechanisms for INE targeting and retention in plant and animal NEs.

Preliminary evaluation of the nature of LBR retention at the NE was conducted using a set of LBR-GFP_5 mutants. Labelling of the NE was perturbed with some of the mutants, indicating that similar domains contribute to LBR retention in plant and animal cells.

LIST OF PUBLICATIONS

JOURNAL ARTICLES:

Irons, S.L., Evans, D.E. and Brandizzi, F. (2003) The first 238 amino acids of the lamin B receptor are targeted to the nuclear envelope in plants. *Journal of Experimental Botany* **54**: 943-950.

ORAL PRESENTATIONS*:

Irons, S.L., Debela, M. H-M., Evans, D.E. and Brandizzi, F. Using the human lamin B receptor targeted to the plant nuclear envelope to study membrane traffic in mitosis. Annual main meeting of the Society for Experimental Biology, April 2003, Southampton, UK.

Evans, D.E., Brandizzi, F. and Irons, S.L. Dynamics of the nuclear envelope and associated endomembranes in the plant cell cycle. SEB Symposium Communication and Gene Regulation at the Nuclear Envelope. Durham, UK. July 2003.

Irons, S.L., Evans, D.E. and Brandizzi, F. New markers for the nuclear envelope in plants. Informal workshop on plant endomembranes. Varenna, Italy. October 2002.

Irons, S.L., Brandizzi, F., Hawes, C., and Evans, D.E. Fluorescent proteins to study nuclear envelope protein trafficking and dynamics in plants: the lamin B receptor. Oxford Brookes University, Research School of BMS Postgraduate Symposium. December 2001.

POSTER PRESENTATIONS*:

Debela, M. H-M., **Irons, S.L.**, Brandizzi, F. and Evans, D.E. Probing plant nuclear envelope dynamics using GFP-constructs. Annual main meeting of the Society for Experimental Biology. Southampton, UK. April 2003.

Irons, S.L., Brandizzi, F. and Evans, D.E. Using the human lamin B receptor to study protein trafficking and dynamics of the plant nuclear envelope. SEB Symposium Communication and Gene Regulation at the Nuclear Envelope. Durham, UK. July 2003.

Irons, S.L., Brandizzi, F., Hawes, C. and Evans, D.E. Fluorescent proteins to study nuclear envelope protein trafficking and dynamics in plants. Oxford Brookes University, Research School of BMS Postgraduate Symposium. December 2002.

* Person or persons presenting work denoted in bold typeface.

ACKNOWLEDGEMENTS

I am grateful to Dr Jan Ellenberg for the kind gift of the original LBR-EGFP construct that forms the basis for this thesis. Thanks to David Evans and Fede Brandizzi for being a supreme supervising team. You have both been great, David with his ever present support and invaluable feedback on the writing of this tome and Fede for always getting that bit extra from me.

Secondly, thanks to all the people that have made my time in Oxford a very positive experience, for a variety of reasons: Tracey Mills (snave!), Chris White, Chloe Osborne, Tracey Carter, Zoe Holloway, Einat Zelinger, Jorunn Johansen, Ulla Neumann, Amanda and Kris Kotzer (the best boarding house in Oxford - thanks guys), Imo Sparks, Maïté Vicré, John Runions, Fabien Puglia and Jude Sheldon. Special thanks to Anne Kearns, Barry Martin and Jan Evins for being free with their knowledge and patient in the face of many questions. Also the weaker half of 'the hardcore' - Richard Hitchman and Rob Graham. And Liz Ritter for being an ideal housemate.

Also thanks to Ben Palmer for a truly wondrous appreciation of Thirst. And to Marie Kelly for being a genuinely lovely person and for the many hours of video watching!

Then thanks to friends from home, especially Sarah White and Paul Robinson. Thanks for your support and a quite impressive volume of email.

Then there is Barbara Kelly. Life is strange in throwing together two pisceans with a shared love of vodka in the same house. How could we not get along! You've been such a great friend. I can't see how I could have got through this without you.

And to my family. Thanks to Nanna Payne, Nanna and Grandad Irons. And last, but so not least, Mum and Dad, you have been so great. Thank you for your support to do whatever I want to do.

CONTENTS

CHAPTER 1. INTRODUCTION

CHAPTER 2. MATERIALS AND METHODS

CHAPTER 5. MUTATIONS IN THE LBR-GFP$_5$ PROTEIN REVEAL DETAILS OF RETENTION OF LBR AT THE PLANT NUCLEAR ENVELOPE

LIST OF FIGURES

CHAPTER 4.

CHAPTER 5.

LIST OF TABLES

LIST OF ABBREVIATIONS

APS	ammonium persulfate
ATP	adenosine tri-phosphate
BSA	bovine serum albumin
BY-2	bright yellow-2
cDNA	complementary deoxyribonucleic acid
CFP	cyan fluorescent protein
CLSM	confocal laser scanning microscope
CX	calnexin
2,4-D	2,4-dichlorophenoxyacetic acid
DIC	differential interference contrast
DNA	deoxyribonucleic acid
dNTP	deoxynucleoside triphosphate
ECA1	endoplasmic reticulum calcium ATPase
ECL	enhanced chemical luminescence
EDTA	ethylenediaminetetraacetate
EGFP	enhanced green fluorescent protein
EM	electron microscopy
ER	endoplasmic reticulum
ERAD	endoplasmic reticulum associated degradation
ERD-2	endoplasmic reticulum retention defective 2
EthBr	ethidium bromide
FLIP	fluorescence loss in photobleaching
FPP	filament-like plant protein
FRAP	fluorescence recovery after photobleaching
GA	Golgi apparatus
GFP	green fluorescent protein
gp210	glycoprotein 210
GTP	guanosine tri-phosphate
HDEL	Histidine-aspartic acid-glutamic acid-leucine
HIV	human immunodeficiency virus
HP1	heterochromatin protein 1

HRP	horse radish peroxidase
Hsp	heat shock protein
INE	inner nuclear envelope
IF	intermediate filament
IP_3	inositol 1,4,5-trisphosphate
IP_4	inositol 1,3,4,5-tetrakisphosphate
IPTG	isopropyl-β–D-thiogalactopyranoside
kDa	kiloDalton
KDEL	lysine-aspartic acid-glutamic acid-leucine
LAP	lamin associated polypeptide
LB	Luria-Bertini
LBR	lamin B receptor
M and S	Murashige and Skoog
MAF1	MFP1 associated factor 1
MAPK	mitogen activated protein kinase
MFP1	matrix attachment region binding filament-like protein 1
MT	microtubule
MTOC	microtubule organising centre
Nag	N-acetylglucosaminyl transferase I
Nag-RFP	N-acetylglucosaminyl transferase I – red fluorescent protein
NE	nuclear envelope
NEBD	nuclear envelope breakdown
NES	nuclear export signal
NLS	nuclear localisation sequence
NMP1	nuclear matrix protein 1
NPC	nuclear pore complex
nt	nucleotide
Nup153	nucleoporin 153
ONE	outer nuclear envelope
PBS	phosphate buffered saline
PBSB	phosphate buffered saline BSA
PBST	phosphate buffered saline Tween 20
PCR	polymerase chain reaction

POM121	pore membrane protein of 121 kD
PPB	pre-prophase band
p.s.i.	per square inch
RanBP2	Ran-binding protein 2
RanGAP	Ran GTPase activating protein
RNase A	ribonuclease A
r.p.m.	revolutions per minute
SDS	sodium dodecyl sulfate
SDS-PAGE	sodium dodecyl sulfate poly-acrilamide gel electrophoresis
SERCA	sarco/endoplasmic reticulum calcium ATPase
sp	signal peptide
SqLCV	Squash leaf curl virus
SRPK	serine/arginine protein kinase
ST	sialyltransferase
SV40	simian virus 40
TBY-2	tobacco bright yellow 2
T-DNA	transferred DNA
TEMED	N,N,N',N'-tetramethylethylenediamine
Ti	tumour inducing
TM	transmembrane
TX-114	Triton X-114
UV	ultraviolet
vir	virulence
WT	wild type
YEB	yeast extract broth
YFP	yellow fluorescent protein

CHAPTER 1.

INTRODUCTION

1. INTRODUCTION

1.1 THE NUCLEAR ENVELOPE

The nuclear envelope (NE) is a unique feature of eukaryotic cells. It consists of a concentric double membrane that encloses the nucleoplasm, separating the genome from the cytoplasm (Dingwall and Laskey 1992). Its lumen is continuous with that of the endomembrane system (Gerace and Burke 1988, Malviya and Rogue 1998, Mattaj 2004). Traffic into and out of the nucleus occurs via pores either by passive diffusion or by active transport, using ATP and GTP as an energy source, and requiring a nuclear localisation sequence for import (Hicks and Raikhel 1995, Stehno-Bittel *et al.* 1995).

The NE is supported by a network of intermediate filaments termed the nuclear matrix; the matrix associates with the NE via several types of receptor (Dingwall and Laskey 1992) and has a similar filamentous ultrastructure in animal and plant cells (Moreno Diaz de la Espina 1995, Rose *et al.* 2003). It is the lamina that holds the NE in position forming the characteristic spherical nuclear profile seen in many eukaryotic cells (Vaughan *et al.* 2000).

The outer nuclear envelope (ONE) is continuous with the endoplasmic reticulum (ER), being covered with ribosomes (Staehelin 1997). It has been shown to contain proteins native to the ER, and as such can be considered as a sub-compartment of the ER. Each of the nuclear membranes has a set of intrinsic and peripheral proteins, characteristic of that particular membrane (Collas and Courvalin 2000) e.g. IP_4 receptors and sarcoplasmic/ER calcium ATPase (SERCA) at the ONE

(Humbert *et al.* 1996) and the lamin B receptor (LBR), lamin-associated polypeptides (LAPs), emerin, nurim, MAN1, matefin, IP_3 receptors (Humbert *et al.* 1996), Myne 1, the nesprin family, ring-finger-binding protein (RFBP), Luma and UNC 84 (Holaska *et al.* 2002) at the inner nuclear envelope (INE; see diffusion retention and NE protein sections for more information). This array of proteins appears to differ between plant and animal cells, with homologues to mammalian NE proteins not as yet identified in plants (Hicks and Raikhel 1995, Meier 2001, Rose *et al.* 2004). Studies of plant nuclear architecture are limited due to inherent difficulties of working with plant cells. Intact plant nuclei are difficult to obtain in large numbers, and many techniques used in animal systems are not applicable to plants due to the cell wall (Moreno Diaz de la Espina 1995).

1.1.1 Nuclear Pores

All nuclear envelopes contain nuclear pores situated where inner and outer nuclear membranes join. The pore consists of multiple copies of around 30 proteins that form the nuclear pore complex (NPC) (Rout *et al.* 2000). The pore channel is approximately 10 nm in diameter and 100 nm long (Panté and Aebi 1994), NPC size varies between species with the *Xenopus* pore complex around 120nm wide, compared to 100nm in yeast (Stoffler *et al.* 1999). Small molecules, between 20 and 70 kD, can passively diffuse through the pore aperture, though this is dependent on cell type, and time taken for diffusion may also differ (Bustamante *et al.* 1995). Larger molecules require nuclear location sequences for transport. Their translocation is driven by ATP and GTP hydrolysis and can require chaperones, such as Hsp 70 (Dingwall and Laskey 1992), and other accessory factors (Melchior and Gerace 1995).

The pore complexes in animal cells are attached to the nuclear lamina, and hence are not dependent on the phospholipid membrane for maintaining their structure (Lyman and Gerace 2001). The use of nucleoporins fused to green fluorescent protein (GFP) has allowed the visualisation of NPC dynamics *in vivo* in animal cells. Daigle *et al.* (2001) produced nucleoporin GFP fusions of POM121, an integral membrane protein localised to the ring spoke region, and Nup153, a peripheral membrane protein found in the nuclear fibrils (forming part of the basket like structural portion of the NPC). These proteins demonstrated different dynamics through the cell cycle, suggesting that the NPC has a core set of proteins with low turnover such as POM121 and other proteins such as Nup153 that show rapid cycling (Daigle *et al.* 2001).

The physical presence of NPCs in plant cells has been known for sometime, as demonstrated by freeze fracture of tobacco cells (Heese-Peck and Raikhel 1998). However, as yet no plant nuclear pore proteins have been characterised (Meier 2001, Rose *et al.* 2004). A recent survey of plant genome databases has revealed 3 proteins which bear similarity to mammalian nucleoporins Nup98 and gp210 (Rose *et al.* 2004). A 100 kDa nuclear matrix protein was recognised by antibodies against animal and yeast nucleoporins; however this protein has not been identified (Scofield *et al.* 1992). The production of plant NPC markers would provide a valuable tool for studying nuclear membrane dynamics *in planta*. A random cDNA cloning approach to isolate GFP-tagged proteins that label novel structures (Escobar *et al.* 2003) gave rise to a construct that labelled punctate structures at the NE, similar to pore labelling observed in mammalian cells. Results of attempts to

fuse the cDNA to yellow fluorescent protein (YFP) and use it in a binary vector are shown in Appendix 2.

1.1.2 Lamins

Lamins are type V intermediate filaments that form the nuclear lamina in animal cells. Lamins are divided into 2 subtypes, A and B, characterised by sequence, mitotic behaviour and tissue specific expression (Vaughan *et al.* 2000). The lamina forms a dynamic peripheral meshwork attached to cytoskeleton (Moreno Diaz de la Espina 1995). They are bound to the inner nuclear membrane by several types of integral membrane protein; these include the LBR (for B type lamins) and LAPs 1 and 2 (for A and B type lamins). The lamin network provides support to the inner nuclear membrane, and as such helps to maintain nuclear size and shape. When lamin assembly is prevented cells contain very small fragile nuclei (Ellis *et al.* 1997). Lamins are involved in NE organisation; NPCs are abnormally distributed in mutant *Drosophila* with depletion of a lamin B homologue. In addition to this, the first stages of NE assembly are also disturbed in the mutant flies (Lenz-Bohme *et al.* 1997). Experiments in cell free systems have suggested that lamins or their inner nuclear membrane receptors are involved in targeting nuclear membrane vesicles to chromatin at telophase, thereby suggesting a structural link between chromatin and the NE (Ulitzur *et al.* 1997).

Plant genomes sequenced to date do not contain lamin homologues (Rose *et al.* 2003, 2004). However previous work using pea nuclear fractions showed immuno-labelling with mammalian anti-lamin B and anti-intermediate filament (IF) antibodies, thus demonstrating the presence of lamin and IF protein epitopes in

plant cells (McNulty and Saunders 1992). Short sequences from intermediate filament (IF) type proteins isolated from plant cells show some sequence similarity to animal lamins (Blumenthal *et al.* 2004). A protein (NMCP1) approximately twice the length of animal lamins containing a long α–helical coiled-coil domain (Masuda *et al.* 1997) has been identified in carrot and *Arabidopsis*. Due to its domain structure and presence in the nuclear matrix, the protein is a possible candidate for a lamin equivalent in plants. A novel plant protein, termed nuclear matrix protein 1 (NMP1) containing α helical coiled-coil domains similar to intermediate filaments has been identified and is present in many plant types (Rose *et al.* 2003). In addition the protein is found in the nuclear matrix fraction, the nuclease resistant, insoluble nuclear substructure that persists after soluble and chromatin-bound proteins and DNA have been removed from the nucleus. Although NMP1 is present in the nuclear matrix it is mainly located in the cytoplasm, differing from animal matrix proteins which are predominantly in the nucleus. Some animal proteins show both cytoplasmic cytoskeletal and nuclear functions and this may be the case with this protein. The differing location may imply a dual cytoskeletal role.

A family of long coiled-coil proteins, the structural motif seen in intermediate filaments, have recently been characterised from tomato, *Arabidopsis* and rice and have been named filament-like plant proteins (FPP; Gindullis *et al.* 2002). The proteins were shown to interact with MAF1 (MFP1 associated factor 1; see section 1.4), a NE associated plant protein, in a yeast two-hybrid assay. The lack of lamin homologues in the *Arabidopsis* genome and interactions of the FPPs with a NE

associated protein suggests that these proteins may perform the function of lamins in plants.

1.1.3 Microtubules

Microtubules (MTs) are fundamental in many cellular processes and have been studied extensively in animal and plant cells by electron microscopy, immunohistochemistry and more recently using fluorescently labelled tubulin and confocal microscopy (Ueda *et al.* 1999, Hasezawa *et al.* 2000, Lloyd and Hussey 2001, Kumagai *et al.* 2003).

Plant MTs display four distinct assemblies that do not have homologues in animal cells and also differ in not having distinct microtubule organising centres (MTOCs) as seen in animals (Lloyd and Hussey 2001). In non-dividing plant cells, cortical microtubules are involved in cell morphology, determining cellulose microfibril deposition (Lloyd and Hussey 2001). During cell division the MTs form 3 distinct arrangements, the preprophase band (PPB), the plant spindle and the phragmoplast. The PPB forms during G2, (see Figure 1.1 for phases of the cell cycle) forming a cortical ring of MTs. This structure depolymerises before metaphase but accurately marks the site of cell plate formation after nuclear division. The spindle is predominantly the same structure as its animal counterpart, except the poles tend to be larger and there are no astral MTs in plant cells. The phragmoplast forms in anaphase as a bundle of MTs which becomes a rapidly growing double ring, the fast growing ends of the MTs associate in the midline of this structure and form the basis on which the new cell wall is laid down (Lloyd and Hussey 2001).

In animal cells the mechanism of nuclear envelope breakdown (NEBD) has been shown to be a result of spindle MT-induced tearing of the nuclear lamina (Beaudouin *et al.* 2002). This has not been shown in plant cells as the interaction between nuclear structures, the nuclear envelope and MTs has yet to be studied in unison. The *Arabidopsis* α tubulin gene, TUA6 has been fused to GFP and used to visualise MTs *in vivo* (Ueda *et al.* 1999).

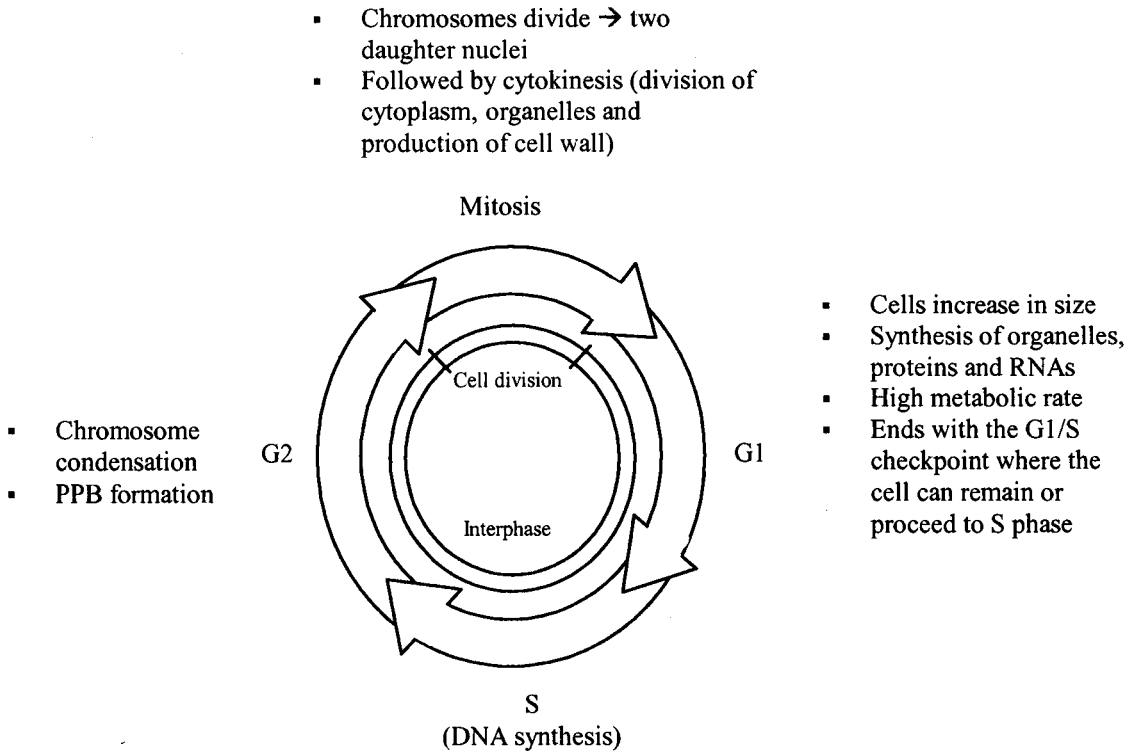

Figure 1.1 The Phases of the Cell Cycle.

1.1.4 The nuclear envelope and endomembrane system

Higher plant cells contain machinery for the synthesis, modification and export of a variety of products. Proteins and many carbohydrates are processed in the endomembrane system, a dynamic functional continuum of the nuclear envelope,

endoplasmic reticulum, Golgi apparatus (GA) and the vacuolar and plasma membranes. The different membrane compartments are inter-connected and materials flow through the pathway, either by direct connections or vesicles. For example, calreticulin is seen in the ER lumen as well as the lumen of the NE (Roderick *et al.* 1997). The molecular composition and function of the stage of the pathway from ER to GA is well described in animal cells (e.g. Lippincott-Schwartz *et al.* 1989, 2001) and is becoming more defined in plants (Andreeva *et al.* 2000, Brandizzi *et al.* 2002c), however transport between the NE and the ER has not been studied in detail in many organisms.

1.2 THE NUCLEAR ENVELOPE AT MITOSIS

The NE is unique in breaking down during cell division and re-forming around the chromatin of the daughter cells (Yang *et al.* 1997). There are two theories that aim to describe the fate of the nuclear membrane during mitosis; vesiculation or ER absorption (Buendia *et al.* 2001, review).

The vesiculation theory is based mainly on work using cell free systems. Experiments with *Xenopus* cell free extracts have shown that the nuclear membranes form vesicles which re-form around chromatin (Vigers and Lohka 1991). The production of cell extracts inherently leads to membrane vesiculation, the presence of vesicles with different proteins and binding characteristics may be due to micro-domains within disrupted continuous membranes i.e. the ER (Buendia *et al.* 2001). *In vitro* nuclear reconstitution in a plant cell free system has been achieved using carrot cell cytosol extract, membrane vesicles extracted from *Xenopus* eggs and demembranated sperm chromatin (Zhao *et al.* 2000). In this

system a double membrane layer formed around sperm chromatin and the re-assembled nuclei showed nucleosomal structures as demonstrated by DNA laddering on digestion with micrococcal nuclease, which is not observed with the chromatin alone. The formation of nuclei is clearly triggered by factors present in the carrot cytosolic extract the information. Extrapolation to NE assembly *in vivo* in plant cells, is limited as the membranes used were not from plants so do not contain native plant proteins that may act in a different way during NE reformation. Nuclear assembly including nucleosome formation has been shown using cell free extracts from tobacco ovules and demembranated *Xenopus* sperm chromatin (Lu and Zhai 2001). Thus plant membranes are capable of *in vitro* nuclear reassembly in a manner similar to that seen with animal models, suggesting similarity in NE formation between the two systems.

In vivo studies have provided evidence for the ER absorption theory. Use of fluorescently labelled NE proteins has shown that labelling persists and moves into mitotic ER membranes followed by subsequent NE re-formation, with fluorescence moving from mitotic ER to the daughter NE *in vivo* in animal cells (Ellenberg *et al.* 1997, Haraguchi *et al.* 2000). The mechanism and sorting of NE membrane proteins during this process has not been studied in plants (Collas and Courvalin 2000). Further evidence for ER absorption is discussed below.

Protein phosphorylation or dephosphorylation has been implicated in NE disassembly during mitosis in animal cells (Foisner and Gerace 1993, Gerace and Foisner 1994, Collas and Courvalin 2000, Otto *et al.* 2001). Lamins are depolymerised on phosphorylation by $p34^{cdc2}$ kinase, the β form of protein kinase C

and mitogen activated protein kinase (MAPK) (Goldberg *et al.* 1999). LAP2 binding of lamin B and chromatin is disrupted by mitosis specific phosphorylation, and LBR is known to undergo phosphorylation at mitosis by kinases such as $p34^{cdc2}$ kinase and SR protein specific kinase (SRPK) (Gerace and Foisner 1994, Nikolakaki *et al.* 1996, Takano *et al.* 2002, 2004). Such protein phosphorylation changes are thought to allow reversible dissociation of inner nuclear membrane proteins and their ligands, effectively removing their anchorage to the nuclear structures and so allowing movement into the ER membranes (see section 1.3.1).

The production of constructs consisting of part of LBR, a mammalian endogenous INE protein and GFP, plus applications of confocal microscopy techniques such as fluorescence recovery after photobleaching (FRAP) and fluorescence loss in photobleaching (FLIP) has allowed study of nuclear membrane dynamics during mitosis in animal cells (Ellenberg *et al.* 1997, Ellenberg and Lippincott-Schwartz 1999, Terasaki *et al.* 2001). Such studies were not previously possible using immunocytological methods.

FRAP is a microscopical technique that involves exposing a specific area or areas of a cell to brief, intense and localised laser beam pulses to bleach the region, with subsequent monitoring of return of fluorescent proteins to the bleached area (see Figure 1.2A). Photobleaching leads to fluorochromes in the bleached area losing their ability to fluoresce. If recovery occurs in a bleached area it is due to movement of new fluorochromes into the exposed area, replacing the bleached proteins. The speed at which recovery occurs provides insight into the dynamics of the fluorescently labelled protein in the membrane.

FLIP involves exposing a specific area of a cell to a continuous laser beam (see Figure 1.2B). This will eventually lead to total ablation of fluorescence in the cell if the fluorochrome is freely diffusible in the membrane/cytoplasm. However, if the protein of interest is immobilised it will not pass through the bleached area and so will not lose fluorescence. This technique provides information on the continuity of membranes and demonstrates the location of immobile fluorescently tagged proteins in transformed cells.

The dynamics of the GFP tagged proteins in animal cells have provided clear evidence for NE protein migration to the ER membranes during mitosis, as demonstrated by co-localisation of the LBR-EGFP construct with known ER markers during cell division (Ellenberg *et al.* 1997). This has also been demonstrated with other NE proteins fused to GFP (full length LBR, emerin, RanBP2, Nup153; Haraguchi *et al.* 2000). Immunofluorescence and confocal images were used to observe the inner NE proteins LAP1, LAP2 and gp210 (a NPC membrane protein) which were shown to co-localise with ER markers at mitosis (Yang *et al.* 1997).

The NE reforms in a step-wise fashion with membranes binding to late anaphase chromosomes. These membranes fuse to form a fenestrated cisternal structure that encloses the nucleus and finally the assembly of the NPCs and lamins at late telophase (Gerace and Foisner 1994, Haraguchi *et al.* 2000).

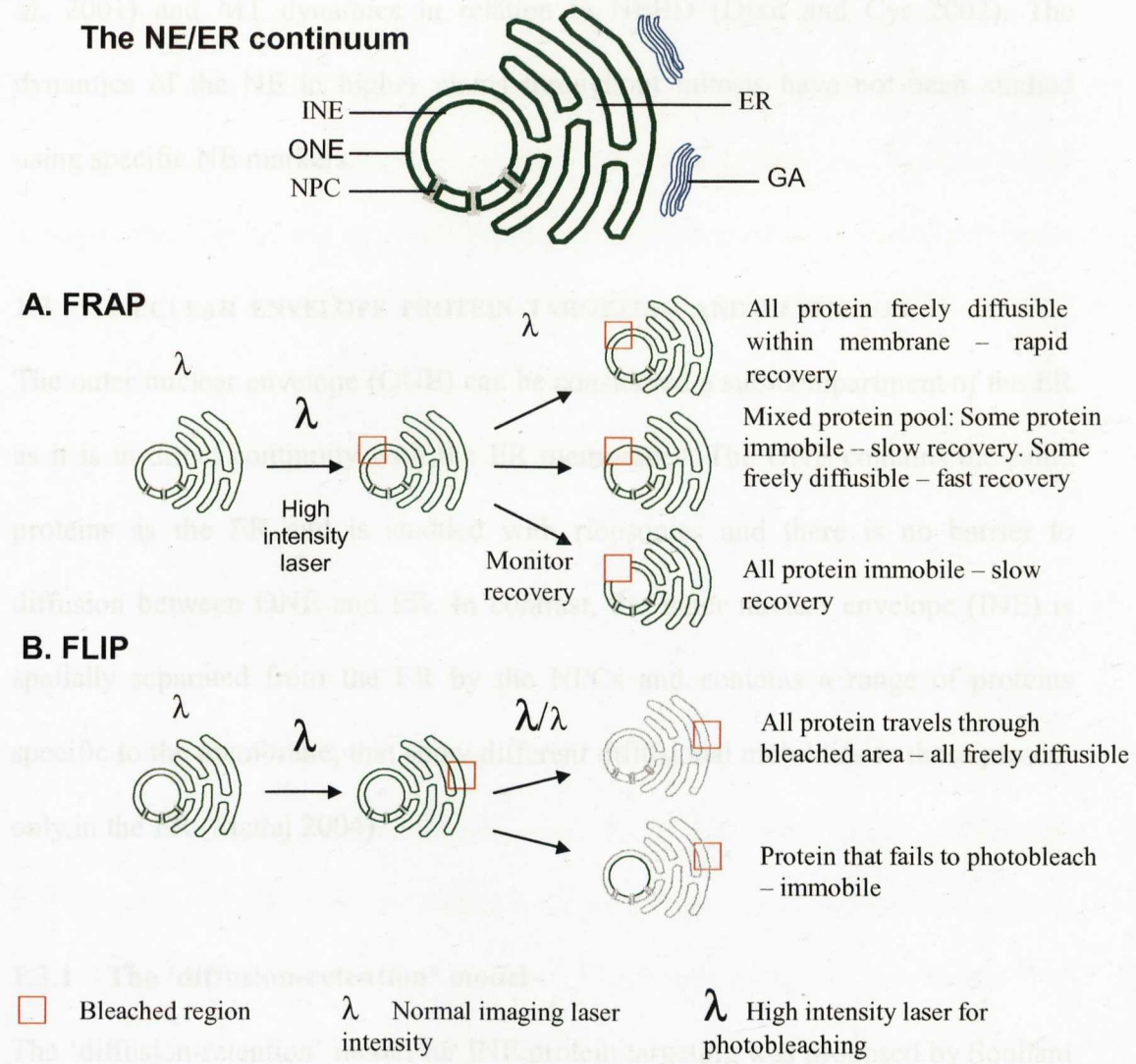

Figure 1.2 Determination of NE/ER protein dynamics using photobleaching techniques. Schematic diagram of the NE/ER continuum. A. Fluorescence Recovery After Photobleaching (FRAP). B. Fluorescence Loss In Photobleaching (FLIP).

Early electron microscopy studies in plants (de la Torre *et al.* 1979) showed a growth in NE from G1 to G2 and a concomitant increase in pore number from G1 to mid S phase inferring that NE structure is related to nuclear activity. In more recent studies, use of fluorescent constructs has provided information about cell signalling proteins, RanGAP and the NE (Rose and Meier 2001, Pay *et al.* 2002), plant nuclear matrix associated proteins and their respective cellular locations (Gindullis and Meier 1999, Gindullis *et al.* 1999, Harder *et al.* 2000, Samaniego *et*

al. 2001) and MT dynamics in relation to NEBD (Dixit and Cyr 2002). The dynamics of the NE in higher plants throughout mitosis have not been studied using specific NE markers.

1.3 NUCLEAR ENVELOPE PROTEIN TARGETING AND RETENTION

The outer nuclear envelope (ONE) can be considered a sub-compartment of the ER as it is in direct continuity with the ER membranes. The ONE contains the same proteins as the ER and is studded with ribosomes and there is no barrier to diffusion between ONE and ER. In contrast, the inner nuclear envelope (INE) is spatially separated from the ER by the NPCs and contains a range of proteins specific to the membrane, that show different diffusional mobilities to those present only in the ER (Mattaj 2004).

1.3.1 The 'diffusion-retention' model

The 'diffusion-retention' model for INE protein targeting was proposed by Soullam and Worman (1995). In the model, proteins are synthesized on the ER and are freely diffusible within the membrane, including the ONE, the proteins move through lateral channels of the NPCs within the nuclear pore membrane. Once in the INE the protein becomes immobilised via interactions with specific ligands that lie close to the NE e.g. for LBR; lamin B, heterochromatin protein 1 (HP1) orthologues, chromatin (Wu *et al.* 2002) and possibly histones H3/4 (Polioudaki *et al.* 2001), LAP 2; lamins and chromatin, emerin; lamins (Wu *et al.* 2002). This immobilisation is observed as a decrease in lateral diffusion constant, as determined by FRAP, between the ER and INE which has been seen with LBR (Ellenberg *et al.* 1997), emerin (Östlund *et al.* 1999) and MAN1 (Wu *et al.* 2002).

During mitosis the dynamics of INE proteins change from predominantly immobile to freely diffusible, with diffusion constants comparable to those of ER proteins (Wu *et al.* 2002). This change can be ascribed to three major events which occur at the start of cell division; the depolymerisation of the lamina, chromatin condensation and NPC disassembly. These changes lead to dissociation of INE proteins with the constituents that immobilise them at the NE; as such the proteins are then free to diffuse within the mitotic ER membranes.

1.3.2 Trans-membrane domains

Trans-membrane (TM) domains contribute to membrane retention; this has been observed in mammalian membranes (Bretscher and Munro 1993, Nilsson and Munro 1994) and in plant membranes, where it was demonstrated that TM domain size affects targeting within the endomembrane system due to membrane thickness (Brandizzi *et al.* 2002a). The TM domain of LBR was shown to contribute to NE targeting of the protein (Smith and Blobel 1993, Soullam and Worman 1995). However proteins with similar TM domains to LBR but which lack the N-terminal nucleoplasmic domain fail to stay at the NE. This suggests that the specific interaction between the nucleoplasmic domain and binding partners within the nucleus is the main factor contributing to the retention of LBR at the INE.

1.3.3 Protein size

The NPCs provide a spatial barrier between the INE and ONE/ER. The lateral channels of the NPC, that the INE proteins must diffuse through in order to enter the nucleoplasmic face of the NE, have a diameter of around 10nm and are located at the edge of the NPC adjacent to the pore membrane (Hinshaw *et al.* 1992). The

channel allows diffusion of nucleo/cytoplasmic globular proteins up to 60kDa between the NE and ER. When native INE proteins such as LBR (Soullam and Worman 1995) and MAN1 (Wu *et al.* 2002) are enlarged they fail to target the NE and hence are retained in the ER. Hence the NPCs play a fundamental role in excluding proteins from the NE and differentiating the INE from the ONE and ER.

1.3.4 Nuclear envelope targeting

Sequences that may target proteins to the INE in animal cells have recently been reported (Meyer *et al.* 2002). From LBR the motif SRSRSR, was suggested to be responsible for INE localisation. This 'RS repeat region' has been associated with chromatin binding (Takano *et al.* 2002), which would immobilise the protein in the INE. The SR motif is present in many chromatin-associated proteins e.g. splicing factors present in mammalian and plant cells (Lazar *et al.* 1995) as well as kinases and phosphatases, and in proteins involved in transcription and cell structure (Boucher *et al.* 2001). Whether the RS sequence serves as a specific targeting signal in its own right, or simply contributes chromatin binding and hence, in the case of LBR, retention of the protein at the NE (see section 1.3.1 and Chapter 5), is yet to be established.

1.3.5 Nuclear localisation sequences

Proteins destined for the nucleus are translated in the cytoplasm and have to be translocated into the nucleus via nuclear pore complexes. For this to occur the proteins have to contain nuclear location sequences (NLSs). These sequences tend to have a high basic amino acid content, usually arginine and lysine, though proline is also observed in some cases. Such sequences are not cleaved by proteases, which

allows the proteins to exit and re-enter the nucleus without modification, thus allowing resident proteins back to the nucleus after nuclear membrane dissipation during mitosis.

There are three general classes of NLS, the most extensively studied being that originally found in the SV40 T-antigen (named the SV40-like NLSs). This class of sequence consists of a single peptide region of basic amino acids (Pro-Lys-Lys-Lys-Arg-Lys-Val) (Kalderon *et al.* 1984). Proteins targeted to the nucleus using the SV40-like NLS have been reported in animals, yeast and plant systems (Hicks and Raikhel 1995).

The second class, which is thought to be the most common targeting mechanism, is the bipartite nucleoplasmin signal (Dingwall *et al.* 1988). It incorporates two basic peptide regions separated by a ten amino acid spacer, though this spacer region can vary in length. There have been many bipartite NLSs identified in plants as well as animals and yeast.

The third class is a basic N terminal sequence seen in the yeast protein Mat $\alpha 2$ and maize transcription factor R. This sequence contains basic and hydrophobic amino acids, with as yet undefined function. This form of NLS does not appear to work in mammalian cells (Hicks and Raikhel 1995). There are also undefined NLSs that do not conform to the criteria listed above as shown in proteins targeted to the nucleus but lacking any of the above NLSs.

Proteins also contain nuclear export signals (NES), important in shuttling of proteins in and out of the nucleus. NESs are composed of short amino acid sequences and provide an export signal independent of their position within the protein. The geminivirus squash leaf curl virus (SqLCV) encodes viral movement proteins including BR1. The BR1 amino acid sequence showed homology to a NES found in HIV Rev protein, *Xenopus* transcription factor IIIA and other proteins that shuttle in and out of the nucleus. The BR1 NES (LEKDTLLIDL), contains hydrophobic residues and several leucine residues that are essential for its function. (Ward and Lazarowitz 1999). When the SqLCV BR1 NES was replaced with the NES from *Xenopus*, transcription factor IIIA nuclear export and viral movement were unaffected, indicating that the pathway of nuclear export is conserved between plants, animal and yeast (Ward and Lazarowitz 1999); however the machinery of nuclear export is yet to be identified.

1.4 PROTEINS ASSOCIATED WITH THE PLANT NUCLEAR ENVELOPE

The plant NE has received relatively little attention in comparison to its mammalian and yeast counterparts. This is mainly due to a lack of markers available for the NE for use in plant cells. However, some work has been done on proteins involved in nuclear transport and architecture.

MAF1 is a novel plant protein located at the NE but not directly attached to it. It is a 152 amino acid protein with a predicted molecular weight of 16.2 kD (Gindullis *et al.* 1999). It is hydrophilic with alternating acidic and basic domains and a high serine and threonine content and is coded for by a single gene in tomato. A MAF1-mGFP-MAF1 sandwich construct was shown to localise at the nuclear periphery

with low expression seen in the cytoplasm and nucleoplasm (Gindullis *et al.* 1999). This was confirmed by immunocytochemistry where MAF1 was predominantly found in a ring like structure around the nucleus, either in or near the NE. After treatment with Triton X-100, which removes most of the outer NE, MAF1 was still found to be tightly associated with the nucleus implying that it is associated with the nuclear matrix. MAF1 and MFP1 (matrix attachment region binding filament-like protein 1) show near identical localisation (Gindullis and Meier 1999) and behave in the same way during nuclear matrix isolation, implying that they are part of the same of strongly interacting nuclear structure. Recent work has shown that MFP1 is predominantly a nucleoid binding protein present in plastids (Jeong *et al.* 2003). The apparent NE labelling previously reported for the protein (Meier *et al.* 1996, Gindullis and Meier 1999, Gindullis *et al.* 1999) was ascribed to the close proximity of plastids to the nucleus in tobacco suspension cells, but the presence of an isoform in the nucleus has not been discounted (Jeong *et al.* 2003).

MAF1-mGFP-MAF1 has been used as a marker of the NE to validate the use of a Golgi marker, N-acetylglucosaminyl transferase, fused to RFP (Nag-RFP) for studies of NEBD and PPB disappearance (Dixit and Cyr 2002). At present the continuous dynamics of MAF1 or MFP1 during the plant cell cycle have yet to be studied.

1.5 NUCLEAR ENVELOPE PROTEINS

At the initiation of this project, a range of possible markers for plant NE and ER proteins were identified by literature survey. Fluorescent constructs of these proteins would allow study of the different sub-compartments of the NE in plant

cells at mitosis. Candidate cDNAs include LBR (Ellenberg and Lippincott-Schwartz 1999), a Ca^{2+}-ATPase, ECA1 (Liang *et al.* 1997, Downie *et al.* 1998; see Appendix 1) and a possible nuclear pore marker (Escobar *et al.* 2003; see Appendix 2). Movement of NE proteins during mitosis using GFP constructs has been visualised in animal cells (Ellenberg and Lippincott-Schwartz 1999, Yang *et al.* 1997), but not in plant cells.

1.5.1 Lamin B receptor

LBR is a constitutively expressed integral membrane protein found in the INE and present in animal cells (Worman *et al.* 1990). It is a 637 amino acid/58kD protein with a large globular N terminal nucleoplasmic domain which is hydrophilic and rich in basic amino acids, and a hydrophobic C terminus consisting of eight transmembrane segments which show high homology to C-14 sterol reductases across plant (Schrick *et al.* 2000) and animal species (Holmer *et al.* 1998). For this reason it has been suggested by Kasbekar (1999) that sterol changes could have a role in NEBD and reformation. The N-terminus of LBR binds to chromatin (Ye and Worman 1994, Pyrpasopoulou *et al.* 1996, Duband-Goulet and Courvalin 2000, Takano *et al.* 2002) which may be of importance in nuclear membrane reassembly at the end of mitosis. LBR also interacts with lamin B (Ye and Worman 1994, Wu *et al.* 2002, Dreger *et al.* 2002) in most, but not all cases (Mical and Monteiro 1998). Binding of LBR and HP1 (Ye *et al.* 1997) does occur, although the interaction of LBR with HP1 may be indirect, via histones H3/4 (Polioudaki *et al.* 2001).

To determine the regions of LBR responsible for nuclear localisation a variety of constructs were made using full, truncated and chimeric constructs of chicken LBR (Smith and Blobel 1993). The amino terminal domain, specifically the first TM domain, containing a uncleaved bipartite type nuclear signal sequence, was found to be responsible for targeting the receptor to the nuclear membrane (Smith and Blobel 1993, Soullam and Worman 1993, Soullam and Worman 1995).

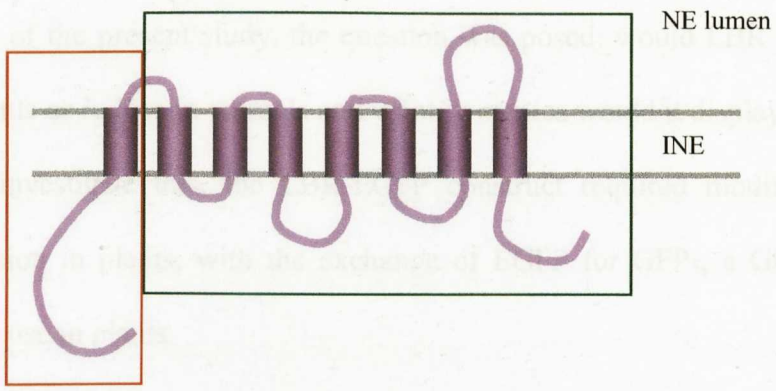

Figure 1.3 Spatial diagram of the full lamin B receptor, indicating regions of importance, sterol reductase region in green box, nucleoplasmic region in red box.

Extensive work has been carried out by Ellenberg *et al.* (1997) using the N terminal 238 amino acids of the lamin B receptor fused to EGFP in animal cells. COS-7 cells were transfected by microinjection or electroporation with an LBR-EGFP construct and its activity observed at mitosis using confocal microscopy. To gain a greater insight into LBR-EGFP, FRAP (see section 1.2) was used to determine whether the tagged protein was freely diffusible in the membranes or immobilised in some way. The LBR-EGFP was targeted to NE membranes in mammalian cells at interphase. There were two populations of LBR-EGFP observed in the cells, which showed differential diffusional mobility in interphase; an immobilised NE population, possibly through binding to lamins or chromatin and a small pool of LBR-EGFP that was freely diffusible in the ER. During mitosis the LBR-EGFP of

the NE becomes highly mobile and disperses to the ER. Nuclear membrane reformation was viewed using time lapse confocal imaging. This showed a redistribution of LBR-EGFP from diffusely distributed ER to membranes tightly associated with chromatin and subsequent expansion to the spherical NE at interphase. When the construct was expressed at high levels it clearly localised with DNA producing NE invaginations.

At the outset of the present study, the question was posed: would LBR localise to the NE in plants as it does in animals and what dynamics would it display in a plant system? To investigate this, the LBR-EGFP construct required modification to allow expression in plants, with the exchange of EGFP for GFP_5, a GFP variant optimised for use in plants.

1.6 TOOLS FOR THE *IN VIVO* STUDY OF THE PLANT NUCLEAR ENVELOPE

In order to study the NE in living plant cells, an *in vivo* marker for proteins of interest, a method of expression and suitable plant material are required. Constructs that label other parts of the plant cell are also necessary to compare the location of different proteins.

1.6.1 Fluorescent Proteins

Green fluorescent protein (GFP) is a naturally fluorescent protein from the jellyfish *Aequorea victoria* that has been used to create fluorescent protein chimeras in intact cells and whole organisms to study many aspects of protein location and movement (Chalfie *et al.* 1994, Tsien 1998, Brandizzi *et al.* 2002b). Creating such a chimera involves identifying and isolating a gene sequence of interest (e.g. for a

NE or ER located protein), generating a construct in which this DNA is fused to the GFP sequence and using a DNA delivery system (for instance that from *Agrobacterium tumefaciens*). This allows transformation of cells or production of whole plants expressing the chimeric protein which can be viewed *in vivo* by fluorescence microscopy. There are a number of GFP spectral derivatives which fluoresce at different wavelengths e.g. yellow fluorescent protein (YFP) and cyan fluorescent protein (CFP) which can also be used to make constructs for protein marking. The range of colours allows the tagging of a number of different proteins and subsequent viewing of their interactions and respective location within the same cell and in real time. NE of animal cells have been extensively studied in this way (Ellenberg *et al.* 1997, Ellenberg and Lippincott-Schwartz 1999, Terasaki *et al.* 2001). Extensive literature searching has shown that the *in vivo* dynamics of the plant NE with specific markers have not been studied.

Several fluorescently labelled proteins have been used as markers of the NE in plants. The relationship between NEBD and preprophase band disappearance (PPB), a plant specific microtubule structure, in tobacco Bright Yellow-2 (TBY-2) suspension cells used a Golgi apparatus (GA) protein, N-acetylglucosaminyl transferase I (Nag), which also localises around the nucleus, as a marker for the onset of NEBD (Dixit and Cyr 2002). The location of plant proteins MFP1 and MAF1 (described in more detail in section 1.4), which are associated with the ONM and nuclear matrix, have been studied using fluorescent constructs (Gindullis and Meier 1999, Gindullis *et al.* 1999, Harder *et al.* 2000, Meier 2000, Samaniego *et al.* 2001, Rose and Meier 2001). These fluorescent constructs have been used for

localisation and protein interaction studies but have not been used to investigate membrane dynamics during mitosis.

1.6.2 Other probes available

In addition to the NE probes described, it is useful to have a range of other fluorescent markers. The use of well characterised fluorescent probes for other regions of the cell such as the ER, alongside a NE marker would allow confirmation of the NE probe destination i.e. whether what appears to be ER location of a NE probe at mitosis is in fact ER and not another structure. There is a range of ER probes fused to GFP or YFP that can be used for co-localisation with tagged NE proteins available in the laboratory. See table 1.1 for details of markers routinely used in our laboratory.

Table 1.1 ER markers available for use in plants.

Protein	*Location*	*Source*
Sporamin signal peptide/KDEL	ER lumen	Boevink *et al.* (1999)
Arabidopsis ERD-2 (H/KDEL receptor)	ER and Golgi	Boevink *et al.* (1998)
Calreticulin	ER and NE lumen	Brandizzi and Hawes (unpublished)
Calnexin	ER and NE membrane	Brandizzi and Hawes (Irons *et al.* 2003)

1.6.3 *Agrobacterium*-mediated plant transformation

Agrobacterium tumefaciens is a gram-negative bacterium that causes crown gall disease in many plants in the natural environment. Crown gall disease is produced

by the integration of *Agrobacterium* T-DNA (transferred DNA), from a large tumour inducing (Ti) plasmid in the bacteria, into the plant genome. There are a range of genes in the T-DNA region, for example, genes responsible for tumour growth induce changes in expression of plant growth factors e.g. auxin and cytokinin which alter normal cell differentiation patterns leading to the formation of crown gall tumours. Research into T-DNA transfer showed that there were three important factors required for successful transfer. Firstly the presence of T-DNA border sequences which flank the T-DNA region, the border sequences consist of direct repeats and are 24 or 25bp long (Van Haaren *et al.* 1988). In general all DNA between the border regions is transferred to the plant genome. Virulence (*vir*) genes are also essential for gene transfer, they are present on the Ti plasmid, but lie outside the T-DNA region (reviewed by Hooykaas and Beijersbergen 1994). The *vir* genes are responsible for transcriptional activation of the *vir* operons and T-DNA processing, transfer into the plant cell and once in the plant, targeting to the nucleus and correct integration into the plant genome. Finally some genes encoded on the bacterial chromosomal are required for bacterial attachment to the plant cells.

As the content of the T-DNA has no bearing on transfer it is possible to change the original genes for other genes of interest which will be incorporated and expressed in the plant genome. In addition, the removal of the T-DNA biosynthetic genes stops tumour formation as there is no stimulus for a change in hormone levels. Thus Ti plasmid based vector systems for expressing specific genes in plant cells have developed for *Agrobacterium*-mediated plant transformation. In a binary vector system (such as pVKH18En6) new genes of interest are cloned into a

plasmid containing non-oncogenic T-DNA. This plasmid is transformed into an *Agrobacterium* strain (e.g. GV3101 containing the Ti plasmid, pMP90) containing a Ti plasmid with *vir* genes but lacking T-DNA.

1.6.4 Plant material for study of NE and mitosis

Agrobacterium containing a binary vector with a gene of interest fused to GFP can be used to transiently and stably transform plant material. Transient expression in *Nicotiana tabacum* leaves allows rapid identification of clones that successfully express in plants. Such transformation involves the high pressure infiltration of *Agrobacterium tumefaciens* containing the construct of choice into the underside of leaves via a needle-less syringe. After three days the fluorescent construct can be observed by fluorescence microscopy (Batoko *et al.* 2000). Production of stably transformed plants provides information about protein location in multiple tissue types that is not possible by transient transformation methods.

Tobacco BY-2 cells are easily transformed with *Agrobacterium* to form stable cell lines expressing fluorescent constructs. TBY-2 cells are amenable to synchronisation of mitosis by the DNA polymerase α inhibitor, aphidicolin (Ikegami *et al.* 1978). Aphidicolin halts cells in G1 phase of the cell cycle and also traps any cell in S-phase. On release from aphidicolin treatment, cells continue through S phase to G2 and into mitosis with greater synchrony than non-treated cells. Using this technique TBY-2 cells provide an ideal system to study mitotic events in stably transformed cells. It is also possible to express multiple fluorescent constructs in the same cell to compare their respective behaviour and interaction *in vivo*.

1.7 AIMS

The lack of markers for the plant NE has led to a lack of *in vivo* research on the NE in higher plants. The aim of my research was to address this gap in knowledge by identifying possible candidate proteins and producing and characterising fluorescent protein chimaeras that specifically label the NE in plant cells. Having identified and produced such a construct the aim of the project was to use the marker to investigate the fate of constituents of the NE during cell division in plant cells. An initial investigation into the nature of the mechanism of protein retention at the NE was also undertaken.

CHAPTER 2.

MATERIALS AND METHODS

2. MATERIALS AND METHODS

2.1 MATERIALS

See Appendix 4 for Strains table.

2.1.1 Water

Water purified by reverse osmosis by an Elgastat Option 3 water purifier (Elga LabWater UK, High Wycombe, UK) was used for making all solutions except plant culture media, which required ultra-pure water (Elga Maxima ultra-pure water purifier). Sterile ultra-pure water (prepared by autoclaving for 20 min at 121°C, 15 p.s.i.) was used for molecular biology protocols.

2.1.2 Chemicals

Chemicals were obtained from Fisher Scientific Supplies (Loughborough, UK), Sigma (Gillingham, UK), and DIFCO (from Beckton Dickinson, Sparks, USA).

2.1.3 Molecular biology reagents

Molecular biology reagents (restriction enzymes, Vent polymerase, dNTPs and T4 DNA ligase) were obtained from New England Biolabs (Hitchin, UK). Oligonucleotides were made by Invitrogen custom primer service (Inchinnan, UK)

2.1.4 Antibiotics

Antibiotics used for bacterial selection and tissue culture were supplied by Melford Laboratory Supplies, Suffolk, UK. Timentin™ (20 mg/ml stock) and carbenicillin, disodium salt (100 mg/ml stock) were dissolved in AnalaR grade methanol. Ampicillin, sodium salt (100 mg/ml stock), kanamycin monosulfate (100 mg/ml

stock) and hygromycin B (40 mg/ml stock) were made up in sterile ultra-pure water. All antibiotics were filter sterilised and stored at –20°C.

2.1.5 Kits

PCR product, DNA and gel band isolation and purification were carried out using an Amersham Pharmacia (Piscataway, USA) GFX^{TM} PCR, DNA and Gel Band Purification kit.

An Amersham Pharmacia Enhanced Chemical Luminescence (ECL) detection system was used to visualise bands on Western blots, according to manufacturer's instructions.

2.1.6 Plant material

Nicotiana tabacum plants (see Appendix 4) were grown in a greenhouse at 21°C, with natural day length illumination, supplemented to 16 h with sodium lighting. For experimental use, plants were transferred to a plant growth room, 24°C with a 14 h light, 10 h dark lighting regime.

Tobacco BY-2 (TBY-2) cells (see Appendix 4) were maintained in Murashige and Skoog (M and S) basal medium pH 5.8, supplemented with sucrose, 2,4-dichlorophenoxyacetic acid (2,4-D) and KH_2PO_4 (see below). Cells were sub-cultured each week (see plant cell culture section) and shaken on an orbital shaker at 130 r.p.m., at 24°C with a 14 h light, 10 h dark lighting regime.

2.1.6.1 Plant growth media

All plant media (see below) was sterilised in an autoclave (121°C, 15 p.s.i, 20 minutes). Antibiotics were added when agar was hand hot, and liquid media at room temperature. Media was stored at 4°C and warmed to room temperature before use. All transformed plant material was autoclaved prior to disposal.

2.1.6.2 Stable plant media

Initial incubation medium (all amounts for 1 litre of medium):

M and S powdered basal medium (2.2 g; without sucrose, indole acetic acid, kinetin, agar; ICN Biomedicals, Costa Mesa, USA), 20 g sucrose. For solid medium 1% w/v DIFCO BactoAgar was added.

Shooting medium:

M and S basal medium (2.2 g), 20 g sucrose, 0.8 mg/L benzylaminopurine (BAP), 1.0 mg/L indolebutyric acid (IBA), 1% DIFCO BactoAgar plus 40 µg/ml hygromycin, 20 µg/ml timentin and 100 µg/ml carbenicillin.

Rooting medium:

M and S basal medium (2.2 g), 20 g sucrose, 0.05 mg/L IBA, 1% DIFCO BactoAgar plus 20 µg/ml timentin and 100 µg/ml carbenicillin. Hygromycin may impair root growth so was excluded from the medium.

2.1.6.3 Tobacco BY-2 cell medium

For 1 litre: 30 g sucrose, 4.3 g M and S medium, 200 µl 1 mg/ml 2,4-D and 3.4 µl 100 mg/ml KH_2PO_4. pH adjusted to 5.8 with KOH. DIFCO BactoAgar (1%) was added for solid medium. Hygromycin (40 µg/ml) was added to liquid and solid media prior to use.

2.1.7 Bacteria

2.1.7.1 Escherichia coli DH5α strain

The DH5α strain of *E. coli* (see Appendix 4) was used to amplify plasmids. *E. coli* were grown in Luria-Bertini broth (LB), Bacto-tryptone (DIFCO) 10 g/L, Bacto-Yeast extract (DIFCO) 5 g/L, NaCl 10 g/L, adjusted to pH 7 with NaOH, autoclaved at 121°C, 15 p.s.i for 20 minutes prior to use. Solid medium was made by adding 1% w/v agar technical no. 3 (Oxoid Ltd., Basingstoke, UK) before autoclaving; antibiotics were added when agar was hand hot.

2.1.7.2 Agrobacterium tumefaciens strain GV3101::pMP90

The *A. tumefaciens* strain (see Appendix 4) used contains a helper Ti plasmid with resistance to gentamycin (10 µg/ml), that is necessary to incorporate the T-DNA regions from the binary plasmid (e.g. pVKH18En6) into the plant genome. *A. tumefaciens* cultures were grown in Yeast Extract Broth (YEB); with (per litre) 5 g beef extract (DIFCO), 1 g Bacto-Yeast extract (DIFCO), 5 g peptone, 5 g sucrose, 2mM $MgSO_4.7H_2O$, autoclaved at 121°C, 15 p.s.i for 20 minutes prior to use. Solid medium was made by adding 1% w/v Bacto-agar (DIFCO) before autoclaving; antibiotics were added when agar was hand hot.

All bacterial suspensions were discarded in Presept disinfectant (Presept effervescent disinfectant tablets, Johnson and Johnson Medical Ltd., Ascot, UK; 1 x 2.5g tablet in 600 ml water). Contaminated glass and plastics were autoclaved prior to washing or disposal.

2.1.8 DNA gel electrophoresis reagents

Gels were cast using BioRad (Hemel Hempstead, UK) gel electrophoresis tanks. TBE at a working concentration of 0.5x was used for DNA gel electrophoresis (Sambrook and Russell 2001). Gels were prepared using 0.5x TBE and electrophoresis grade agarose, the percentage of agarose used depended on the size of DNA fragment being visualised (Sambrook and Russell 2001). Ethidium bromide (50 µg/ml) was added to the agarose before casting the gel. Samples were mixed with 6x DNA electrophoresis gel loading buffer IV (0.25% w/v bromophenol blue, 40% w/v sucrose; Sambrook and Russell 2001) prior to loading onto the gel. Loading buffer was stored at –20°C.

2.1.9 SDS-polyacrylamide gel electrophoresis (SDS-PAGE) and western blotting reagents

Gels were cast in a BioRad Mini Protean II unit. Goggles and nitrile gloves were worn when handling acrylamide.

Separating gels were poured simultaneously; for 2 mini-gels, 6 ml 30% w/v acrylamide (National Diagnostics Ultra pure Protogel. Atlanta, Georgia, USA), 2.1 ml 3M TrisCl pH 8.8, 150 µl 10% w/v SDS solution, 6.7 ml H_2O, 8.3 µl TEMED (N,N,N',N'-tetramethylethylenediamine) and 50 µl 10% APS (ammonium persulfate). A layer of methanol was placed over the gel while it was polymerising to prevent oxygen from diffusing into gel thus preventing polymerisation.

A stacking gel was poured over the separating gels when they had set. For 2 mini-gels, 1.25 ml 30% w/v acrylamide, 500 µl TrisCl 1M pH 6.8, 5 ml 20% w/v

sucrose solution, 75 µl 10% w/v SDS solution, 650 µl H_2O, 10 µl TEMED and 19 µl 10% w/v APS were mixed and poured over the separating gel and the comb inserted. When the stacking gels had polymerised they were wrapped in damp paper towels and placed at 4°C in a sealed plastic container until required.

Gels were run using stocks of 2x SDS gel loading buffer, 5x stock Tris-glycine electrophoresis buffer (used at 1x working concentration), made and used as described in Sambrook and Russell (2001). Western blotting was carried out using 10x Transfer buffer stock, 10x PBS (1x concentration), 1x PBS Tween (PBST), 1x PBS and blocking solution (1x PBST plus 5% w/v skimmed milk powder), also made and used as in Sambrook and Russell (2001).

2.1.10 Constructs/Vectors

The plant binary vector pVKH18En6 (Batoko *et al.* 2000) was used to transform plants via *Agrobacterium*-based methods (see section 2.2.2). The pVKH18En6 vector is based on the pVKH18 vector (Moore *et al.* 1998), with the methotrexate resistance marker replaced by a hygromycin selectable marker. The multiple cloning site is flanked by a 35S mosaic virus promoter, which is enhanced six times (En6), and a nopaline synthase terminal sequence. The plasmid provides kanamycin resistance in transformed bacteria (*E. coli* and *A. tumefaciens*).

2.1.10.1 pVKH18En6-LBR-GFP_5

The pVKH18En6-LBR-GFP_5 plasmid (Irons *et al.* 2003) was constructed by digesting the pVKH18En6 ERD2-GFP_5 vector with *Bam*HI and *Sac*I, to excise the ERD2-GFP_5 construct. The *Bam*HI/*Sac*I cut LBR-GFP_5 overlapping PCR product

was ligated into the cut vector. Further information regarding the production of the LBR-GFP_5 fusion can be found in chapter 3 and appendix 5. The LBR-GFP_5 mutants were cloned in the same manner (details in chapter 5 and appendices 4 and 5).

2.1.10.2 pVKH18En6-sp-EYFP-HDEL

The spYFP-HDEL construct (Irons *et al.* 2003) was kindly provided by Federica Brandizzi (Oxford Brookes University). The ER-targeted yellow fluorescent protein (spYFP-HDEL) was generated by insertion of a c-myc tagged EYFP (Clontech) downstream of a sporamin signal peptide at a *Sal*I/*Sac*I site of an existing sporamin signal peptide-GFP_5-HDEL construct cloned into pVKH18En6 binary vector (see Appendix 4).

2.1.10.3 pVKH18En6-sp-GFP_5-Calnexin TM

The GFP_5-calnexin construct (Irons *et al.* 2003) was kindly provided by Federica Brandizzi (see Appendix 4). GFP_5 fused at the 5' end to a sporamin signal peptide and bearing a glycosylatable region (Batoko *et al.* 2000) was fused to the last 236 base pairs of *Arabidopsis* calnexin (Huang *et al.* 1993). A spacer of seven amino acids was inserted between the GFP_5 and the calnexin sequence. The construct was inserted between the *Bam*HI and *Sac*I sites of pVKH18En6 (Batoko *et al.* 2000).

2.2 METHODS

2.2.1 Molecular cloning

Standard molecular biology techniques were adopted (Sambrook and Russell 2001).

2.2.1.1 Polymerase Chain Reaction (PCR)

PCR was performed using a MJ Research, Inc. (Weltham, USA) PTC-100 Programmable Thermal Controller. PCR reaction mixture was: 1 µl template DNA, 10 µl Thermopol buffer, 1 µl 100 mM $MgSO_4$, 3 µl 100 mM dNTP mix, 1 µl 100 pmol forward primer, 1 µl 100 pmol reverse primer, 82 µl sterile distilled water and 1 µl Vent polymerase. The reaction mixture was held for 3 minutes at 95°C before adding the polymerase. Vent polymerase was used for all cloning to as it has higher fidelity, due to proof reading activity, than conventional Taq polymerase; thus the likelihood of mis-incorporated bases is reduced.

The PCR cycles used are shown in table 2.1. The annealing temperature and elongation times for specific products are provided in the relevant results chapters (LBR; chapter 3, mutants; chapter 5). Annealing temperature of oligonucleotides was determined using the formula $3(GC)+2(AT) = T_m$. For PCR a temperature 2-5°C lower than the calculated T_m of the oligonucleotides was used for the annealing stage (annealing temperature was optimised for each PCR to get maximal specificity).

Table 2.1 Details of the PCR cycles.

Temperature	*Time*	*Number of cycles*	*Stage*
95°C	5 minutes	1	Denature
95°C	20 seconds	20-30	Denature
Depends on oligo Tm (normally between 50 and 60°C)	30 seconds		Anneal
72°C	Depends on length of product (~1000 bp/min)		Elongation
72°C	5 minutes	1	Elongation

The oligonucleotide sequences used in the production of the constructs are shown in Table 2.2, details of their use are given in the relevant results chapters (LBR; chapter 3, mutants; chapter 5, appendix 5).

Table 2.2 Oligonucleotide sequences used in construct production. *Red letters represent restriction sites. Pink letters represent point mutations.*

Construct	*Oligo name*	*Oligo sequence (5')*
LBR-GFP_5	SI16	GTCGGCGGATCCATGCCAAGTAGGAAATTTG CC
	SI17	GCGTCCGAGCTCTTATTTGTATAGTTCATCCA TGCC
	SI13	CCAGTCGACGTGGGATCTTTCTGTTTACACAT CAACAGC
	SI14	CAGAAAGATCCCACGTCGACTGGAGAACTTG TTTCAAATGG
Δ1-60LBR-GFP_5	SI37	GACCGTGGATCCATGAGGCAAAGGAAAGGT GGC
LBR S80A-GFP_5	PM1	CGAGGGAGTCGAGCAAGGTCACGCTCC
	PM2	GGAGCGTGACCTTGCTCGACTCCCTCG
LBR S82A-GFP_5	PM3	AGTCGATCAAGGGCACGCTCCCGATCC
	PM4	GGATCGGGAGCGTGCCCTTGATCGACT
LBR S84A-GFP_5	PM5	TCAAGGTCACGCGCCCGATCCCCTGGT
	PM6	ACCAGGGGATCGGGCGCGTGACCTTGA
LBR S86A-GFP_5	PM7	TCACGCTCCCGAGCCCCTGGTCGACCA
	PM8	TGGTCGACCAGGGGCTCGGGAGCGTGA

Overlapping PCR was used to produce fluorescent protein fusions. Two PCRs were performed to amplify the fluorescent protein and protein of interest (PCR 1 and 2 in Figure 2.1). Oligonucleotides used in these reactions (B and C in Figure 2.1) were designed to have overlapping complementary ends that would anneal in a third PCR (PCR 3 in Figure 2.1), where the two previous products would be joined together using the 5' and 3' terminal oligonucleotides (A and D in Figure 2.1).

The first two PCRs were carried out as described for general PCR. The overlapping reactions contained the two template DNAs from the previous PCR reactions, overlapping PCR reaction mixture (1 µl PCR 1, 1 µl PCR 2, 10 µl Thermopol buffer, 1 µl 100 mM $MgSO_4$, 3 µl 100 mM dNTP mix, 1 µl 100 pmol forward primer, 1 µl 100 pmol reverse primer, 81 µl sterile distilled water, 1 µl Vent polymerase). The reaction mixture was held for 3 minutes at 95°C before adding the polymerase.

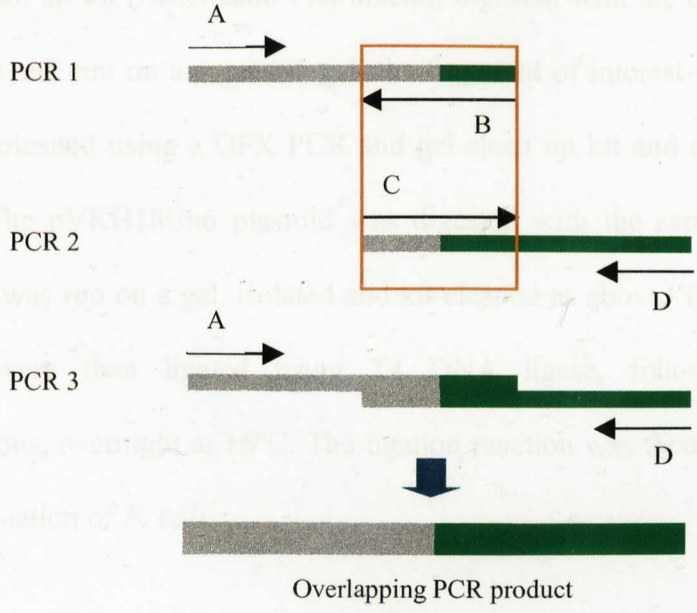

Figure 2.1 Schematic diagram showing the stages of an overlapping PCR. The homologous overlapping region is enclosed in the orange box. Oligonucleotides are denoted A-D.

The first two PCRs were carried out as described for general PCR. The overlapping reactions contained the two template DNAs from the previous PCR reactions, overlapping PCR reaction mixture (1 µl PCR 1, 1 µl PCR 2, 10 µl Thermopol buffer, 1 µl 100 mM $MgSO_4$, 3 µl 100 mM dNTP mix, 1 µl 100 pmol forward primer, 1 µl 100 pmol reverse primer, 81 µl sterile distilled water, 1 µl Vent polymerase). The reaction mixture was held for 3 minutes at 95°C before adding the polymerase.

2.2.1.2 Ligations

PCR products were designed to incorporate specific restriction sites at their 5' and 3' ends (LBR-GFP_5 and mutants – *Bam*HI/*Sac*I). The sites chosen were dependent on the sequence of the gene and the restriction sites in the multiple cloning site of the pVKH18En6 binary vector (the restiction sites in pVKH18En6, in 5' to 3' order are; *Xba*I, *Bam*HI, *Sma*I, *Kpn*I, *Sac*I). The PCR products were cleaned using a GFX PCR clean up kit (Amersham Pharmacia), digested with the appropriate restriction enzymes and run on an agarose gel, the fragment of interest was excised from the gel and cleaned using a GFX PCR and gel clean up kit and eluted in 50 µl sterile water. The pVKH18En6 plasmid was digested with the same enzymes. The cut plasmid was run on a gel, isolated and kit cleaned as above. The cleaned insert and vector were then ligated using T4 DNA ligase, following manufacturer's instructions, overnight at 16°C. The ligation reaction was then used in a heat shock transformation of *E. coli.*

2.2.1.3 Production of competent *Escherichia coli* DH5α

A 100µl aliquot of stock competent cells was used to inoculate 5 ml LB (no antibiotics), the culture was shaken at 200 r.p.m. overnight at 37°C. From the overnight culture 4 ml was used to inoculate 400 ml fresh LB (in conical flask), shake for ~2 hours (or until optical density reached between 0.2 and 0.3 at 600nm against LB blank). During the incubation RF1 and RF2 solutions were prepared (see below) and 8 x 50 ml tubes chilled on ice.

RF1 (low Ca^{2+})

Chemical concentrations	*For 100 ml (for 200 ml cells)*
100mM KCl	0.7460 g
50mM $MnCl_2.4H_2O$	0.9895 g
30mM CH_3COOK (Potassium acetate)	3 ml (from 1M CH_3COOK pH 7.5 stock)
10mM $CaCl_2.2H_2O$	0.1470 g
15% w/v glycerol	15 g

Add KCl, $MnCl_2$, $CaCl_2$, CH_3COOK pH to 5.8, add glycerol and filter sterilise.

RF2 (high Ca^{2+})

Chemical concentrations	*For 50 ml (for 200 ml cells)*
10mM MOPS	0.1047 g
10mM KCl	0.0373 g
75mM $CaCl_2.2H_2O$	0.5513 g
15% w/v glycerol	7.5 g

Add MOPS, KCl and $CaCl_2$ pH to 6.8 with NaOH, add glycerol and filter sterilise.

When the correct optical density was obtained, cells were decanted into cooled tubes and incubated on ice for 15 minutes. The tubes were then centrifuged (10 minutes, 3000 r.p.m., 4°C) and the supernatant was discarded to hypochlorite. The pellets were gently resuspended in 5 ml RF1, then a further 15 ml RF1 was added and the suspensions combined to 4 tubes. Tubes were incubated on ice for 15 minutes, then centrifuged (10 minutes, 3000 r.p.m., 4°C) supernatant was discarded and each pellet very gently resuspended in 8 ml RF2. The cells were divided into

aliquots of 200-400 µl, in chilled 1.5 ml microfuge tubes, and were snap frozen in liquid nitrogen and stored at –70°C.

2.2.1.4 Heat shock transformation of *E. coli*

Competent *E. coli* cells were thawed on ice and added to a 1.5 ml tube containing plasmid DNA or ligation reaction (50-100ng plasmid or 20 µl ligation reaction to 200 µl cells). The *E. coli* were incubated on ice for 20 minutes and then placed into a 42°C water bath for 2 minutes. LB (600 µl) was added to the heat shocked cells which were incubated with shaking (100 r.p.m.) at 37°C for 1 hour. Cells were then pipetted onto a LB agar plate (supplemented with appropriate antibiotic; pVKH18En6 – kanamycin 100 µg/ml) at room temperature and spread with a flame-sterilised glass spreader. Plates were incubated overnight at 37°C.

2.2.1.5 Plasmid preparation

Colonies were picked from antibiotic plate using a sterile pipette tip and placed in 5 ml LB supplemented with antibiotic (pVKH18En6 – kanamycin 100 µg/ml). The inoculated tubes were incubated at 200 r.p.m. on a shaking incubator for up to 16 hours at 37°C. The plasmids were extracted from the liquid cultures using the alkaline lysis mini DNA preparation method described.

2.2.1.6 Alkaline lysis mini DNA preparation using Qiagen buffers – 'Minipreps'

Cultures (5 ml) were precipitated by centrifugation for 5 minutes at 3,000 r.p.m. in a Sorvall 6,000D centrifuge. Supernatant was discarded to bleach. Each pellet was resuspended in 250 µl buffer P1 (30 mM Tris, 10 mM ethylenediaminetetraacetate

(EDTA) pH 8.0, 100 µg/ml RNaseA), transferred to sterile 1.5 ml tubes and incubated on ice for 10 minutes. P2 buffer (250 µl; 200 mM NaOH, 1% SDS) was added and gently inverted to mix. Buffer P3 (350 µl; 3 M potassium acetate pH 5.5) should be added no longer than 5 minutes after adding the P2, and the tubes were centrifuged for 10 minutes at 13000 r.p.m at 4°C in a Heraeus microfuge Fresco (Bishop's Stortford, UK). Supernatant was transferred to fresh tubes and 425 µl of ice-cold isopropanol was added. Tubes were centrifuged for 20 minutes at 13000 r.p.m. at 4°C. Supernatant was removed and the pellet was washed twice with 300 µl ice cold 70% ethanol, with 5 min, 4°C, 13000 r.p.m. centrifugations between each wash. Finally the pellets were dried at 37°C for around 30 minutes and resuspended in 30 µl sterile distilled water.

2.2.1.7 DNA gel electrophoresis

PCR products, plasmid samples and restriction enzyme digests were separated on agarose gels (see section 2.2.1.6 for materials) containing ethidium bromide, against DNA ladders of known fragment sizes (100 bp and 1 kb ladders, NEB). Samples were mixed with 6x DNA electrophoresis gel loading buffer IV (see section 2.1.8) prior to loading onto the gel. Gels were run between 30 and 70 V.

Bands were visualised using a Flowgen UV light box (Lichfield, UK) and images captured using a Uvitec Uvisave gel documentation system (Cambridge, UK).

2.2.1.8 Sequencing reactions

The plasmids were digested to determine the correct size of insert was in place. Two positive clones for each construct were sequenced using BigDye terminators

version 3 (Applied Biosystems, Warrington, UK). Sequencing was performed by the University of Oxford, Department of Biochemistry DNA Sequencing Laboratory (see Appendix 5 for details). The sequenced plasmids were used to transform *A. tumefaciens*.

2.2.1.9 Production of competent *Agrobacterium* (GV3101 : :pMP90)

A single colony was picked using a sterile pipette tip and placed in 5 ml YEB plus 10 µg/ml gentamycin. The culture was placed in shaking incubator at 28°C, 150 r.p.m. and grown to saturation (around 20 hours). A 200 µl aliquot was taken from the 20 hour culture and used to inoculate 20 ml fresh YEB plus antibiotic. The culture was incubated overnight shaking at 28°C. From the 20 ml overnight culture 16 ml used to inoculate 400 ml of fresh medium (400 ml in 2 L flask or 2 x 200 ml in 1 L flasks). The culture was grown for ~3 hours shaking at 28°C.

Cells were transferred to 50 ml falcon tubes and chilled on ice, then harvested by centrifugation (15 minutes, 3500 r.p.m., 4°C). The pellet was gently resuspended in 200 ml (combine to 4 tubes) ice cold 1mM HEPES buffer pH 7.5 (filter sterilised). Cells were centrifuged (15 minutes, 3500 r.p.m., 4°C) and the pellet gently resuspended in 100 ml ice cold 1mM HEPES buffer pH 7.5 (combine cells to 2 tubes, 50 ml/tube). Cells were pelleted by centrifugation (15 minutes, 3500 r.p.m., 4°C) and resuspended in 10 ml (5 ml/tube) ice cold 1mM HEPES/10% glycerol pH 7.5 (filter sterilised). The cells were collected again by centrifugation (15 minutes, 3500 r.p.m., 4°C) and gently resuspended in 1.6 ml (800 µl/tube) ice cold 1mM HEPES/10% glycerol pH 7.5. Aliquots of 40 µl resuspended cells were placed into 1.5 ml microfuge tubes, snap frozen in liquid nitrogen and stored at –70°C.

2.2.1.10 Heat shock transformation of *Agrobacterium*

Competent *Agrobacterium* were thawed on ice, mixed gently with 0.5-1 µg DNA and incubated on ice for 5 minutes. The cells were then placed in liquid nitrogen for 5 minutes and then transferred to a 37°C incubator for 5 minutes. 1 ml of YEB was added and the cells shaken at 150 r.p.m. at 28°C for 2-4 hours. A 200 µl aliquot of the cells was then plated onto YEB agar plates containing an appropriate antibiotic (e.g. 100 µg/ml kanamycin for pVKH18En6 plus 10 µg/ml gentamycin) and incubated for 2 days at 28°C. From these plates, liquid cultures were established by picking colonies with a sterile pipette tip and placing in a 30 ml sterile tube containing 5 ml YEB plus selectable antibiotic. The cultures were shaken at 150 r.p.m overnight at 27°C.

2.2.2 *Agrobacterium*-mediated transformation of plant material

2.2.2.1 Agrobacterium-mediated transient transformation of *Nicotiana tabacum*

The optical density of the *Agrobacterium* culture was determined against YEB at 600 nm absorbance using a Perkin Elmer (Boston, USA) UV/Vis Lambda 3B Spectrophotometer. The culture was diluted 1:2-1:5 culture:fresh medium to produce readings within range for the spectrophotometer. The optical density of bacterial culture was then calculated so each culture was infiltrated at the same density (0.1 for LBR and mutants, 0.02-0.05 for calnexin).

Agrobacterium suspended in infiltration medium was taken up into a 1 ml sterile syringe. The syringe tip was placed firmly against the underside of a leaf and the syringe plunger gently pressed, thereby forcing the bacterial culture through the stomata and into the leaf mesophyll. The suspension can be seen diffusing through

the leaf. Infiltration was repeated in different areas of the leaf until the 1 ml suspension was used up.

2.2.2.2 Transformed *Agrobacterium* stocks

To make frozen stocks of transformed *Agrobacterium* 1.5 ml overnight suspension culture was placed into a sterile microfuge tube and centriguged for 5 minutes at 6000 r.p.m. The supernatant was removed using a Gilson pipette fitted with a sterile P1000 tip and the pellet resuspended in 1 ml infiltration medium (see media section). The bacteria were centrifuged for 5 minutes at 6000 r.p.m. The supernatant was removed, the pellet was resuspended in 600 µl infiltration medium plus 400 µl autoclaved glycerol, mixed thoroughly and snap frozen in liquid nitrogen. The frozen stocks were stored at -80°C. The frozen samples were used to re-establish liquid *Agrobacterium* cultures without re-transforming cells. To start cultures from frozen stabs a sterile pipette tip was used to transfer a small amount of frozen culture to a 30 ml sterile tube containing 5 ml YEB plus selectable antibiotic which was then shaken overnight at 27°C.

2.2.2.3 Agrobacterium-mediated stable transformation of *Nicotiana tabacum*

Stably transformed plants were generated via *Agrobacterium tumefaciens* mediated transformation as described by Hadlington and Denecke (2001). See Figure 2.2 for flow diagram of the transformation process. All procedures were carried out in a laminar flow hood unless stated otherwise. Sterile leaf squares (lower epidermis on the medium) were incubated with 400 µl of an overnight agrobacterium culture in initial incubation medium (see section 2.1.6.2), whilst gently agitated (50 r.p.m. in shaking incubator), at 28°C for 20 minutes. Leaf squares were then plated on solid

initial incubation medium with no antibiotics and incubated in the dark for 3 days at 28°C.

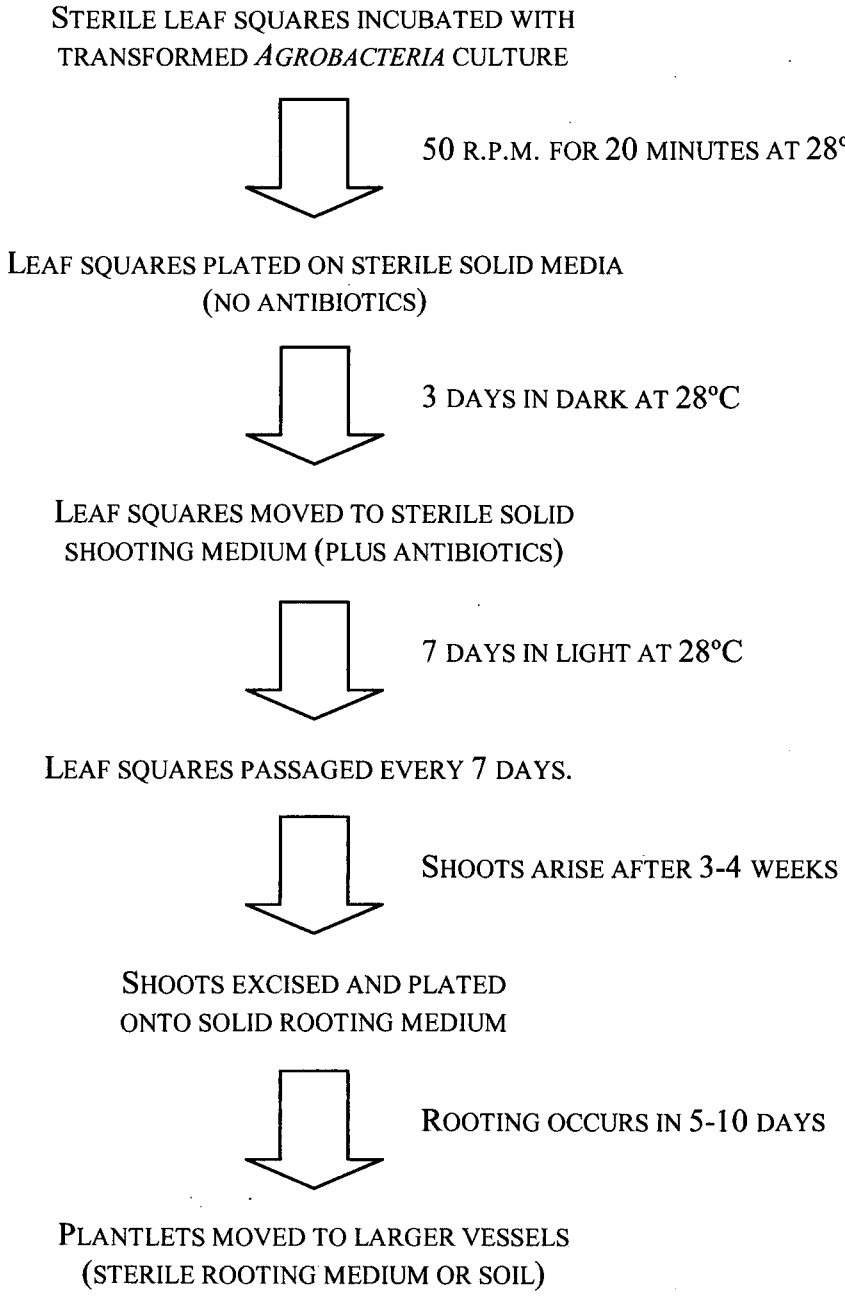

Figure 2.2 Flow diagram of the stable transformation of *Nicotiana tabacum*

After 3 days, the leaf squares were moved to solid shooting medium (see section 2.1.6.2), supplemented with 40 µg/ml hygromycin (to select transformed plant cells) and 100 µg/ml carbenicillin and 20 µg/ml timentin (to control *Agrobacterium* growth). Incubation continued at 28°C in light conditions. Leaf squares were

moved to fresh plates every 7 days, and excess bacteria were removed by blotting leaf squares on sterile filter paper.

When shoots appeared, they were excised and plated onto rooting medium (see section 2.1.6.2). Rooting occurred in 5-10 days. The plantlets were moved to Phytatrays (Sigma, Gillingham, UK) containing rooting medium. The plants were then either moved to soil or grown in larger sterile culture vessels. When the plants finished flowering, seeds were collected, bagged and stored for future use.

2.2.2.4 Agrobacterium-mediated stable transformation of tobacco BY-2 cells

Stable BY-2 cell transformation was achieved as described in Saint-Jore *et al.* (2002). In summary, 1 ml of 3 day old *N. tabacum* BY-2 suspension culture cells were incubated with 50 µl of a 20 h *Agrobacterium* culture for 2 days. The cells were then washed by pipetting cells into sterile tubes where they sank to the bottom. The excess medium was removed and the cells were gently resuspended in fresh autoclaved media. The sinking/resuspension sequence was repeated twice, finally resuspending cells in 1 ml medium. The washed cells were spread onto solid TBY-2 medium containing the appropriate selective antibiotics (for pVKH18En6; 40 µg/ml hygromycin, 100 µg/ml carbenicillin and 20 µg/ml timentin). After a month, micro-calli appeared. The micro-calli were moved onto fresh plates (9 calli per plate) of solid TBY2 medium supplemented with appropriate antibiotics. Calli were passaged every month onto fresh plates of TBY-2 solid medium supplemented with antibiotics. Transformed calli were identified with a Leica stereo fluorescence microscope using UV illumination and GFP1 and GFP3 filters. After 3 passages selected calli were used to establish suspension cultures. Calli

used for suspension were passaged onto three separate plates (rather than the usual two as used for routine passage of calli) prior to starting the suspensions.

Double transformation was achieved as described in Saint-Jore *et al.* (2002). Wild type TBY-2 cells were incubated with 50 µl each of two *Agrobacterium* cultures, transformed with different constructs, for two days. The cells were washed, plated onto antibiotic plates, and selected as previously described.

2.2.3 Synchronisation of mitosis in tobacco BY-2 cells using aphidicolin

Cells (1ml stationary phase, 4 or more days after passage) were passaged into 20 ml fresh medium including 5 µg/l aphidicolin (stock 5 mg/ml in DMSO) and hygromycin (40 µg/l). Cells were incubated for 24 hours at 27°C with shaking at ~130 r.p.m. The cells were washed with 500 ml of fresh medium using a sterile fine nylon filter; cells were poured onto the filter and immersed in medium. Washing was achieved by gentle agitation of the nylon filter in the washing medium, which was frequently changed. Cells were resuspended in 20 ml of medium plus hygromycin, and shaken at 28°C for 10 hours (peak cell division after release from aphidicolin block occurs 10-12 hours post release) prior to observation using the confocal laser scanning microscope (CLSM, see below).

2.2.4 Preparation of living plant tissue for observation using the confocal laser scanning microscope

For imaging expression in leaves, a 1cm square piece of leaf was excised and placed with the lower epidermal surface facing upwards on a glass slide (20 x 70 mm, Fisher). A drop of water was placed on the leaf surface and a coverslip (22 x

55mm, 0 thickness, Fisher) gently lowered on to the sample. Excess water was removed by gently placing a tissue on one edge of the coverslip.

For imaging TBY-2 cells, 50-100 µl of cells were taken from a suspension culture and put on a slide prior to observation. Samples were analysed at room temperature.

2.2.5 Imaging

Confocal imaging was performed using an inverted Zeiss (Welwyn Garden City, UK) LSM 510 Laser Scanning Microscope fitted with 40x and 63x oil immersion objectives. For imaging expression of GFP constructs alone or in combination with YFP we used the single- and multi-track facilities of the confocal microscope, respectively as described by Brandizzi *et al.* (2002c). For imaging GFP and ethidium bromide (EthBr), the 488 nm excitation line of an argon ion laser (GFP) and the 543 nm excitation line of the helium laser (EthBr) were used alternately. Fluorescence was detected using a 488/543 nm dichroic beam splitter and 505-530 nm band pass filter for GFP and 560 nm long pass filter for EthBr. Image processing (image manipulation, addition of scale bars) was accomplished with the LSM 5 Image Browser (Zeiss) and Adobe (San Jose, USA) PhotoShop 5.5 software.

Ethidium bromide staining involved incubation of leaf tissue or BY-2 suspension cultures with EthBr (50 µg/ml) and 50 µg/ml RNase A (Sigma) for 30 minutes at room temperature (Brandizzi and Caiola 1998).

2.2.6 Membrane and protein isolation and analysis

2.2.6.1 Protein isolation

It was important to establish whether the LBR-GFP_5 construct was membrane-integral. This was assessed using Triton X-114 (TX-114) partition as described by Bordier (1981). 0.2 - 1.0 mg/ ml of protein in a crude extract of leaf tissue and BY-2 cells in 10 mM Tris-HCl, 150 mM NaCl, 0.5-1.0% TX-114 on ice, prepared as described below.

2.2.6.2 Pre-condensation of Triton X-114

Prior to use, the TX-114 was condensed to remove hydrophilic molecules as described by Bordier (1981). In brief, 20 g of TX-114 plus 16 mg butylated hydroxytoluene was added to 980 ml 10 mM Tris-HCl pH 7.4, 150 mM NaCl. The mixture was placed at 0°C, mixed using a magnetic stirrer until the solution cleared. The flask was then incubated overnight at 30°C and the solution separated into two phases – a large aqueous phase and a smaller detergent phase. The aqueous phase was removed and replaced by fresh 10 mM Tris-HCl pH 7.4, 150 mM NaCl. This condensation was repeated a further 2 times. Finally the enriched TX-114 phase was removed and used as the stock for subsequent experiments. The concentration of the stock TX-114 was determined by measuring absorbance at 277 nm (using a Perkin Elmer (Boston, USA) UV/Vis Lambda 3B Spectrophotometer with UV light and quartz cuvettes against a buffer blank). A 1% TX-114 solution has an absorbance of ~28 at 277 nm.

2.2.6.3 Phase separation of membrane proteins using Triton X-114

Stably or transiently transformed leaf tissue or 2 ml BY-2 cells (0.5-1.0 g) were crushed on ice with 50 µl extraction buffer (10 mM Tris HCl, 150 mM NaCl, 0.5-1.0% Triton-X114). Samples were centrifuged for 3 min at full speed at 4°C. Supernatant was decanted to a new tube and the volume brought up to 250 µl with buffer. Sample (50 µl) was retained for total protein content evaluation.

Protein sample was gently overlaid on a 300 µl sucrose cushion containing: 6% sucrose, 10 mM Tris HCl, 150 mM NaCl, 0.06% Triton-X114. Samples were incubated for 3 minutes at 30°C, then centrifuged for 3 minutes at 30°C at 300 *g* using a Sorvall 6000D (Bishop's Stortford, UK) with swinging bucket rotor. The detergent phase was a small 'oil drop' at bottom of tube under the sucrose cushion. The upper aqueous phase was removed to a new tube. Fresh Triton-X114 (0.5% w/v) was added and dissolved at 0°C, and the sucrose cushion tube retained. The protein mixture was overlaid on the old sucrose cushion and incubated for 3 minutes at 30°C. The tubes were centrifuged for 3 minutes at 30°C at 300 *g*. The aqueous phase was rinsed with 2% Triton-X114 (samples were shaken and allowed to separate) and this detergent fraction was discarded. Triton-X114 and buffer were added to aqueous and detergent phases to obtain approximately equal volumes and concentrations of salt and surfactant. Proteins were precipitated before separation by SDS-PAGE as the presence of Triton interferes with separation of proteins.

2.2.6.4 Protein precipitation

Bovine serum albumin (BSA; 20 µl of 10 mg/ml stock) was added to 600 µl protein. Saturated ammonium sulphate solution (900 µl) was added and mixed by

inversion. The tubes were incubated on ice for a minimum of 2 hours. The tubes were then centrifuged for 10 minutes, 13000 r.p.m. at 4°C in a benchtop microfuge. Supernatant was removed carefully, the tubes were centrifuged for 10 minutes at 13000 r.p.m. at 4°C. The supernatant was carefully removed. Buffer TE 50/2 (120 µl; 50 mM Tris, 2 mM EDTA) was added to the pellet and incubated on ice for 30 minutes. The pellet was then gently resuspended. Protein samples were separated by SDS-polyacrylamide gel electrophoresis (SDS-PAGE; see section 2.1.9 for reagents and below for method).

2.2.6.5 SDS-polyacrylamide gel electrophoresis

An equal amount of 2x SDS gel loading buffer (Sambrook and Russell 2001) was added to the protein samples, which were then heated at 94°C for 5 minutes. Samples were the placed on ice and then immediately centrifuged at 13000 r.p.m. for 1 minute at room temperature. Samples (15 µl) were loaded onto the pre-prepared gel (see section 2.1.9 for details).

Electrophoresis was performed in denaturing conditions using a discontinuous buffer system (Laemmli 1970). SDS polyacrylamide gels (12%, pH 8.8) with stacking gels (pH 6.8) were prepared using a BioRad Mini Protean II unit (see section 2.1.9).

The gels were prepared for use by removing the gel combs, and washing the wells with deionised water to remove unpolymerised acrylamide and the well walls were straightened with a blunt needle where necessary. Gels were then mounted in the electrophoresis apparatus. 1x Tris-glycine electrophoresis buffer was added to the

middle reservoir and then the tank and, the apparatus agitated to remove air bubbles. Wells were washed out with electrophoresis buffer using a bent hypodermic needle. The gels were then loaded using a 15 µl Hamilton syringe, the syringe being washed between samples using buffer from the bottom reservoir. Any unused wells were loaded with 1x loading buffer. The gels were run at 100 V until the dye front reached the running gel at which point the current was increased to 180 V. The run was complete when the dye front reached the end of the gels, approximately 1 h. The gels were stained with Coomassie blue dye to reveal proteins present, or electrophoretically transferred to nitrocellulose membrane (Western blotted) for immunostaining.

2.2.6.6 Western blotting

Western blotting (Sambrook and Russell 2001) was performed using the BioRad mini-blot system for wet blotting, with transfer for 1 h at 100 V onto Schliecher and Schuell 0.45 µm nitrocellulose membrane. The membranes were blocked with PBST 5% skimmed milk powder, then immersed in primary antibody in PBST 5% skimmed milk powder (anti-GFP 1:3000 dilution) overnight at 4°C. Primary antibody was washed off and a secondary antibody added (goat anti rabbit conjugated to horse radish peroxidase (HRP) 1:10,000 in PBST 5% milk). Proteins were visualised using an ECL detection system (Amersham Pharmacia, UK) according to manufacturer's instructions.

2.2.7 Electron microscopy

Two embedding methods were employed, LR White resin to retain antigenicity for immunogold labelling and Spurr resin for preservation of ultrastructural features.

2.2.7.1 Fixation for immunogold labelling

Leaf material was prepared for electron microscopy using the progressive lowering of temperature (PLT) technique as described by Gunawardena *et al.* (2001) with the exception of the fixative used. In the present study, leaf material was fixed for 1 h in 1% paraformaldehyde/1% glutaraldehyde in 0.1 M Na-Cacodylate buffer (pH 6.9).

For immunogold labelling, sections were treated as described in Gunawardena *et al.* (2001) using as anti-GFP primary antibody (Molecular Probes, Leiden, The Netherlands) diluted 1:3000 in PBS BSA (1%). Control grids were incubated in the absence of primary antibody. Sections were then washed (3 x 10 min.) in PBS BSA 1% fish gelatin before incubation for 1h at room temperature in secondary antibody (10 nm-gold conjugated goat anti-rabbit secondary antibody, British Biocell, Cardiff, UK) diluted 1: 20 with 1% fish gelatin in PBS BSA (1%). Sections were then post-stained using uranyl acetate and lead citrate (Reynolds 1963) before examination. Sections were then viewed using a JEOL 1200 EXII transmission electron microscope (Welwyn Garden City, UK).

2.2.7.2 Fixation for ultrastructural study

Leaf samples were processed at room temperature and embedded in Spurr resin (TAAB Laboratories, Reading, UK). Leaf discs (2 mm diameter) were fixed for 40

minutes in 1% glutaraldehyde, 1% paraformaldehyde in 0.1 M sodium cacodylate buffer pH 6.9 plus 2% sucrose, a small amount of polyoxyethylene laurly ether (Brij 35) and 1 mg/ml $CaCl_2$. Discs were washed 4 x 10 minutes with 0.1M sodium cacodylate buffer pH 6.9, then transferred to 1% aqueous osmium tetroxide for 1 h. Samples were then washed 4 x 10 minutes with filtered ultra-pure water and incubated overnight at 4°C in 0.5% uranyl acetate. Samples were rinsed for 10 minutes with ultra-pure water then dehydrated in a water/ethanol (v/v) series 10%, 20%, 30%, 50% for 30 minutes each, 70% 2 x 30 minutes, 90 1 x 30 minutes, 100% and 100% dried ethanol (over anhydrous sodium sulphate) each 3 x 20 minutes.

Samples were then infiltrated with increasing levels of Spurr resin (pre-mixed medium grade from TAAB Laboratories). Infiltration began with 25% resin v/v with dried ethanol at room temperature for 1 h, then 50%, 75% and 100% for 1 h each and overnight in 100% resin. Samples were kept in 100% resin for 8 h, changing the resin periodically, then left overnight and for a further 8 h. Specimens were placed in fresh resin before placing in silicone embedding moulds for polymerisation.

Specimens were placed in a 70°C oven for 10 hours to polymerise. Samples were then removed from the moulds prior and prepared for sectioning. Sections were cut using Reichert-Jung (Vienna, Austria) Ultracut E, and RMC (Boeckeler Instruments Inc., Tucson, USA) MT XL microtomes using glass knives for thick sections and a diamond knife (Drukker International, Cuijk, The Netherlands) for thin and ultra-thin sections.

CHAPTER 3.

PRODUCTION, AND CHARACTERISATION OF

LBR-GFP$_5$ PROTEIN EXPRESSION

IN PLANT CELLS

3. PRODUCTION, AND CHARACTERISATION OF LBR-GFP_5 PROTEIN EXPRESSION IN PLANT CELLS

3.1 INTRODUCTION

The NE, a concentric double membrane perforated by nuclear pores, is a unique feature of eukaryotic cells. The ONE is in continuum with perinuclear ER and hence the components of the ER and ONE membranes and lumen are very similar. The INE contains a functionally distinct group of proteins, which include those involved in maintaining the structure of the nucleus by their interaction with the nuclear lamina (Schuler *et al.* 1994, Ye and Worman 1994).

To date there has been little research concerning NE organisation and protein composition in plants (see Meier 2001 for a review). The absence of markers specifically localised to the plant NE for use in *in vivo* studies has impeded progress in the area. Thus there is little information regarding the dynamics of the plant NE during progression through the cell cycle as shown by specific markers in living cells, an area studied in depth in mammalian cells (see Introduction 1.2).

Searches of the higher plant protein and DNA sequence databases do not show plant homologues to INE proteins identified in mammals, for instance, LBR, nurim, emerin and MAN1.

Previous GFP and immuno-labelled plant proteins (e.g. RanGAP, MAF1, MFP1; Rose and Meier 2001, Gindullis and Meier 1999) that are located at the plant NE were also found to localise with other subcellular structures and thus lack the

specificity needed for exclusive analysis of the properties of the NE. Work using RanGAP-GFP fusions in *Arabidopsis* showed a discontinuous distribution of fluorescence suggestive of nuclear pore association, rather than NE membrane (Pay *et al.* 2002). This is consistent with its role in nuclear transport. Immunofluorescence labelling during mitosis showed RanGAP co-localising with microtubules. Immunolabelling of the protein-degrading 26S proteasome showed NE labelling, as well as labelling of other structures (Yanagawa *et al.* 2002). During mitosis the proteasome labelling co-localised with the microtubules of the mitotic spindle.

The dynamics of the mammalian NE have been successfully investigated using a GFP-fusion with the N-terminal lamin-B receptor domain (Ellenberg *et al.* 1997). The LBR is a constitutively expressed 58kDa integral membrane protein of the INE (Worman *et al.* 1990, Holmer *et al.* 1998). It is present in animal, but not plant or fungal cells. The C-terminal domain is very similar to the sterol reductase family found in plants (Schrick *et al.* 2000) but this domain is not necessary for targeting of LBR to the NE in animal cells (Smith and Blobel 1993). The protein has 8 transmembrane domains and a large N-terminus in the nucleoplasm to which the lamins and chromatin bind (Ye and Worman 1994, Schuler *et al.* 1994, Takano *et al.* 2002). These protein-protein and protein-DNA interactions are responsible for its retention in the INE (Soullam and Worman 1993, 1995). The carboxyl-terminal domain binds to B-type lamins and HP1-type chromatin proteins (Ye and Worman 1994, 1996, Ye *et al.* 1997). Studies using truncated LBR indicate that the N-terminus contains a bipartite nuclear localisation signal (NLS) and that the first TM domain is necessary and sufficient for protein targeting to the INE (Soullam and

Worman 1993, 1995, Smith and Blobel 1993). The NE targeting of human LBR has also been demonstrated in yeast (Smith and Blobel 1994). When the N-terminal 238 amino acids of the LBR, comprising the nucleoplasmic N terminal region and one TM domain, was fused to enhanced GFP (EGFP) the fusion localised to the NE and to a lesser extent the ER, on expression in COS-7 cells (Ellenberg *et al.* 1997). This LBR-EGFP chimaera has allowed the *in vivo* dynamics of interphase and mitotic cells in mammalian cells to be followed (Ellenberg *et al.* 1997, Gerlich *et al.* 2001, Beaudouin *et al.* 2002). See Introduction 1.2 for more detail.

Successful targeting of heterologous proteins in plants has been previously reported. The C-terminal 52 amino acids of the rat sialyltransferase (ST), which is absent in plants, was sufficient to localise a GFP fusion to the plant Golgi in tobacco plants and BY-2 cells (Boevink *et al.* 1998, Saint-Jore *et al.* 2002). In the light of this positive targeting, the use of a mammalian INE protein as an *in vivo* marker in plant cells was explored.

To obtain a potential *in vivo* marker for studying the dynamics of the plant NE, the human LBR-EGFP chimaera (Ellenberg *et al.* 1997) was optimised for expression in plant cells by the replacement of EGFP by GFP_5 (Haseloff *et al.* 1997). The fusion construct was transiently and stably expressed in tobacco plants and the location and dynamics of the encoded protein evaluated.

3.2 RESULTS

3.2.1 Production of the LBR-GFP$_5$ construct

The LBR-GFP$_5$ cDNA fusion was produced by overlapping PCR (reaction conditions described in Materials and Methods section 2.2.1.1). LBR was amplified from the LBR-EGFP plasmid (donated by Dr J. Ellenberg, EMBL Heidelberg) by PCR using oligonucleotides SI16 (5`gtcggcggatccatgccaagtaggaaatttgcc) and SI13 (5`ccagtcgacgtgggatctttctgtttacacatcaacagc) with an annealing temperature of 58°C and elongation time of 40 seconds. GFP$_5$ was amplified using oligonucleotides SI14 (5`cagaaagatcccacgtcgactggagaacttgtttcaaatgg) and SI17 (5`gcgtccgagctcttatttgtatagttcatccatgcc) with an annealing temperature of 62°C and elongation time of 40 seconds. These products were then used as templates in a third PCR in which the two coding regions were fused together and amplified using oligonucleotides SI16 and SI17 (annealing temperature 52°C and elongation time of 1 min 25 sec). The fusion construct was designed to have 5' *Bam*HI and 3' *Sac*I restriction sites for insertion into the polycloning site of pVKH18En6 (Figure 3.1).

The pVKH18En6 LBR-GFP$_5$ plasmid was cloned using standard molecular techniques (Materials and Methods 2.2.1 and Appendix 5) and was used to transform an *A. tumefaciens* strain containing a disarmed Ti plasmid (pMP90; Introduction 1.6.3). The transgenic *Agrobacterium* strain was used to transiently express the LBR-GFP$_5$ protein in *N. tabacum* leaf epidermal cells.

3.2.2 Transient expression of LBR-GFP$_5$ in tobacco leaf cells

The subcellular location of the LBR-GFP$_5$ protein in tobacco leaf cells was determined using a Zeiss LSM 510 Laser Scanning Microscope (see Materials and

Methods 2.2.5). Leaf segments were observed three days after infiltration with transformed *A. tumefaciens* culture. Fluorescence was found to localise at the periphery of the nucleus in interphase (marked by a white arrow, Figure 3.2A). The NE location of fluorescence in the cells was confirmed by staining chromatin with ethidium bromide (shown in red, Figure 3.2B). On imaging, GFP fluorescence was clearly observed surrounding the ethidium bromide labelled nuclear contents, consistent with labelling of the NE (Figure 3.2C). Chloroplast autofluorescence was also present and is indicated by a white arrow in Figure 3.2C. In single cells the LBR-GFP_5 construct clearly labelled the NE (Figure 3.2D) with low fluorescence in the cortical ER (Figure 3.2E). The level of NE labelling differed between cells due to the nature of the transient expression system. The transient expression system allows rapid screening of constructs, however there is no way of controlling how much protein each cell will produce as they are likely to have been infected with a different number of bacteria, thus producing varying levels of protein expression. A low level of ER labelling was frequently observed in cells that were expressing high levels of the fusion protein.

3.2.3 Comparison of LBR-GFP_5 location with ER markers

The subcellular distribution of LBR-GFP_5 labelling in cells transiently expressing the LBR-GFP_5 protein (Figure 3.3A-B) was compared with cells expressing a GFP_5-calnexin fusion (spGFP_5CX, Figure 3.3C-D) and ER targeted/retained GFP_5 (spGFP_5-HDEL; Figure 3.3E-F), which are ER membrane and soluble markers, respectively (see Introduction 1.6.2 and Materials and Methods 2.1.10).

Fluorescence of LBR-GFP_5 located predominantly to the nuclear periphery (Figure 3.3A). Overall there was minimal fluorescence observed at the cell cortex in cells expressing LBR-GFP_5 (Figure 3.3B); however, a small subset of transformed cells displayed a low level of ER fluorescence when greatly over-expressing the LBR-GFP_5 protein.

In cells expressing a truncated form of calnexin, an ER resident integral membrane protein, (Irons *et al.* 2003) GFP fluorescence was present at the NE as well as the ER in accordance with the continuity of NE and ER membranes (Figure 3.3C). In contrast to the LBR-GFP_5 labelling these cells also contained a clearly labelled cortical ER network (Figure 3.3D). The ER lumen marker spGFP-HDEL gave similar patterns of fluorescence to calnexin, with GFP fluorescence located at the NE (Figure 3.3E) and in a clearly defined cortical ER network (Figure 3.3F).

3.2.4 Stable expression of LBR-GFP_5 in *Nicotiana tabacum*

Plants stably expressing LBR-GFP_5 protein were produced in order to study the location of the chimaera in different cell types. Stable plants originate from a single transformed cell and as such every cell in a stable plant should express the labelled protein at the same level when controlled by a constitutive promoter.

When tobacco epidermal cells stably expressing LBR-GFP_5 were analysed with the imaging settings for GFP fluorescence, bright fluorescence was localised at the rim of the nuclei (a typical NE labelled with GFP is indicated by a white arrow), strongly indicating labelling of the NE (Figure 3.4A and C). The NE in the stable plants showed a uniform level of GFP fluorescence. On staining with ethidium

bromide these cells showed intense red fluorescence localised at the nucleoplasm (Figure 3.4B-C). At higher magnification, NE labelling was observed in single cells stably expressing the LBR-GFP_5 protein (Figure 3.4D). Ethidium bromide staining of the same cell provided clear labelling of the nucloplasm (Figure 3.4E). When the GFP and ethidium bromide images were merged GFP labelling was specific to the nuclear rim, with nucleoplasmic GFP fluorescence not apparent (Figure 3.4F). Fluorescence was not detected in the cortical endoplasmic reticulum (Figure 3.4G).

Stable expression allows the imaging of cell types that are not amenable to the transient transformation method. The guard cells of the stomata show NE localisation of the LBR-GFP_5 protein (Figure 3.4H), confirmed by the dual imaging of GFP and ethidium bromide (Figure 3.4I). In petal cells NE labelling was also observed, together with some cortical ER labelling (Figure 3.4J). An autofluorescent chromoplast is also present (white arrow, Figure 3.4J). Pollen granules on the petals also showed NE labelling with LBR-GFP_5 (Figure 3.4K; autofluorescent structures were also present within the pollen granules indicated by arrows). In root cells, fluorescence was present in the vacuole and excluded from the nucleus (Figure 3.4L; nucleus marked with white arrow).

3.2.5 Mobility of LBR-GFP_5 determined by FRAP

The diffusional mobility of LBR-GFP_5 and spGFP_5CX were determined by monitoring fluorescence recovery after photobleaching (FRAP; as described in Introduction 1.2). LBR-GFP_5 showed a slow recovery of fluorescence after photobleaching with a recovery curve gradient of 2.07 (for curve see Figure 3.5A),

compared to spGFP$_5$CX with a steeper curve (Figure 3.5B) and gradient of 1.58. The gradient represents the rate of fluorescence recovery, from time of photobleaching to the time at which a steady state of recovered fluorescence is established, with a gradient of 1 showing faster rate of recovery than a gradient of 2. The slower recovery of LBR-GFP$_5$ suggests that an immobile fraction of fluorescently tagged protein is present at the NE. SpGFP$_5$CX shows a faster recovery of fluorescence than LBR-GFP$_5$, supporting previous descriptions of the protein being freely mobile within the membrane but membrane integral.

3.2.6 Location of the LBR-GFP$_5$ protein by immunogold labelling

In order to investigate further the sub-cellular localisation of the LBR-GFP$_5$ chimaera an ultrastructural study was undertaken by electron microscopy. Antibodies to GFP and immunogold immunocytochemistry were used to detect the location of the expressed protein in the stable transformants. Gold particles were localised at the NE in leaf epidermal cells expressing the construct (Figure 3.6A) but not in non-transformed controls (Figure 3.6B). It was not possible to discriminate between INE, ONE and NE lumenal staining because in the indirect immunostaining technique a secondary antibody to GFP was used for detection. The GFP domain of the construct is anticipated to be in the NE lumen, anchored to the membrane by the LBR domain. However, the combined size of the primary and secondary antibodies limit the resolution of the technique.

3.2.7 Phase separation of integral membrane proteins using Triton X-114

LBR is an integral membrane protein in mammalian cells (Soullam and Worman 1993, 1995). As plant cells were used as a heterologous system for LBR-GFP$_5$

expression it was necessary to establish whether the protein was also membrane integral in plants. To assess this a phase separation assay (Bordier 1981) was performed. The assay is based on partitioning total cellular extracts between an aqueous phase and a detergent phase obtained by extraction with the detergent Triton X-114 (TX-114); membrane integral proteins partition into the detergent enriched phase, while soluble proteins partition with the aqueous phase. As membrane and soluble markers of the endomembrane system, spGFP$_5$CX and sp-GFP$_5$-HDEL were adopted respectively.

SDS-polyacrilamide gel electrophoresis (SDS-PAGE) was performed on aliquots from the total protein, soluble and TX-114 phases for each of the constructs. Samples were transferred to a nitrocellulose membrane by electrophoresis (Western blotting) and they were then labelled with an anti-GFP primary antibody followed by a HRP conjugated secondary antibody. Proteins were then visualised using an ECL system (see Materials and Methods 2.2.6.6).

Figure 3.7 shows the separated and transferred proteins visualised by ECL. The LBR-GFP$_5$ and spGFP$_5$CX protein bands partitioned in the detergent phase, confirming that the constructs are membrane integral. The dual bands in LBR-GFP$_5$ and spGFP$_5$-CX total and TX-114 fraction lanes (lanes 1 and 3, and 4 and 6, respectively) are likely to be the result of incomplete protein glycosylation. The spGFP$_5$-HDEL fusion partitioned in the aqueous phase, as expected, while LBR-GFP$_5$ was absent from this phase. The dual bands seen in HDEL total and aqueous lanes are a result of degradation. Both LBR-GFP$_5$ and spGFP$_5$CX soluble protein phases also contained clear bands of the same molecular weight as free GFP. The

presence of this soluble GFP is likely to be due to the degradation of the fusion constructs.

3.3 DISCUSSION

The amino terminal 238 amino acids of the human LBR were fused to GFP_5 in order to produce a possible *in vivo* marker for the plant NE. Characterisation of LBR-GFP_5 by confocal microscopy of plant tissue transiently (Figure 3.2) and stably (Figure 3.4) expressing the protein indicated that this fusion was an appropriate marker for the study of NE dynamics as it showed NE localisation, with minimal labelling of other sub-cellular structures. Electron microscopy confirmed the location of the GFP fusion to the NE. Biochemical investigations indicated that LBR-GFP_5 expressed heterologously in plants was membrane integral, as it is in animal cells.

By stably expressing the chimaeric protein in whole plants under a 35S constitutive promoter the location of LBR-GFP_5 in a variety of tissues was assessed (Figure 3.4). In most cells (leaf epidermis, pollen) NE location was observed, with some ER labelling present in petal cells. Root cells showed clear fluorescence in the vacuole lumen. This vacuolar fluorescence present in root, but not in leaf, cells is likely to be due to the exposure of the aerial plant growth to blue light. When GFP absorbs blue light at acidic pH the fluorophore becomes susceptible to proteinase attack, resulting in protein degradation and quenching of fluorescence (Tamura *et al.* 2003). This explanation is corroborated by the observation of soluble protein bands of the same molecular weight as GFP found when protein extracts from cells expressing GFP labelled proteins were subjected to phase partition using TX-114.

The ONE is considered to be a domain of the ER and in functional continuum with it. Thus ONE and ER proteins, and ER and NE lumenal proteins can be expected to show very similar, if not identical distribution (Mattaj 2004). However, when LBR-GFP_5 distribution was compared with the ER marker calnexin, a clear difference in distribution was observed, with calnexin localised in the ER and NE, while LBR was largely restricted to the NE. This suggests that the LBR-GFP_5 is localised to and retained in the INE.

The targeting of the amino-terminal 238 amino acids of the human LBR to the higher plant NE shows that NE protein targeting and anchoring mechanisms can be achieved in plant cells. Previous studies have shown that the LBR N terminus located in the nucleoplasm, contains a bipartite NLS together with one TM domain, is necessary for retention at the INE (Smith and Blobel 1993, Soullam and Worman 1993). It is thought that LBR is retained at the mammalian INE by a diffusion-retention mechanism in which LBR binds to lamin B and chromatin (Soullam and Worman 1995, see Introduction 1.5.1). By using FRAP the retention of LBR-EGFP at the NE during interphase has been demonstrated (Ellenberg *et al.* 1997). The dissociation of the protein and resulting diffusion within the ER during mitosis has also been observed with this method (Ellenberg *et al.* 1997). The 'diffusion-retention' mechanism has been demonstrated in animals and, in the present study, suggested to occur in plants. When the recovery rates of LBR-GFP_5 and spGFP_5CX were compared using FRAP, the gradient of the calnexin fluorescence recovery curve was greater than that of LBR, showing a faster rate of fluorescence recovery for calnexin. The difference in recovery implies that there is an immobile (bound) population in the total pool of LBR, whose fluorescence is restored when the

unbleached protein dissociates from its binding interactions and is replaced by new fluorescent protein. The recovery process will take longer for a bound protein in comparison to an unbound one, as unbound protein is freely mobile in the membrane, and as such can move away from the bleached area and be replaced with unbleached protein.

Use of the phase partition (Bordier 1981) procedure to separate integral membrane and soluble proteins showed that spGFP$_5$-CX, a known membrane protein, partitioned to the TX-114 fraction and behaved in the same way as LBR-GFP$_5$. This strongly suggests that LBR-GFP$_5$ is present as an integral membrane protein in plant cells. SpGFP$_5$-HDEL, which is not membrane-integral, was present in the aqueous fraction only, further corroborating the validity of the technique.

For each of the fluorescent constructs used in the phase separation assay, the subsequent blots contained protein bands with a similar molecular weight to soluble GFP. These GFP bands are likely to be due to the degradation of the fusion proteins, with the resulting degradation products being found in the vacuole lumen, as observed in root cells expressing LBR-GFP$_5$. The presence of a single GFP band, rather than a ladder of degraded protein, is suggested to be due to the high stability of GFP in acid and proteolytic conditions found in the vacuole, whilst the protein of interest is less resistant and hence is degraded rapidly leaving the free GFP (Tamura *et al.* 2003).

The sub-cellular distribution of LBR-GFP$_5$ raises several questions regarding the targeting of proteins to NE in plants. Database searches reveal that plants do not

have identifiable molecular homologues of LBR and other mammalian NE proteins. Yet the basic architecture of the nucleus consisting of a roughly spherical form enclosed by a double membrane, appears to be similar in plants, animals and yeast. The lack of INE protein homology between plants, animals and fungi raises the possibility of different evolutionary routes of gross nuclear architecture, as well as the finer aspects of protein targeting and retention strategies employed in different organisms.

Plants have nuclear intermediate-filament like proteins with structural motifs similar to mammalian nuclear lamins (see Introduction 1.1.2), but with different amino acid sequences (Gindullis *et al.* 2002, Rose *et al.* 2003). Immunolabelling using anti-vertebrate lamin antibodies has produced nuclear labelling in plant cells. This implies the presence of a common epitope in animals and plants (Beven *et al.* 1991, McNulty and Saunders 1992, Minguez and Moreno Diaz de la Espina 1993).

The presence of intermediate-filament like proteins and concomitant lack of lamin genes in plants (see 3.1 Introduction) suggests that the plant NE may have a unique composition that has developed in a different way to the vertebrate NE. Yeast also lacks lamins and as such may have nuclear structure closer to plants than animals. The lack of protein homology could also indicate a divergence of NE architecture in plants, mammals and fungi, with the presence of a rigid cell wall affording some protection to the nucleus and as such leading to reduced structural complexity and protein interactions at the NE. Alternatively the architecture of the nucleus may be common to plants, mammals and fungi, but with plants having evolved a different array of proteins that produce a comparable end result. Another possible

explanation for failure to detect homologues of the mammalian lamins in plants may result from the failure of current plant databases to fully represent all plant genes.

Using confocal and electron microscopy and biochemical techniques the LBR-GFP_5 fusion has been shown to label the plant NE *in vivo*. The production of this marker facilitates the study of the dynamics of the NE in plant cells during mitosis (Chapter 4). By mutating specific amino acids in the LBR protein the domains responsible for the targeting and retention of LBR at the plant NE may be identified (Chapter 5).

Figure 3.1 LBR-GFP$_5$ pVKH18En6 cloning site map.

RB - right border, pA - poly A, Hyg^R – hygromycin resistance gene encoding hygromycin phosphotransferase (in plants), PNOS – nopaline synthase promoter, Km^R – kanamycin resistance gene encoding neomycin phosphotransferase II (bacteria), TNOS – nopaline synthase terminator, 35S En6 – 6 times enhancer 35S promoter, LB – left border.

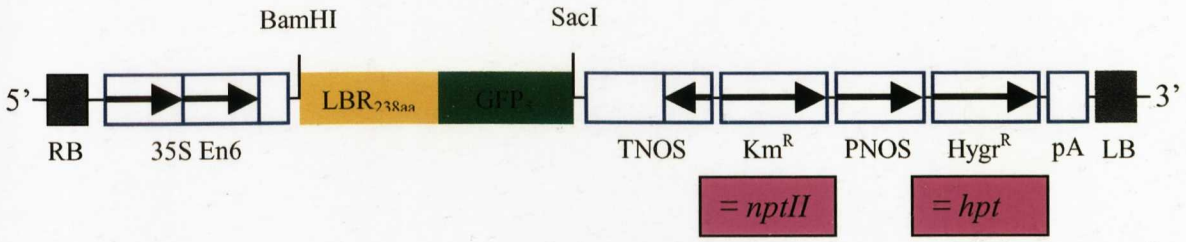
BamHI
SacI
5'
3'
LBR238aa
GFP
RB
35S En6
TNOS
KmR
PNOS
HygrR
pA
LB
= nptII
= hpt

Figure 3.2 Transient expression of the LBR-GFP_5 protein in tobacco leaf epidermal cells.

A. GFP fluorescence in tobacco leaf epidermal cells transiently expressing LBR-GFP_5, nuclear rim labelling marked with arrow.

B. Ethidium bromide stained tobacco leaf epidermal cells (same cells as A).

C. Merged image of A and B, GFP and ethidium bromide labelling in epidermal cells transiently expressing LBR-GFP_5. Autofluorescent plastid marked with arrow.

D. GFP fluorescence in single leaf epidermal cell expressing LBR-GFP_5.

E. Same cell as D, view of cell cortex showing GFP labelling of ER in leaf epidermal cell expressing LBR-GFP_5.

Scale bars = 10 µm.

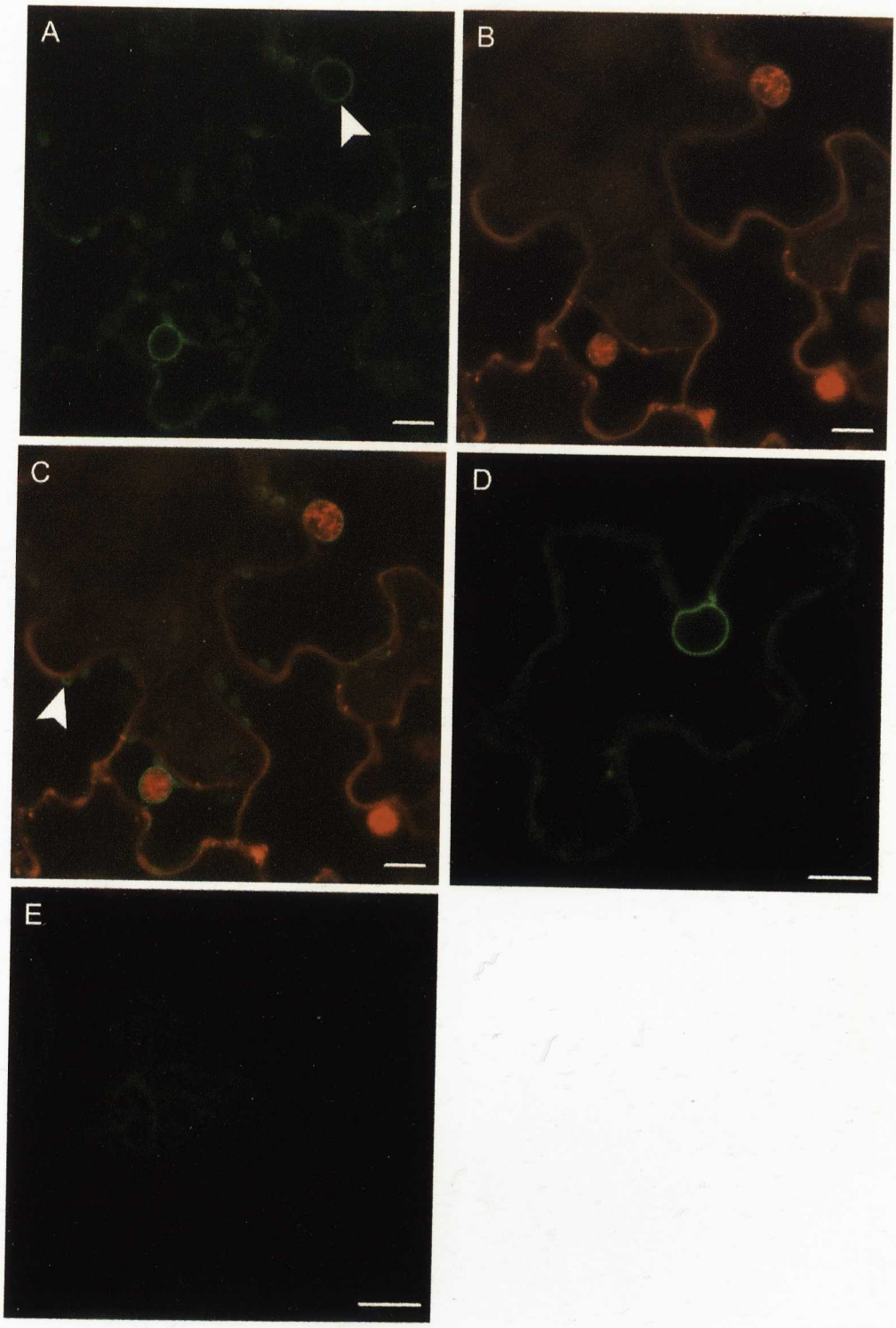
A
B
C
D
E

Figure 3.3 Comparison of NE and ER labelling of LBR-GFP_5 and ER resident proteins $spGFP_5$-HDEL and $spGFP_5$-Calnexin on transient expression in tobacco leaf epidermal cells.

A. LBR-GFP_5 located at the NE in leaf epidermal cell.

B. Same cell as A, view of cell cortex showing LBR-GFP_5 located in ER in leaf epidermal cell.

C. $SpGFP_5$-Calnexin located at the NE in leaf epidermal cell.

D. Same cell as C, view of cell cortex showing $spGFP_5$-Calnexin GFP_5 located in the ER in leaf epidermal cell.

E. $SpGFP_5$-HDEL located at the NE in leaf epidermal cell.

F. Same cell as E, view of cell cortex showing $spGFP_5$-HDEL GFP_5 located in the ER in leaf epidermal cell.

Scale bars = 10 µm.

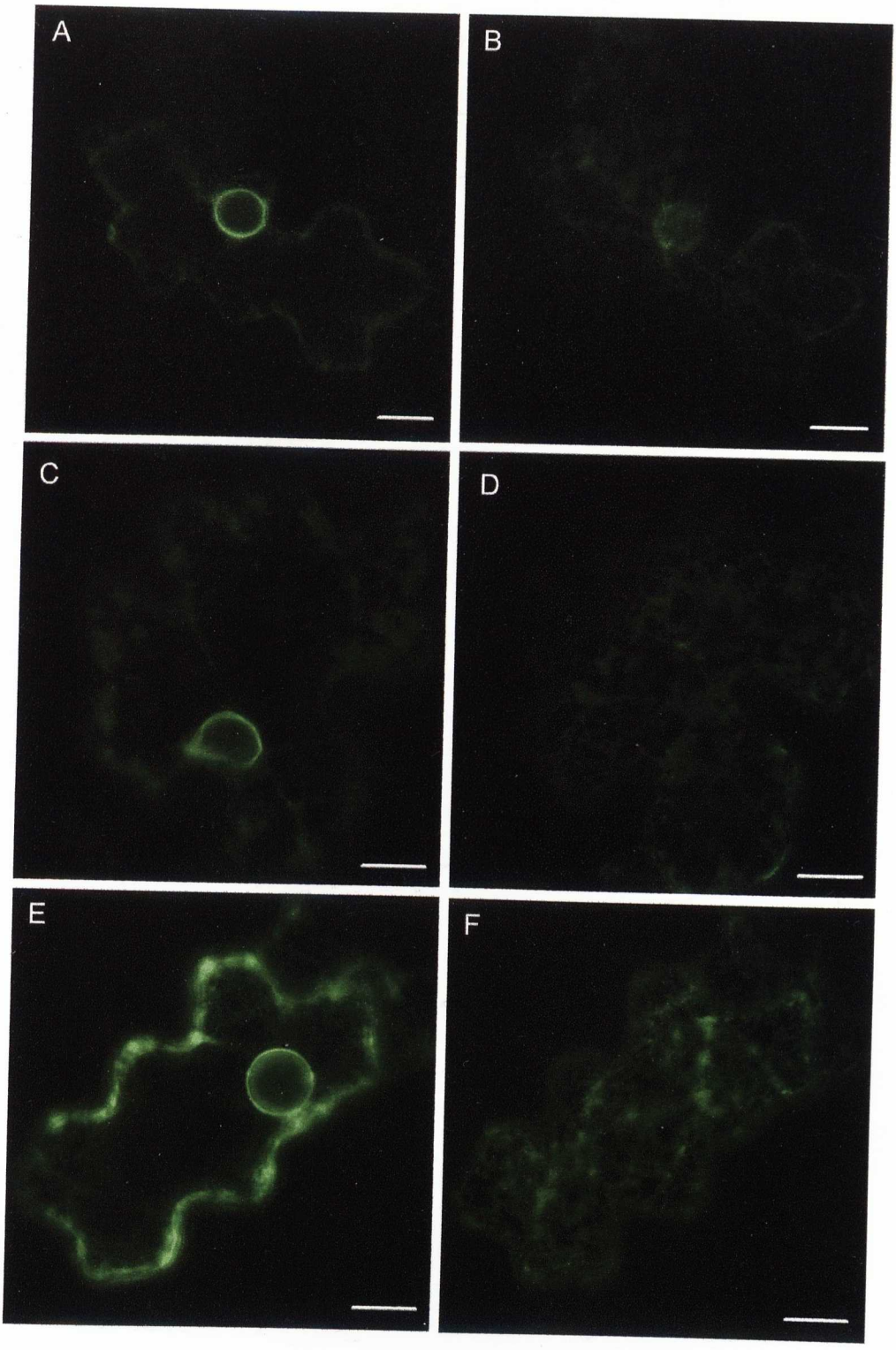
A
B
C
D
E
F

Figure 3.4 Stable expression of the LBR-GFP$_5$ protein in a range of tobacco cell types.

A. GFP location in leaf epidermal cells stably expressing LBR-GFP$_5$.

B. Same cells as A, ethidium bromide stained leaf epidermal cells.

C. Merged image of A and B.

D. GFP location in single leaf epidermal cell stably expressing LBR-GFP$_5$.

E. Same cells as D, ethidium bromide stained leaf epidermal cell.

F. Same cell as D showing GFP labelling and ethidium bromide staining.

G. View of cell cortex of leaf epidermal cell stably expressing LBR-GFP$_5$.

H. GFP labelling in stomatal guard cells stably expressing LBR-GFP$_5$.

I. Same cell as H, GFP and ethidium bromide labelling in guard cell.

J. GFP location in petal cells stably expressing LBR-GFP$_5$, autofluorescent plastid marked with arrow.

K. Higher magnification of petal cells expressing LBR-GFP$_5$, autofluorescent structure marked with arrow.

L. GFP location in root cells stably expressing LBR-GFP$_5$, nucleus marked with arrow.

Scale bars = A-C, G 20 µm, D-F, H-L 10 µm.

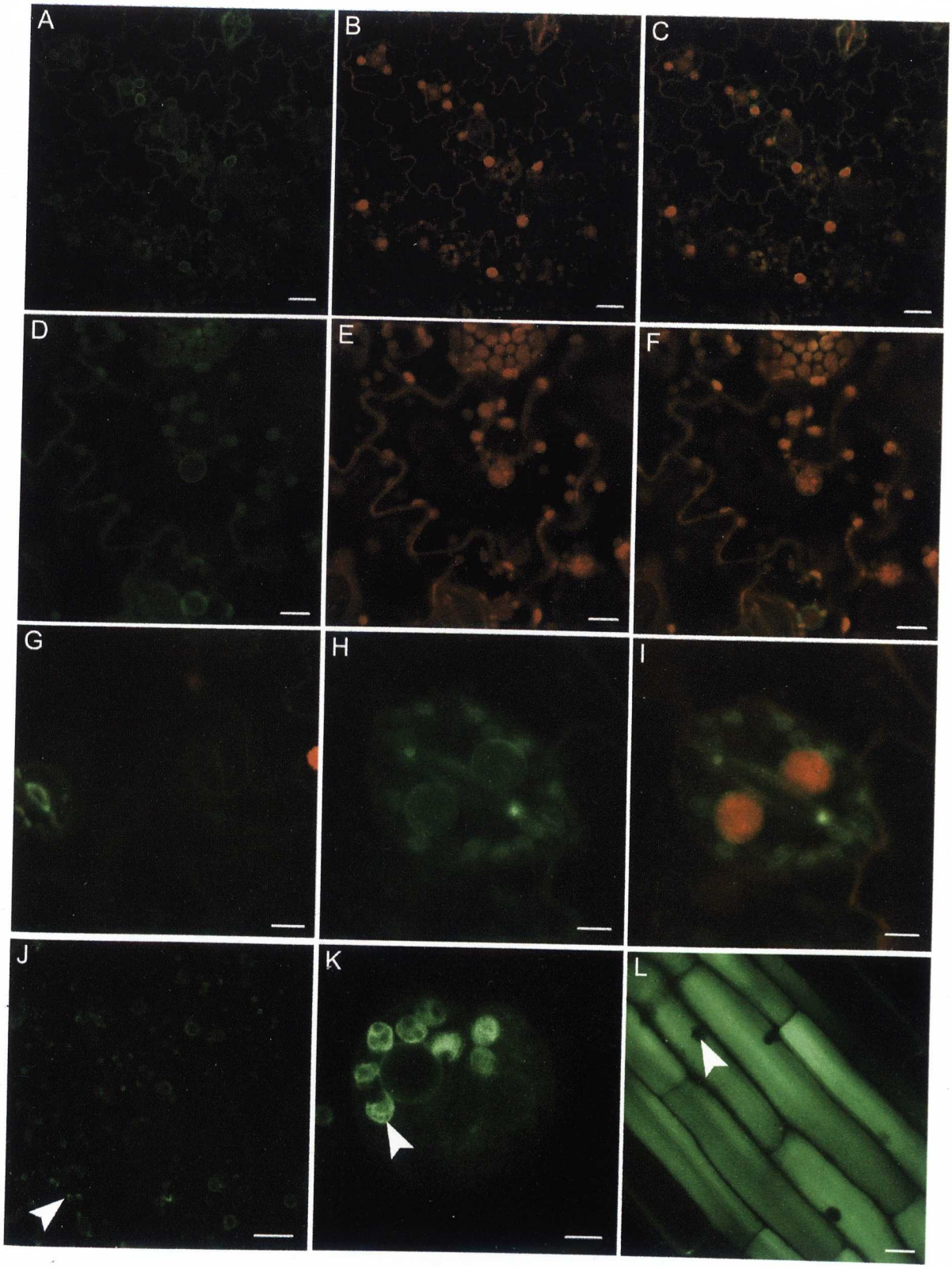
A
B
C
D
E
F
G
H
I
J
K
L

Figure 3.5 Mobility of LBR-GFP$_5$ as determined by fluorescence recovery after photobleaching (FRAP).

A. Graph showing fluorescence recovery after photobleaching of LBR-GFP$_5$ in NE of transiently transformed tobacco leaf epidermal cell.

B. Graph showing fluorescence recovery after photobleaching of spGFP$_5$CX in NE of transiently transformed tobacco leaf epidermal cell.

A.

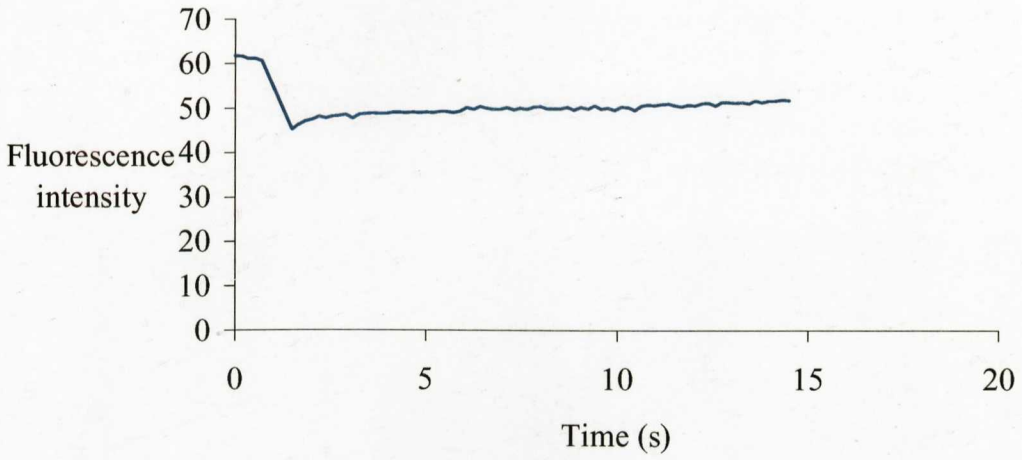
70
60
50
40
30
20
10
0
Fluorescence intensity
0
5
10
15
20
Time (s)

B.

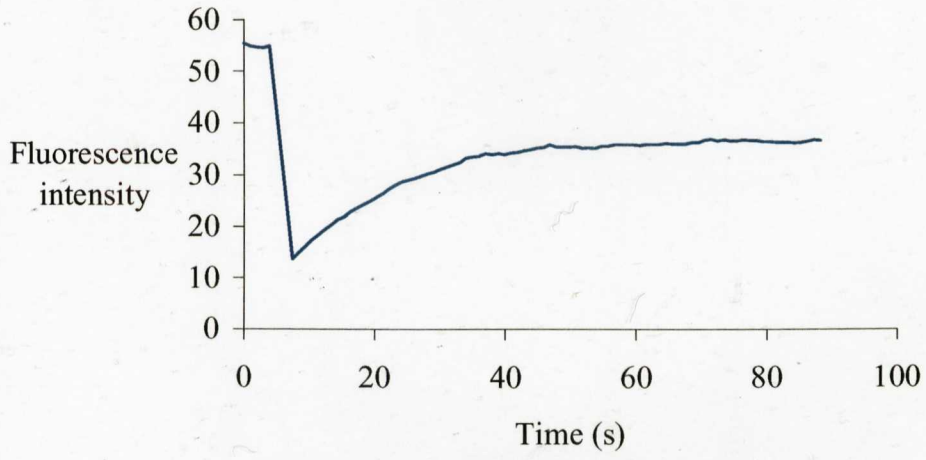
60
50
40
30
20
10
0
Fluorescence intensity
0
20
40
60
80
100
Time (s)

Figure 3.6 Electron microscope immunocytochemistry of LBR-GFP$_5$ distribution at the nuclear envelope of a stably expressing LBR-GFP$_5$ tobacco leaf epidermal cell.

A. Sections were stained with anti-GFP primary antibody, followed by secondary 10nm gold antibody. Arrows indicate the position of gold particles. The position of the inner NE (INE) and outer NE (ONE) are indicated.

B. Control in which no primary antibody was added.

Scale bars = 100 nm.

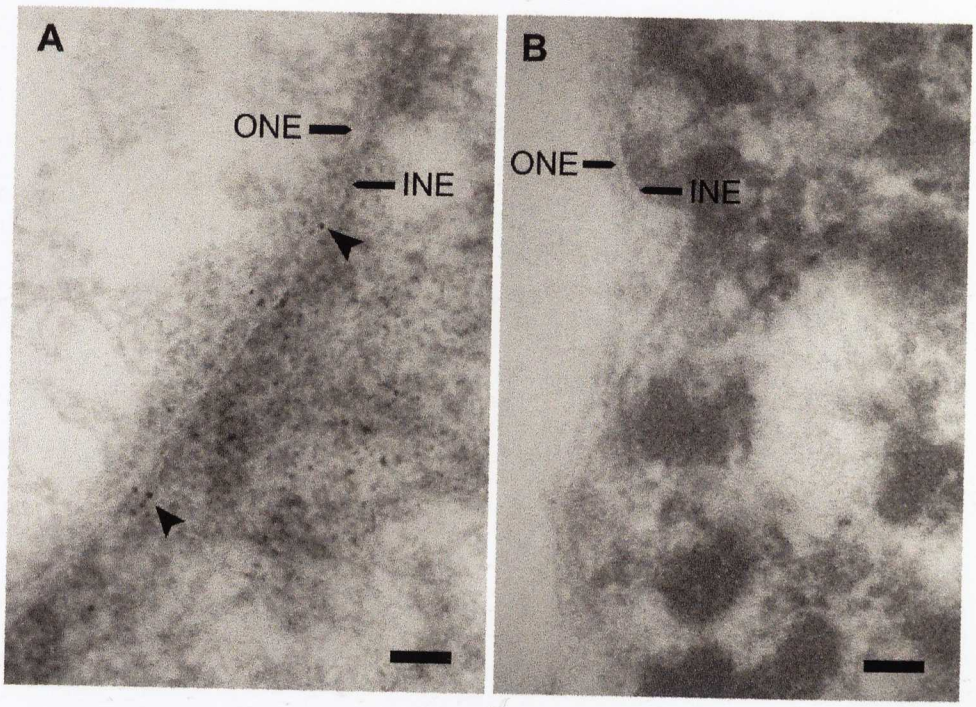
A
ONE
INE
B
ONE
INE

Figure 3.7 Western blot of GFP_5 protein constructs extracted from plant material, separated using a Triton X-114 phase separation assay and visualised by ECL blot.

Lane 1. LBR-GFP_5 total protein extract.

Lane 2. LBR-GFP_5 aqueous fraction.

Lane 3. LBR-GFP_5 Triton X-114 fraction.

Lane 4. SpGFP_5-CX total protein extract.

Lane 5. SpGFP_5-CX aqueous fraction.

Lane 6. SpGFP_5-CX Triton X-114 fraction.

Lane 7. SpGFP_5-HDEL total protein extract.

Lane 8. SpGFP_5-HDEL aqueous fraction.

Lane 9. SpGFP_5-HDEL Triton X-114 fraction.

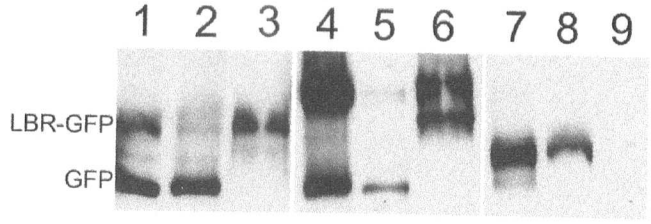
1 2 3 4 5 6 7 8 9
LBR-GFP
GFP

CHAPTER 4.

STUDY OF NUCLEAR ENVELOPE DYNAMICS DURING MITOSIS IN PLANT CELLS USING LBR-GFP_5

4. STUDY OF NUCLEAR ENVELOPE DYNAMICS DURING MITOSIS IN PLANT CELLS USING LBR-GFP_5

4.1 INTRODUCTION

In the previous chapter it was shown that when the amino terminal 238 amino acids of the mammalian LBR were fused to GFP_5 and expressed in plant cells, NE localisation of the construct was observed. This *in vivo* NE marker facilitates the study of the dynamics of the NE during the cell cycle in plant cells, previously not possible due to a lack of markers specific to the plant NE.

The proteins of the mammalian INE are well described (reviewed by Holmer and Worman 2001). With the use of fluorescent protein fusions and microscopy techniques such as FRAP and FLIP (Introduction 1.2) it has been demonstrated that all of the INE proteins examined to date are immobilised at the NE during interphase (e.g. LBR; Ellenberg *et al.* 1997, emerin; Östlund *et al.* 1999, nurim; Rolls *et al.* 1999, MAN1; Wu *et al.* 2002). This immobility supports the diffusion-retention model, which proposes that proteins are bound at the INE by interactions with ligands within the nucleoplasm. During mitosis these interactions are uncoupled through changes in phosphorylation (Worman and Courvalin 2000), which allows formerly tethered proteins to diffuse within the membrane continuum (Soullam and Worman 1993, 1995). Live cell imaging of dividing cells expressing LBR-EGFP showed that the fluorescent protein chimaera migrated to the ER during division and was present in a freely diffusible form, in contrast to its predominantly immobilised interphase state (Ellenberg *et al.* 1997). The location of LBR-EGFP through the ER membranes during mitosis provides evidence to

dispute the theory that the breakdown of the NE during mitosis is due to vesiculation (see Introduction 1.2), as proposed from *in vitro* experiments using fractionated *Xenopus* oocytes (Vigers and Lohka 1991).

The association of plant endomembranes with the mitotic apparatus has been demonstrated by electron microscopy (EM) in a range of plants, including barley (Hepler 1980), *Tradescantia* stamen cells (Hepler 1985) and maize root (Hawes *et al.* 1981). These studies provided a wealth of information about spindle architecture and enabled informed speculation as to the dynamic membrane changes that occur during mitosis. Imaging of biological specimens presents a dichotomy; whilst EM provides excellent ultrastructural resolution, this detail is gained with the loss of the ability to observe membranes *in vivo*. In contrast, live cell imaging allows the observation of membrane dynamics in real time, but with significant loss of spatial resolution compared to EM. In the case of mitosis, it has been suggested, on the basis of EM images, that the NE joins the ER membranes during mitosis (Hepler 1980, Hawes *et al.* 1981). However this absorption has not been visualised *in vivo* due to the lack of specific markers for the NE for EM or light microscopy.

As previously detailed (Introduction 1.4) research on plant NE dynamics has been hindered by a lack of readily available markers that specifically target the NE. Fluorescent protein chimaeras that target the ER and ER/Golgi (e.g. spYFP-HDEL, ERD2-GFP, $spGFP_5$-CX), also highlight the NE (see chapter 3). This labelling is due to the direct continuity of the NE and ER membranes and lumen and is not due to specific targeting or retention at the NE. An ER/Golgi marker was used as a

marker for NE breakdown in a study of PPB formation and division in tobacco BY-2 (TBY-2) cells, providing interesting information on microtubule (MT) interaction with the NE and on MT changes during mitosis (Dixit and Cyr 2002).

Tobacco BY-2 cells have been used to study many aspects of plant cell and molecular biology through the cell cycle including cytokinesis (Samuels *et al.* 1995), proteasome location (Yanagawa *et al.* 2002), MT dynamics (Dixit and Cyr 2002, Kumagai *et al.* 2003) and gene expression (Breyne *et al.* 2002, Dambrauskas *et al.* 2003). TBY-2 cells are amenable to mitotic synchronisation using aphidicolin (Nagata *et al.* 1992, Nagata and Kumagai 1999), a DNA polymerase α inhibitor (Ikegami *et al.* 1978) that arrests cells at the G1/S boundary together with any cells that are in S-phase. On removal of the aphidicolin the majority of the cells are released from G1 and the cell cycle progresses to S phase and into division. This provides a population of cells in which a significant proportion are dividing at the same time and hence is an ideal system to use when studying cell division. TBY-2 cells are also easy to transform using *A. tumefaciens*, producing cells stably expressing protein chimaeras (Geelen and Inzé 2001).

The LBR-GFP_5 chimaera was used as a vital marker to specifically follow NE dynamics during the cell cycle in plant cells *in vivo*.

4.2 RESULTS

Tobacco BY-2 cells were stably transformed with LBR-GFP_5 alone, and in combination with spYFP-HDEL and the location of fluorescence of the constructs followed through mitosis (see Materials and Methods 2.2.2.3).

4.2.1 LBR-GFP_5 location in interphase tobacco BY-2 cells

In TBY-2 cells stably expressing LBR-GFP_5 bright fluorescence was found to localise mainly at the NE (Figure 4.1A). Faint labelling of the cortical ER was also detected. TBY-2 cells stably transformed with LBR-GFP_5 showed a similar level of NE labelling as the previously described for stably transformed plants (Chapter 3.2.4). On repeated passage of the TBY-2 cultures the level of ER labelling increased. This meant that only cells that had undergone less than 4 passages were used for the studies described in this thesis. ER labelling with LBR-GFP_5 was found on transient expression in tobacco leaf cells and has also been observed in mammalian cells (Ellenberg *et al.* 1997).

4.2.2 LBR-GFP_5 highlights NE dynamics in tobacco BY-2 cells

The distribution of LBR-GFP_5 was observed during mitosis at different stages of division in several cells (Figures 4.1-4.3). In interphase cells, NE fluorescence was consistently observed (Figure 4.1A). With the NE intact, at prophase the NE begins to break down. GFP fluorescence was observed around the condensed prophase chromosomes (Figure 4.1B), as labelled with ethidium bromide (shown in red, Figure 4.1C and D). GFP fluorescence was present in tubular structures connecting the NE to the cortical ER at the periphery of the cell (indicated by arrow, Figure 4.1D). In prometaphase the defined labelling typical of the NE was no longer

present, with fluorescence distributed throughout the membranes of the mitotic spindle (Figure 4.2A). During metaphase the LBR-GFP_5 fluorescence continued to be located in a membranous meshwork which was continuous with ER, with the chromosomes aligned on the metaphase plate visible as an area of membrane exclusion (metaphase plate indicated by arrow, Figure 4.2B). As the daughter chromosomes migrated to opposite poles of the cell in anaphase, fluorescence was observed in tubular structures resembling tubular ER (tubular ER indicated with arrow, Figure 4.3A) at the division plate between the two daughter nuclei. In early telophase, as new NEs form around the new daughter nuclei, recruitment of LBR-GFP_5 fluorescence around the nuclei was observed (marked with arrow, Figure 4.3B), with labelling of the mitotic membranes also remaining. As telophase progressed the fluorescence around the new NE became more pronounced, with a decrease in peripheral membrane network labelling. The NEs at this stage appeared crenalated in form, with a uniform distribution of fluorescence (as indicated by arrow, Figure 4.3C). Labelling of the phragmoplast was also observed between the new daughter nuclei. Towards the end of telophase as the daughter NE became more rounded, the strong labelling of the phragmoplast persisted as the new dividing cell wall formed between the daughter cells (marked by arrow, Figure 4.3D).

4.2.3 Fluorescence distribution in a single cell during division

Using TBY-2 cells stably expressing LBR-GFP_5 and synchronised with aphidicolin, it was possible to follow single cells undergoing division. A typical example (3 cells were observed undergoing division) of fluorescence distribution in a cell progressing from late metaphase to the end of telophase is shown in Figure

4.4. The sequence shown took approximately one hour, consistent with the observation that mitosis takes around 2 hours in TBY-2 cells (Vos *et al.* 1999).

As in the cell shown in figure 4.3D, the late metaphase cell expressing LBR-GFP$_5$ showed fluorescence distributed through the ER membranes (time 0-1216s, Figure 4.4). Tubular membranous structures were observed through the mitotic apparatus (indicated with arrow, Figure 4.4, time 1274-1507s). As division progressed through anaphase the fluorescence of the membranes moved towards opposite poles as the chromosomes separated (time 0-1536s, Figure 4.4). In telophase the ER membranes encircled the newly formed daughter nuclei (1624s, Figure 4.4), with new NE forming around each nucleus in the middle of the membranous networks (2069s, Figure 4.4). Fluorescence of the phragmoplast (marked with empty arrow, Figure 4.4), the structure which is the basis for forming the dividing cell wall, forms between the nuclei and develops rapidly across the cell as more wall is assembled (2069-3585s, Figure 4.4). The newly re-formed nuclei partitioned into the two daughter cells and appeared to become closer to the phragmoplast with time (2069-3585s, Figure 4.4). The animated version of the dividing cell shown in Figure 4.4 is included as an AVI movie (Appendix 3).

4.2.4 Double labelling of TBY-2 cells with LBR-GFP$_5$ and spYFP-HDEL

TBY-2 cells co-expressing LBR-GFP$_5$ (Figure 4.5A and B) and spYFP-HDEL (Figure 4.5C and D), a soluble ER marker, showed similar levels of GFP and YFP fluorescence at the NE (Figure 4.5A and C respectively). Within the ER a higher level of YFP fluorescence (Figure 4.5D and F) was observed in comparison to

LBR-GFP_5 (Figure 4.5B and F). This confirms the specificity of NE labelling by LBR-GFP_5.

TBY-2 cells expressing LBR-GFP_5 and spYFP-HDEL were observed during mitosis. At interphase both GFP and YFP fluorescence were located at the NE (Figure 4.6A-C). The GFP was also observed in bright immobile punctate structures (marked with an arrow (Figure 4.6A). At prophase both fluorochromes were found to label the dissipating NE (Figure 4.6D-F). In metaphase, indicated by chromosome alignment at the midline of the cell, GFP and YFP fluorescence were co-localised throughout the membranes of the mitotic spindle (Figure 4.6G-I). GFP labelling was again present in punctate structures (denoted by arrow, Figure 4.6G). In anaphase, co-localisation of LBR-GFP_5 and spYFP-HDEL continued (Figure 4.6J-L) and punctate structures were present in the GFP labelled membranes (as marked by arrow, Figure 4.6J) and were absent from the YFP population (Figure 4.6K). The tubular membrane between the separating chromosomes structures (marked by arrow, Figure 4.6L and as previously seen in Figure 4.3A and 4.4) was labelled with both the fluorescent markers. During telophase, labelling of the re-formed daughter NE and phragmoplast by both GFP and YFP was observed (Figure 4.6M-O). This co-localisation of LBR-GFP_5 with spYFP-HDEL through cell division provides further evidence that the NE protein locates to the ER during mitosis.

4.3 DISCUSSION

The LBR-GFP_5 fusion protein was used as a specific marker of the NE to follow the fate of the NE during mitosis in plant cells. Expression of the protein in TBY-2

cells showed NE fluorescence similar to that previously described in transient and stable expression in leaf epidermal cells (Chapter 3). During mitosis the fluorescence was observed in the membranes of the mitotic apparatus (Figure 4.1-3), on co-expression with spYFP-HDEL an ER lumenal marker, co-localisation of GFP and YFP labelling was seen (Figure 4.5 and 4.6). The results indicate that after NE breakdown LBR-GFP_5 is found in the membranes of the ER, and that the protein is recruited into the new NE of the daughter cells from this ER membrane population.

The location of LBR-GFP_5 through mitosis in TBY-2 cells suggests that components of the plant NE migrate to the ER pool after NE breakdown, and that the NE of the daughter cells re-forms from that pool. This migration of NE protein to the ER during mitosis has been previously observed in mammalian cells (Ellenberg *et al.* 1997) and as such shows conservation in the fate of the NE in plant and animal cells during mitosis. The association of ER derived membranes with the plant mitotic spindle has been well described in early ultrastructural EM studies (Hepler 1980, Hawes *et al.* 1981), DIC microscopy (Hepler 1985, Vos *et al.* 2000) and more recent immunolabelling of calreticulin and RanGAP (Denecke *et al.* 1995, Pay *et al.* 2002) and fluorescently labelled live cell imaging of ER and Golgi apparatus proteins (Nebenführ *et al.* 2000, Saint-Jore *et al.* 2002). The use of LBR-GFP_5 to mark the NE has provided a tool to visualise the association of NE and ER elements during mitosis *in vivo*; such associations have not been conclusively proven previously due to constraints imposed by the use of fixed, and hence dead, specimens (EM and immunofluorescence) or through observation of non-labelled live cells by DIC microscopy and the lack of specific NE markers.

Comparison of the timing of mitosis in TBY-2 cells expressing LBR-GFP_5 with other cell types, both transformed and wild-type, indicates that expression of the fusion protein does not appear to perturb the duration of mitosis. Mitosis in TBY-2 cells has been shown to take around 2 hours (see table 4.1). In cells expressing LBR-GFP_5 the progression from anaphase to the end of cytokinesis took 1 hour, comparable for the same stages in TBY-2 cells expressing γ-tubulin fused to GFP (Kumagai *et al.* 2003). Compared with *Tradescantia*, the duration of division is similar, with anaphase to cytokinesis in *Tradescantia* taking 50 minutes (Vos *et al.* 2000), slightly shorter than observed in TBY-2 cells, in this and other studies (see Table 4.1).

Table 4.1 Duration of cell division in a range of cell types.

Organism	***Duration of mitosis***	***Labelling***	***Reference***
Tradescantia stamen hair cells	Prophase – anaphase (~35 minutes)	DIC images	Hepler (1985)
Tradescantia stamen hair cells	Anaphase – cytokinesis (~50 min)	DIC images	Vos et al. (2000)
TBY-2 cells (plant suspension culture) untransformed	2h	Hoechst stain for MI	Herbert *et al.* (2001)
TBY-2 cells	Anaphase to cytokinesis (~1h)	LBR-GFP_5	This thesis
TBY-2 cells	Prophase – cytokinesis (~2h 25 min; Anaphase to cytokinesis 1h)	GFP-γ-tubulin	Kumagai *et al.* (2003)

Plant cells contain unique structural features during mitosis; these include the preprophase band and the phragmoplast (see Introduction 1.1.3). The phragmoplast

is the site of synthesis for the cell wall that divides the daughter cells and its site is predicted by the site of the preprophase band (Lloyd and Hussey 2001). Electron micrographs of dividing maize cells have shown that the phragmoplast is a site of extensive membrane congregation (Hawes *et al.* 1981). The location of part of the mitotic ER protein population within the phragmoplast indicates that it is a site of extreme membrane activity, with apparently non-specific proteins being trapped within the membrane mass. The absence of labelling at the cell wall on completion of cell division indicates the redistribution of proteins to their specific destinations, or subsequent degradation.

The fluorescent spot-like structures found in TBY-2 cells, present during interphase and mitosis (Figure 4.6), are thought to be an artefact of protein over-expression. Such structures have also been observed in yeast cells expressing an avian form of LBR (Smith and Blobel 1994). In these cells LBR was found to be located at the NE and was also observed as punctate brightly-labelled structures that were shown to be stacks of membrane, as visualised by immunofluorescence and transmission electron microscopy (Smith and Blobel 1994). It was suggested that these membrane stacks were the result of accumulation of membrane containing over-expressed LBR when the NE was saturated with the protein (Smith and Blobel 1994). The increase in ER labelling observed after repeated passages of TBY-2 cells expressing LBR-GFP_5 may also be due to over-expression of the fusion protein leading to a 'backing-up' of excess protein into the ER membranes. This was previously suggested to occur in plant cells over-expressing protein leading to dilated NE and ER membranes (Crofts *et al.* 1999).

Labelling of plant NE by a mammalian NE protein and the subsequent labelling of the ER during mitosis as in animal cells may point to similarities between mammalian and plant nuclei. As previously considered in Chapter 3 the labelling of the plant NE by the LBR-GFP_5 fusion may be due to conservation of nuclear architecture but in view of the lack of protein similarity between plant and animal cells, via a different evolutionary path to that which resulted in the animal nucleus (see General Discussion). The finding that LBR-GFP_5 is localised in the ER during mitosis in plant cells, as in animal cells, implies a level of conservation in the way in which the NE is disassembled in the different kingdoms, with continuity of NE and ER persisting through mitosis, rather than membrane disappearance by vesiculation. It is possible that protein breakdown and synthesis contributes to breakdown of the NE. However the continued high level and steady presence of fluorochrome which is seen throughout mitosis suggests that it is the original protein pool that is present through mitosis.

It has been suggested that recruitment of LBR around the daughter nuclei after division is initially due to chromatin binding during the mid-part of anaphase (Ellenberg *et al.* 1997, Haraguchi *et al.* 2000), which occurs before reformation of the nuclear lamina (Ellenberg *et al.* 1997). It is likely that the binding of chromatin is the main factor that retains LBR at the NE in plants: LBR has been shown to bind chromatin in a non-sequence specific manner (Duband-Goulet and Courvalin 2000, Takano *et al.* 2002). As such, if LBR is correctly folded and inserted into the ER membrane then the chromatin-binding region of the protein will be exposed to the nucleoplasm and chromatin, thus providing a way for the LBR protein to be anchored via chromatin interactions. In chapter 3 it was shown that extraction of

LBR-GFP$_5$ from plant cells expressing the protein yielded an integral membrane protein, which indicates that the protein is correctly folded in plant cells. In mammalian cells, LBR has been shown to interact with lamin B and heterochromatin protein 1 (HP1) as well as chromatin (Ye and Worman 1994, 1996, Ye *et al.* 1997). Plants lack homologues to mammalian lamins (Meier 2001, Rose *et al.* 2004), but do contain HP1 homologues (Gaudin *et al.* 2001; more details Chapter 5), therefore HP1 interactions may play a part in LBR retention in plant cells. Expression of a human HP1 isoform in TBY-2 cells showed interaction with histone H3, and indicated conservation of chromatin organisation between plants and animals (Fass *et al.* 2002). The presence of HP1 homolgues in plants means that interactions may occur between HP1 and LBR in the plant nucleoplasm as has been shown in animal cells (Ye and Worman, 1996, Ye *et al.* 1997). LBR interactions in the plant nucleus are reported in Chapter 5.

When LBR-GFP$_5$ was used as a marker of the NE in dividing tobacco TBY-2 cells fluorescence was found to localise in the ER during division, as demonstrated by co-expression of spYFP-HDEL, a known ER marker. Such ER location of LBR-EGFP during mitosis has previously been described in mammalian cells (Ellenberg *et al.* 1997) so the data presented here strongly suggest that the plant NE is absorbed into the ER during division as in animal cells. Reformation of the NE around daughter nuclei is also observed to follow a similar pattern to that which is seen in mammalian cells, being recruited around the mid anaphase chromatin. As such, it seems likely that the NE reassembles in a similar fashion to its mammalian counterpart. The interactions that contribute to the localisation of LBR to the NE in plant cells are examined in Chapter 5.

Figure 4.1 Location of fluorescence in tobacco BY-2 cells stably expressing LBR-GFP$_5$ at interphase and prophase.

A. An interphase TBY-2 cell expressing LBR-GFP$_5$.

B. A TBY-2 cell in prophase cell expressing LBR-GFP$_5$.

C. Same cell as B, stained with ethidium bromide.

D. Merged image of B and C, NE-ER tubule indicated with white arrow.

Scale bars = 10 µm.

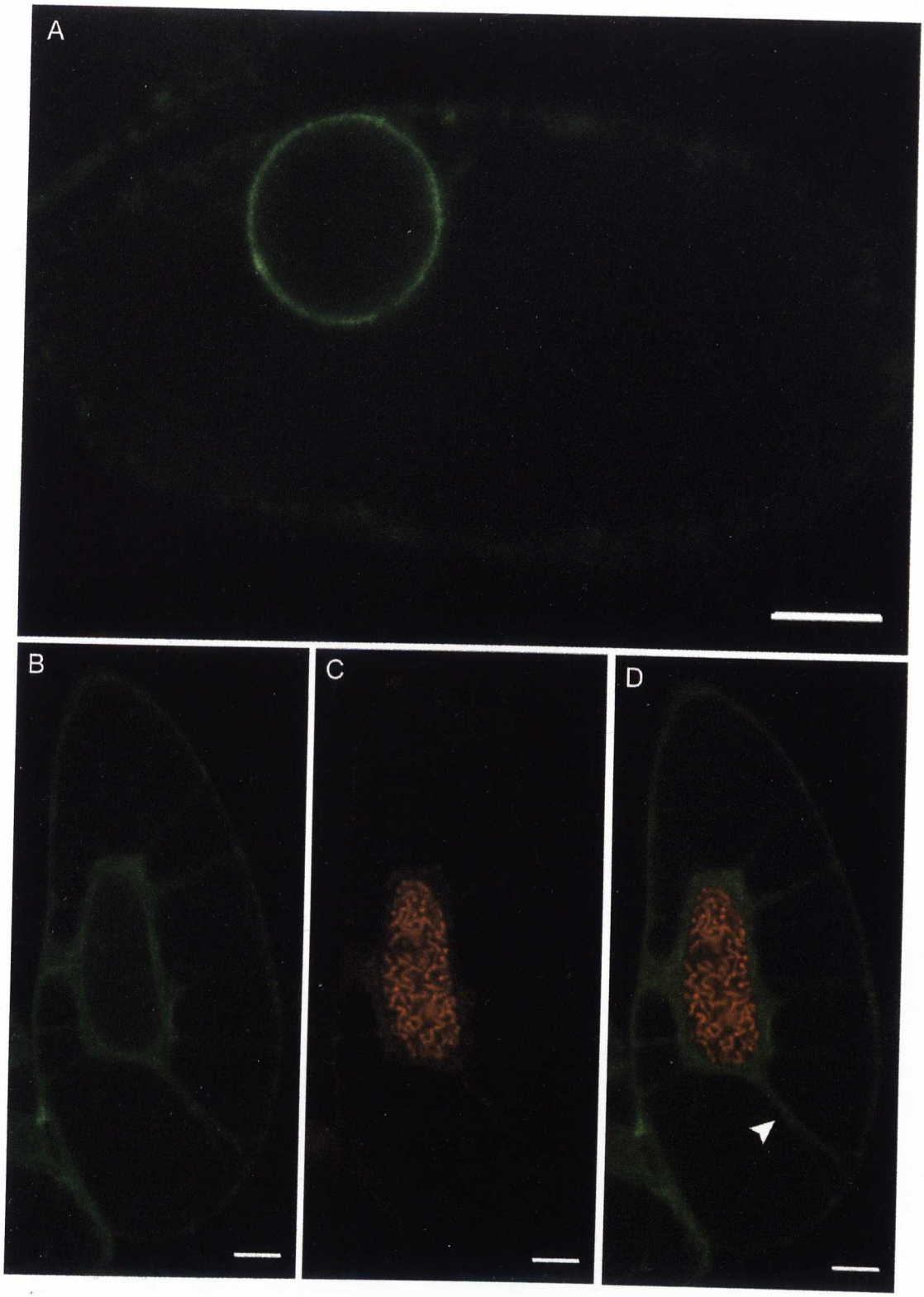
A
B
C
D

Figure 4.2 Location of fluorescence in tobacco BY-2 cells stably expressing LBR-GFP$_5$ at prometaphase and metaphase.

A. A TBY-2 cell in prometaphase expressing LBR-GFP$_5$, NE-ER tubule indicated by white arrow.

B. Metaphase in a TBY-2 cell expressing LBR-GFP$_5$, metaphase plate indicated by white arrow.

Scale bars = 10 μm.

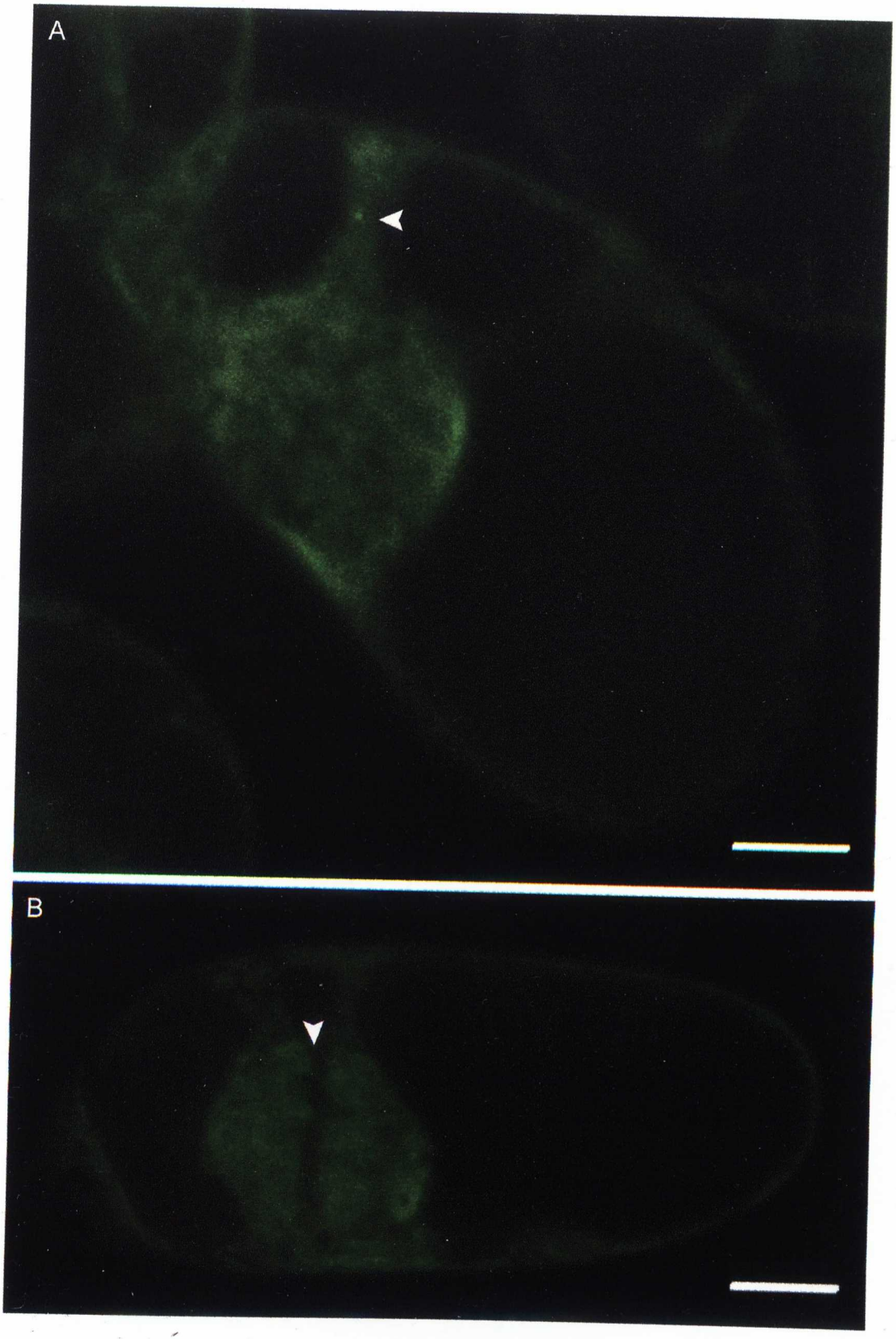
A
B

Figure 4.3 Location of fluorescence in tobacco BY-2 cells stably expressing LBR-GFP$_5$ at anaphase and telophase.

A. A TBY-2 cell in anaphase expressing LBR-GFP$_5$, tubular ER indicated by white arrow.

B. A TBY-2 cell in late anaphase expressing LBR-GFP$_5$, the forming NE is indicated by a white arrow.

C. A TBY-2 cell in telophase expressing LBR-GFP$_5$, re-formed NE indicated by white arrow.

D. A TBY-2 cell in late telophase expressing LBR-GFP$_5$, phragmoplast indicated by white arrow.

Scale bars = 10 µm.

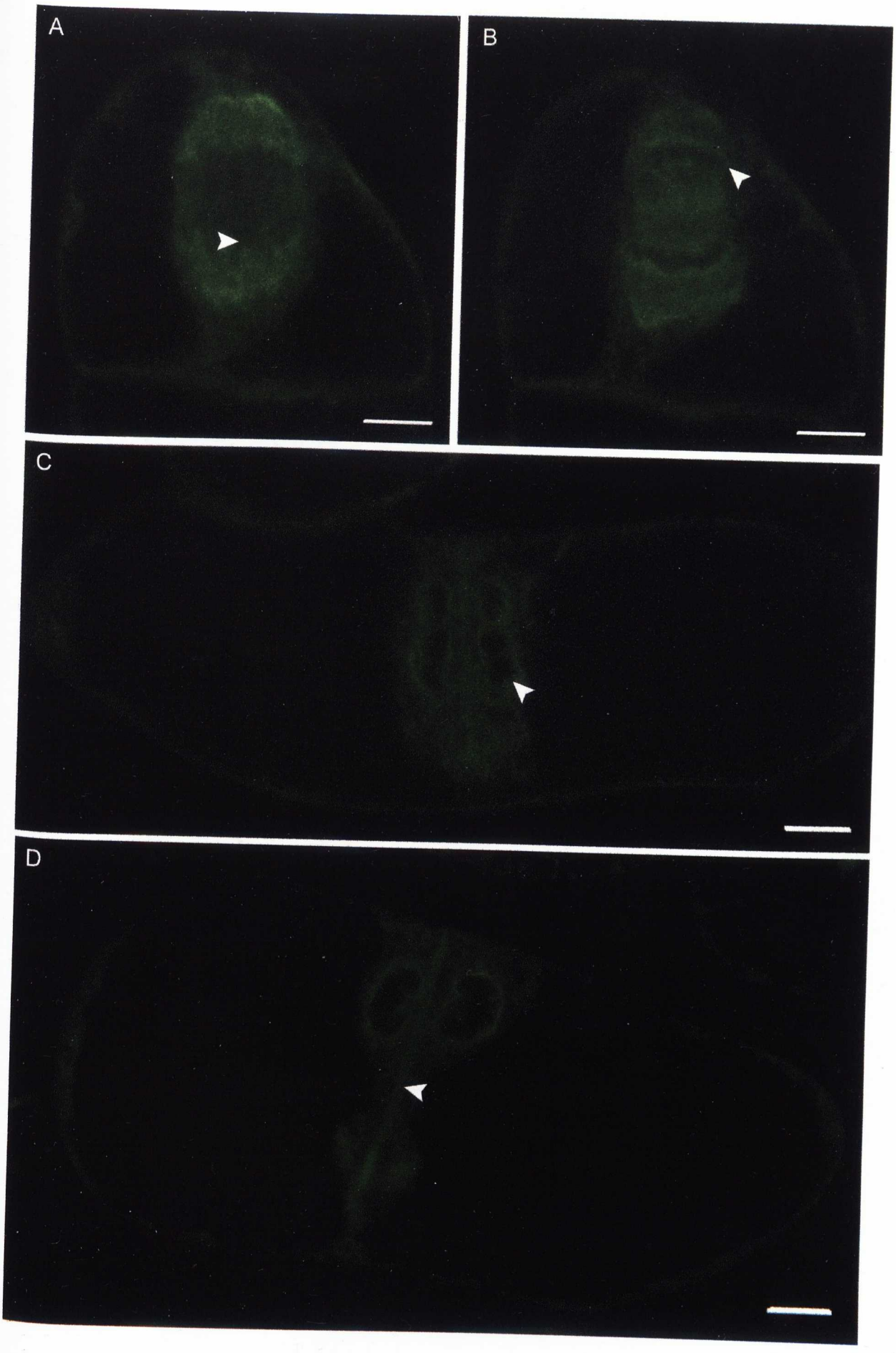
A
B
C
D

Figure 4.4 Location of LBR-GFP$_5$ fluorescence in a single cell during mitosis, from late metaphase.

Numbers refer to time, in seconds, elapsed from start of images. Cells in late metaphase expressing LBR-GFP$_5$ show fluorescence distributed through the ER membranes (time 0-1216s). Tubular membranous structures form through the mitotic apparatus (arrow, time 1274-1507s). As division progresses the membranes move towards opposite poles as the chromosomes separate (time 0-1536s). The ER membranes encircle the newly formed daughter nuclei (1624s). The NE begins to form around each nucleus (2069s). The phragmoplast (marked with empty arrow), which is the basis for the cell wall formation in dividing the cells, forms between the nuclei. It grows radially across the cell as more wall is assembled (2069-3585s).

Scale bar = 20 μm.

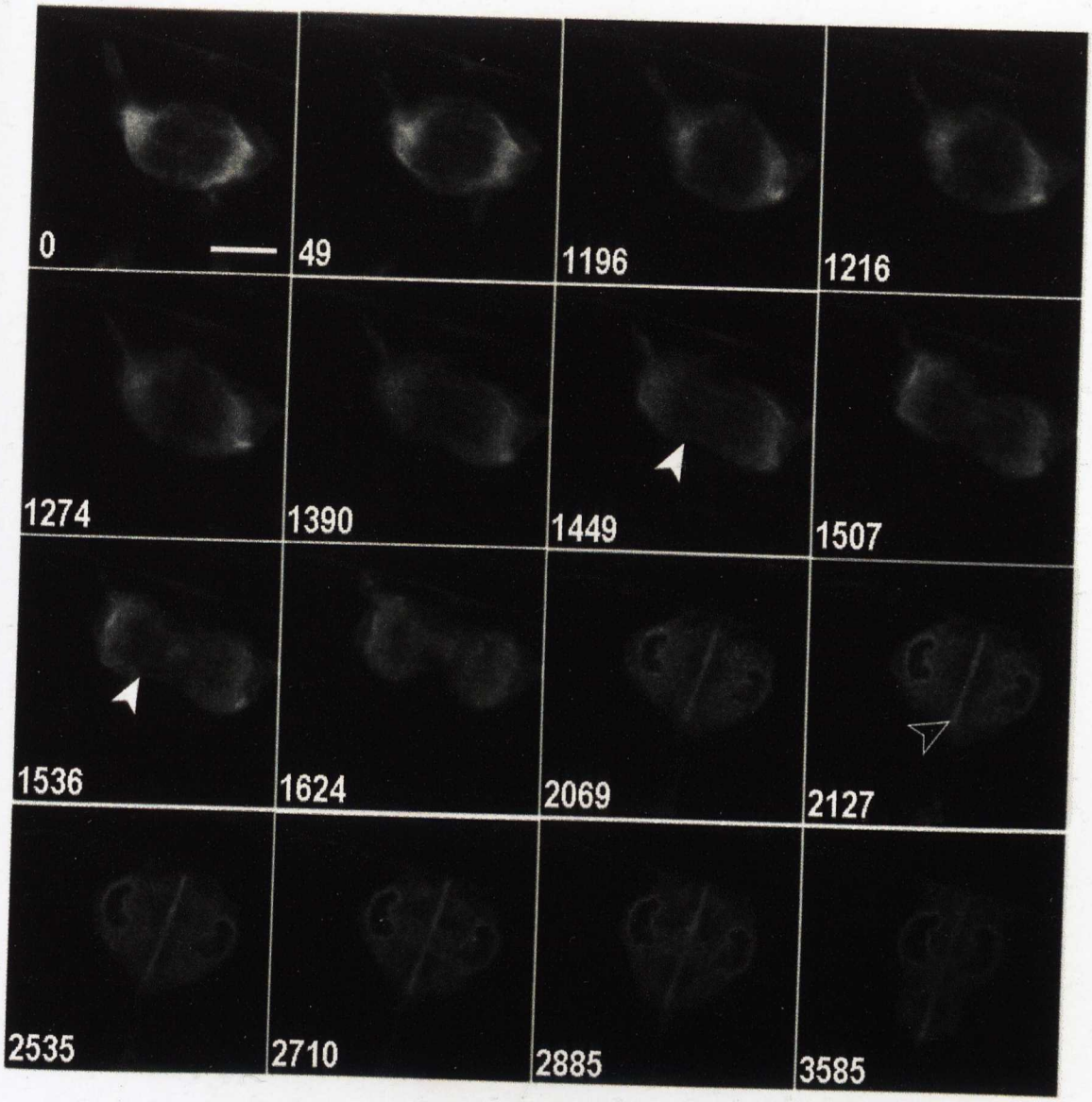
0
49
1196
1216
1274
1390
1449
1507
1536
1624
2069
2127
2535
2710
2885
3585

Figure 4.5 Fluorescence location of LBR-GFP$_5$ and spYFP-HDEL expressed in the same cell, at the nuclear envelope and cortical endoplasmic reticulum.

A. LBR-GFP$_5$ labelling at the NE in a TBY-2 cell expressing LBR-GFP$_5$ and spYFP-HDEL.

B. LBR-GFP$_5$ labelling at the ER in a TBY-2 cell expressing LBR-GFP$_5$ and spYFP-HDEL.

C. spYFP-HDEL labelling at the NE in a TBY-2 cell expressing LBR-GFP$_5$ and spYFP-HDEL.

D. spYFP-HDEL labelling at the ER in a TBY-2 cell expressing LBR-GFP$_5$ and spYFP-HDEL.

E. Merged GFP and YFP fluorescence at the NE in a TBY-2 cell expressing LBR-GFP$_5$ and spYFP-HDEL.

F. Merged GFP and YFP fluorescence at the ER in a TBY-2 cell expressing LBR-GFP$_5$ and spYFP-HDEL.

Scale bars = 10 µm.

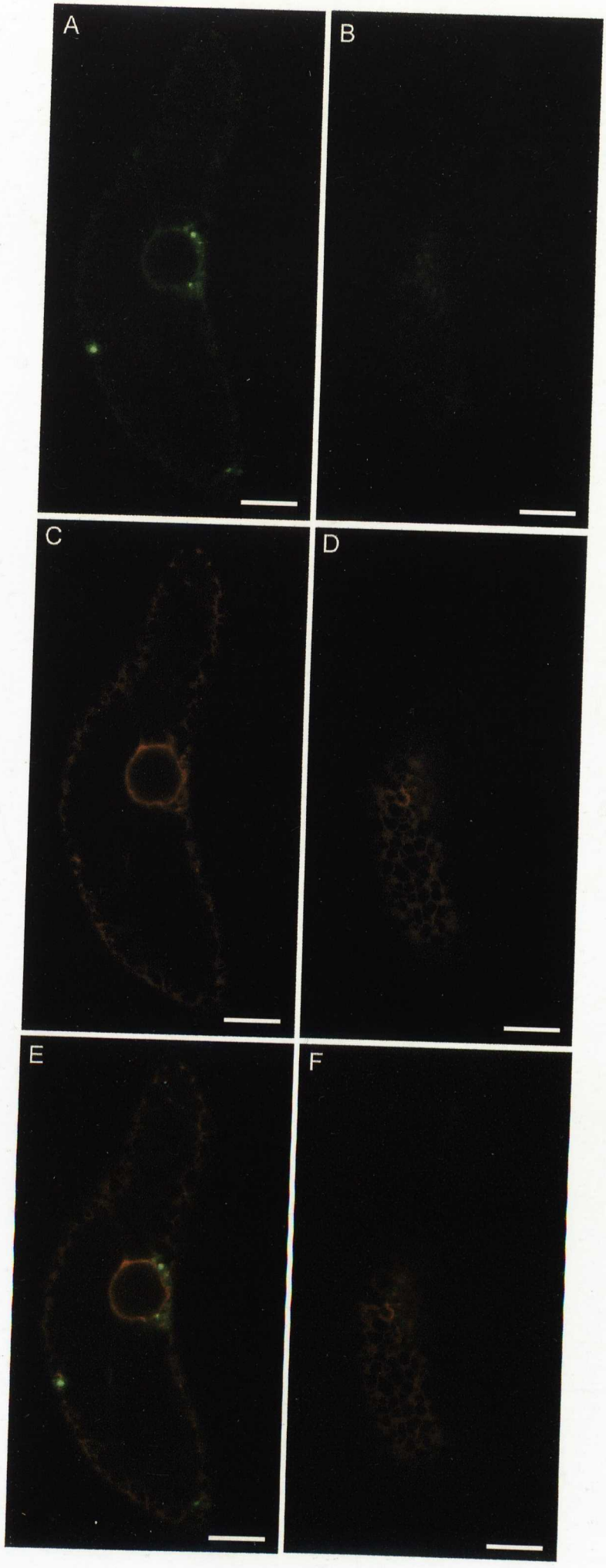
A
B
C
D
E
F

Figure 4.6 Fluorescence location of LBR-GFP$_5$ and spYFP-HDEL in tobacco BY-2 cells at different stages of mitosis.

A. LBR-GFP$_5$ labelling of the NE at interphase in a TBY-2 cell expressing LBR-GFP$_5$ and spYFP-HDEL. Arrow indicates bright punctate fluorescent structure.
B. spYFP-HDEL labelling of the NE at interphase in a TBY-2 cell expressing LBR-GFP$_5$ and spYFP-HDEL (same cell as A).
C. Merged GFP and YFP fluorescence at the NE in an interphase TBY-2 cell expressing LBR-GFP$_5$ and spYFP-HDEL (same cell as A and B).
D. LBR-GFP$_5$ labelling of the NE at prophase in a TBY-2 cell expressing LBR-GFP$_5$ and spYFP-HDEL.
E. spYFP-HDEL labelling of the NE at prophase in a TBY-2 cell expressing LBR-GFP$_5$ and spYFP-HDEL (same cell as D).
F. Merged GFP and YFP fluorescence at the NE in a prophase TBY-2 cell expressing LBR-GFP$_5$ and spYFP-HDEL (same cell as D and E).
G. LBR-GFP$_5$ labelling at metaphase in a TBY-2 cell expressing LBR-GFP$_5$ and spYFP-HDEL. Arrow indicates bright punctate fluorescent structure.
H. spYFP-HDEL labelling at metaphase in a TBY-2 cell expressing LBR-GFP$_5$ and spYFP-HDEL (same cell as G).
I. Merged GFP and YFP fluorescence in a metaphase TBY-2 cell expressing LBR-GFP$_5$ and spYFP-HDEL (same cell as G and H).
J. LBR-GFP$_5$ labelling at anaphase in a TBY-2 cell expressing LBR-GFP$_5$ and spYFP-HDEL. Arrow indicates bright punctate fluorescent structure.
K. spYFP-HDEL labelling at anaphase in a TBY-2 cell expressing LBR-GFP$_5$ and spYFP-HDEL (same cell as J).
L. Merged GFP and YFP fluorescence in an anaphase TBY-2 cell expressing LBR-GFP$_5$ and spYFP-HDEL (same cell as J and K). Arrow indicates labelling of tubular ER structures.
M. LBR-GFP$_5$ labelling at telophase in a TBY-2 cell expressing LBR-GFP$_5$ and spYFP-HDEL.
N. spYFP-HDEL labelling at telophase in a TBY-2 cell expressing LBR-GFP$_5$ and spYFP-HDEL (same cell as M).
O. Merged GFP and YFP fluorescence in a telophase TBY-2 cell expressing LBR-GFP$_5$ and spYFP-HDEL (same cell as M and O). Arrow indicates dual labelling at forming phragmoplast.

Scale bars = 10 µm.

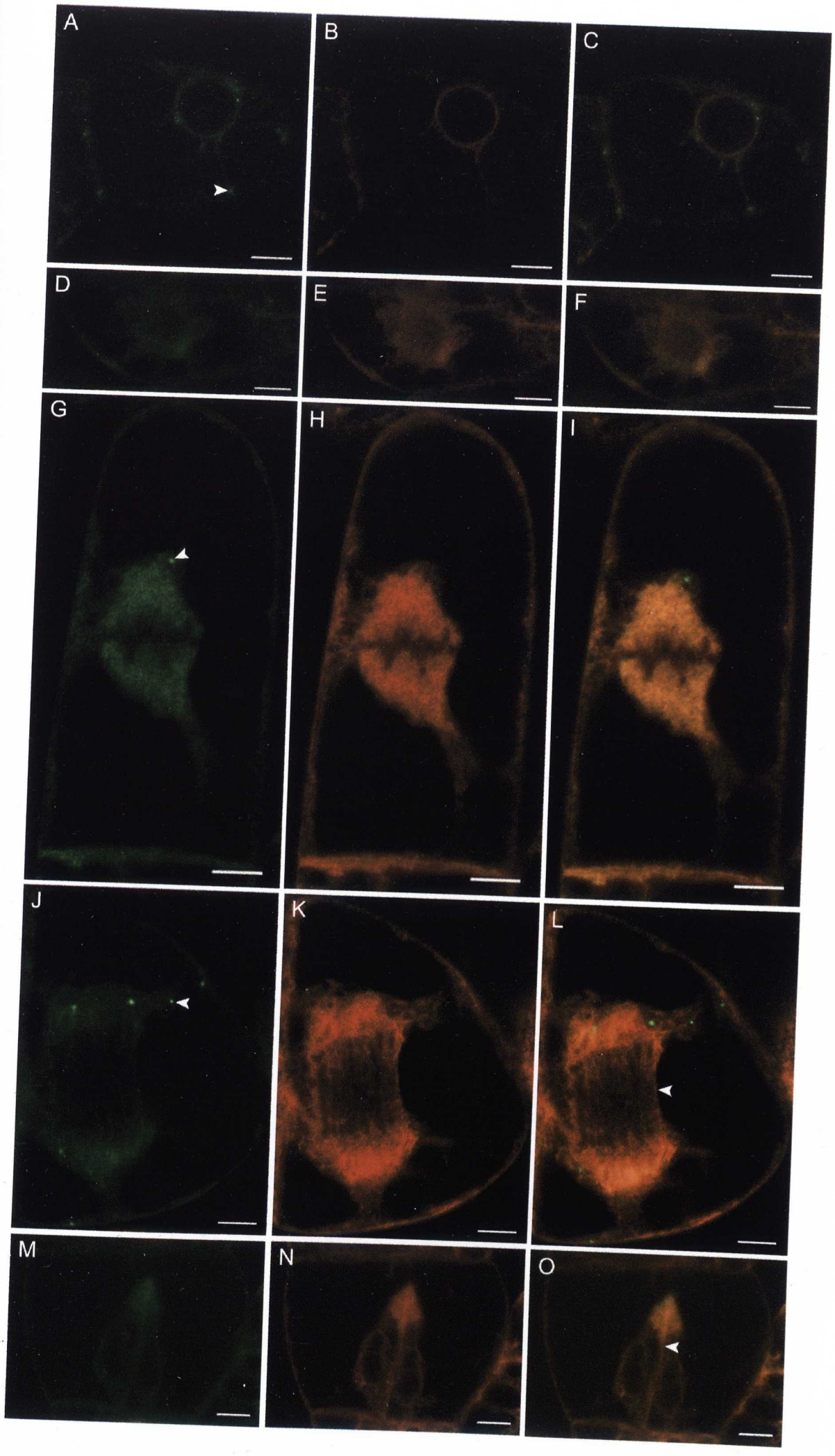
A
B
C
D
E
F
G
H
I
J
K
L
M
N
O

CHAPTER 5.

MUTATIONS IN THE LBR-GFP$_5$ PROTEIN REVEAL DETAILS OF RETENTION OF LBR AT THE PLANT NUCLEAR ENVELOPE

5. MUTATIONS IN THE LBR-GFP$_5$ PROTEIN REVEAL DETAILS OF RETENTION OF LBR AT THE PLANT NUCLEAR ENVELOPE

5.1 INTRODUCTION

As described in the introduction (1.4), at the outset of this project the lack of identified endogenous plant NE proteins led to the search for a heterologous protein marker for *in vivo* visualisation of the plant NE. In the preceding results chapters it has been shown that GFP$_5$ fused to the amino terminal domain of the mammalian LBR was an effective marker for the plant NE. This marker was employed as a tool to study the dynamics of the NE during mitosis, which had previously not been specifically labelled *in vivo*. The labelling of the plant NE with this non-native protein indicates that NE targeting and retention mechanisms may exist in plant cells.

5.1.1 Protein targeting to the nucleus

Most nuclear proteins contain nuclear localisation signals (NLSs; see Introduction 1.3.5, Hicks and Raikhel 1995) that are functional in animal, fungal and plant cells (Hicks and Raikhel 1995). The motifs are recognised by receptors that form part of the nuclear pore complex and allow transport into the nucleus. The transport of LBR may be by simple diffusion through the lateral channels of the NPC. Alternatively, the bipartite NLS in the nucleoplasmic domain of LBR may be recognised by NLS receptors and the nucleoplasmic domain transported through the nuclear pore, 'dragging' the TM domains along the pore channel membrane and into the INE as it goes (Soullam and Worman 1993). Once in the NE, proteins that reside there are proposed to be anchored in place, predominantly by binding to ligands in the nucleus

such as chromatin, chromatin associated proteins and lamins (Ye and Worman 1994, and see Holmer and Worman 2001 for a review).

5.1.2 Retention of the lamin B receptor at the nuclear envelope in animal cells

Several regions of LBR have been suggested to contribute to the anchoring of LBR at the NE in mammalian cells. These include a putative lamin binding region in the N terminal 60 amino acids (Worman *et al.* 1988, Ye and Worman 1994, Dreger *et al.* 2002), a chromatin binding region encoded in amino acids 53-88, including an RS repeat region (Ye and Worman 1994, Duband-Goulet and Courvalin 2000, Takano *et al.* 2002, 2004) and a putative HP1 association site between amino acids 88 and 211 (Ye and Worman 1996, Ye *et al.* 1997).

The binding of LBR to chromatin and proteins is linked to phosphorylation status, with protein phosphorylation leading to dissociation of the LBR from chromatin (Takano *et al.* 2002, 2004), nuclear proteins p34/p32 (Nikolakaki *et al.* 1997) and HP1 (Ye *et al.* 1997). Such phosphorylation events occur at the onset of mitosis and are likely to contribute to the breakdown of the NE at prometaphase (Burke and Ellenberg 2002, review) and may prevent premature reassembly of the NE (Nikolakaki *et al.* 1997). At the end of mitosis de-phosphorylation events occur (Courvalin *et al.* 1992). These changes, which make the LBR competent to bind chromatin, lamin B and HP1 lead to the recruitment of membrane around the daughter nuclei (Chaudhary and Courvalin 1993, Ye and Worman 1994). LBR is one of the first proteins to be found at the re-forming NE during anaphase in mammalian cells (Foisner and Gerace 1993, Chaudhary and Courvalin 1993, Haraguchi *et al.* 2000).

5.1.2.1 Lamin binding

The interactions between LBR and lamin B were first demonstrated *in vitro* during the early characterisation of the protein (Worman *et al.* 1988, Ye and Worman 1994). The association was also observed on heterologous expression of LBR in yeast (Smith and Blobel 1994). More recently, a domain-presenting expression system used to demonstrate nucleus specific interactions showed that lamin B recruited LBR (and vice versa) to vimentin bodies (aggregates formed from a temperature sensitive filament forming protein) thus indicating an *in vivo* interaction between the two proteins (Dreger *et al.* 2002). Some data have been presented which indicates that LBR does not bind lamin B, and that the lamina associates with the NE by a CAAX motif alone (Mical and Monteiro 1998). During mitosis, lamin B is thought to remain associated with membranes by interaction of the protein's C-terminal farnesyl motif with the membrane, the association of lamin B with LBR and other NE proteins may also persist through division (Meier and Georgatos 1994). Phosphorylation within parts of the RS region (see Chromatin binding section 5.1.2.2) of LBR in mitosis does not affect binding to lamin B (Nikolakaki *et al.* 1997).

Lamin sequence homologues have not been identified in the plant genomes sequenced to date (Mewes *et al.* 2002, Rose *et al.* 2004). Plant genomes do encode proteins with α helical coiled-coil motifs similar to lamins but with different peptide sequences (Gindullis *et al.* 2002, Rose *et al.* 2003). These proteins may be functionally analogous to mammalian lamins, possibly forming part of the lattice-like nuclear matrix that can be isolated from plant cells (Samaniego *et al.* 2001).

5.1.2.2 Chromatin binding

Expression and immunofluorescent detection of a truncated form of LBR, comprising amino acids 1-203 of the protein lacking a TM domain, showed uniform nucleoplasmic labelling consistent with binding to chromatin, rather than the nuclear rim staining that would occur if LBR was binding with lamin B alone (Smith and Blobel 1993, Soullam and Worman 1993). Early studies of LBR demonstrated that the protein could bind to double stranded DNA *in vitro* (Ye and Worman 1994). More recently the RS motif (shown in red, Figure 5.1) within the protein has been shown to bind chromatin in biochemical studies (Takano *et al.* 2002, 2004). Serines in the RS region (Ser^{76}, Ser^{78}, Ser^{80}, Ser^{82}, Ser^{84}) are phosphorylated by a serine/arginine kinase, whilst an upstream Ser^{71} is phosphorylated by $p34^{cdc2}$ kinase, an important kinase in mitotic events (Nikolakaki *et al.* 1997). The phosphorylation is likely to modulate the interactions of LBR with other proteins e.g. p34/32, the effect on chromatin binding remains unresolved (Nikolakaki *et al.* 1997). Some evidence suggests that phosphorylation of Ser^{71} contributes to dissociation of LBR and chromatin (Takano *et al.* 2002).

The N-terminal domain of LBR also contains Ser/Thr-Pro-X-X motifs (example highlighted in green in Figure 5.1) which are involved in DNA binding (Worman *et al.* 1990, Smith and Blobel 1993), and are found in histones and proteins involved in gene regulation (Suzuki 1989).

5.1.2.3 Heterochromatin protein 1

Heterochromatin protein 1 (HP1) is part of a family of gene regulators. The protein has been shown to associate with transcriptional regulators and proteins involved in

chromatin remodelling (Kourmouli *et al.* 2001) as well as LBR (Ye and Worman 1996, Ye *et al.* 1997). During mitosis, phosphorylation of threonine residue 68 of LBR by $p34^{cdc2}$ protein kinase, upstream of RS region may disrupt HP1 binding (Ye *et al.* 1997). HP1 interaction with LBR is thought to occur in the globular protein domain, between amino acids 88 and 211 (Ye *et al.* 1997, Takano *et al.* 2002). A role has been suggested for HP1 and LBR interaction in membrane targeting to chromatin at the end of mitosis (Buendia and Courvalin 1997).

An *in vitro* binding assay showed that LBR preferentially associates with histones H3/H4 leading to the proposal that binding of LBR to HP1 was indirect via these histones (Polioudaki *et al.* 2001). In plant cells expressing human HP1γ fused to GFP, HP1γ was located in discrete domains in interphase nuclei and in the cytoplasm during mitosis (Fass *et al.* 2002). *In vitro* HP1γ was shown to bind to plant histone H3 prepared from tobacco cells (Fass *et al.* 2002). Homologues of HP1 are present in plants, mutations in this gene result in altered plant development - possibly as a result of its role in gene regulation (Gaudin *et al.* 2001).

5.1.2.4 Other nuclear envelope targeting determinants

At a fundamental physical barrier level, nucleoplasmic domain size effects NE location with proteins of ~45kD size able to freely enter the nucleus, whilst domains of ~67kD and above are excluded (Soullam and Worman 1995). Full length LBR is 56kD and as such falls below the exclusion size.

It has been suggested that LBR may be retained within the INE by homodimerisation of TM domains, thereby forming complexes that are too large to diffuse through the

lateral nuclear pore channels and preventing the exit of the protein from the INE by way of complex size (Smith and Blobel 1993).

Trans-membrane domain length is also implicated in protein targeting to the NE, although not in retention (Smith and Blobel 1993, Soullam and Worman 1993). TM domain length has been shown to have a role in protein targeting to parts of the plant endomembrane system, though not specifically the NE (Brandizzi *et al.* 2002a).

5.1.3 Aims

The identification of possible factors that contribute to the labelling of the NE by LBR was addressed by the production of a range of LBR-GFP_5 fusions. These contained mutations or deletions in regions that are involved in the retention of the protein in animal cells in order to identify binding regions holding the protein at the plant NE.

5.2 RESULTS

5.2.1 Deletion of the lamin binding domain of LBR

The first 60 amino acids of LBR were removed from the LBR-GFP_5 fusion by PCR directed truncation, using oligonucleotides SI17 and SI37 with an annealing temperature of 50°C and an elongation time of 1 min 18 seconds. The truncated fusion was cloned into binary vector pVKH18En6 in *Bam*HI/*Sac*I sites (see Appendix 5. Construct referred to henceforth as Δ1-60LBR-GFP_5). The pVKH18En6 Δ1-60LBR-GFP_5 vector was used to transform *A. tumefaciens*, which were used to transiently transform tobacco leaf epidermal cells by pressure infiltration (see Materials and Methods). Cells were imaged three days after infiltration using an

inverted Zeiss LSM 510 confocal laser scanning microscope. Preparation of samples for imaging is described in Materials and Methods 2.2.4.

5.2.2 Location of lamin binding deletion mutant

On observation of transiently expressed Δ1-60LBR-GFP_5 in tobacco leaf epidermal cells a range of subcellular distribution was observed. Some cells showed NE labelling similar to wild type, and in many cases the NE was slightly distended (marked with arrow; Figure 5.2A, also C). Clear ER labelling was observed in these cells (Figure 5.2B and D). The NE lumen appeared enlarged in some cells (Figure 5.2C) with the ER showing a normal labelling (Figure 5.2D). Nucleoplasmic labelling was observed in a significant subset of transformed cells (Figure 5.2E and G). In cells where nucleoplasmic labelling was observed, clear ER labelling was also apparent (Figure 5.2F), in some instances the cortical ER showed altered morphology with MT-like labelling (Figure 5.2G and H). Some punctate fluorescent mobile structures were also seen in a number of cells (marked with arrow, Figure 5.2H).

5.2.3 Production of RS mutants

The RS region mutations were designed to impair phosphorylation of the serines within the RS motif; these residues have been shown to play a role in chromatin association (see section 5.1). To achieve this, a set of point mutations were introduced by PCR directed mutagenesis to replace the serines (polar amino acid) with alanines (a small non-polar amino acid). The LBR wild type RS motif and mutated sequence (mutated bases and amino acids highlighted in red) for each of the point mutations are shown in Figure 5.3.

The mutations were incorporated into a set of oligonucleotide primers (named PM1-8; see Materials and Methods 2.2.1.1) which were used in a three-step overlapping PCR procedure to produce a single nucleotide change. Primer pairs PM 1 and 2 (S80A), 3 and 4 (S82A), 5 and 6 (S84A), 7 and 8 (S86A) were used to produce single point mutation with primers for the original LBR-GFP_5 sequence (SI16 and SI17 Materials and Methods 2.2.1.1, also see Figure 5.4 for details of overlapping PCR). The mutated LBR-GFP_5 fusions were ligated in to the *Bam*HI/*Sac*I site of pVKH18En6 and used to transform *Agrobacterium* and tobacco as the Δ1-60LBR-GFP_5 mutant (see start of results section, Chapter 2 section 2.2.2 and Appendix 5).

5.2.4 Localisation of RS mutants: S80A

LBR-GFP_5 with a single S80A point mutation was found to localise in the NE and ER of some cells (Figure 5.5A and B). In 71% of cells (n = 89) expressing the construct, highly fluorescent inclusions within the nucleus were observed (Figure 5.5C and F). On staining of DNA with ethidium bromide (shown in red; Figure 5.5D and G) the fluorescent structures excluded chromatin as indicated by a lack of ethidium bromide labelling in regions where GFP fluorescence was apparent (marked with arrow, Figure 5.5D and G). When the GFP and ethidium bromide images are merged chromatin was clearly seen within the fluorescent structures (Figure 5.5E and H). Stacked images taken through nuclei with inclusions showed that some of the structures were tube-like, going completely through the nucleus or contained within the nucleoplasm (Figure 5.6), whilst others showed a punctate morphology, and all were immobile within the nucleus (but the nuclei were moving as usual). Preliminary FRAP data indicated the inclusions did not show recovery after photobleaching (Figure 5.7).

Ultrastructural observation by electron microscopy of cells expressing the S80A mutated protein showed that the inclusions were formed by multiple membrane layers (Figure 5.8A-E). The structures observed enclosed chromatin (marked with arrows, Figure 5.8B and C). Membrane invaginations traversing the nuclei in cells expressing the mutated protein were also observed (Figure 5.8F and G).

A variety of *Agrobacterium* infiltration concentrations were used to see if the appearance of the inclusions was dosage dependent. Inclusions appeared with similar frequency at each concentration (from 0.01OD to 0.5) and resulted in no appreciable change in expression or transformation level.

5.2.5 Localisation of RS mutants: S82A

Tobacco leaf epidermal cells expressing LBR-GFP_5 with a S82A point mutation showed fluorescence distributed at the NE (Figure 5.9A and C) and within the ER (Figure 5.9B and D). This is similar to the non-mutated wild-type protein location. In some cells nucleoplasmic labelling (Figure 5.9E) and tubular cortical ER (Figure 5.9F) was seen. Nuclear inclusions were not observed in cells expressing this mutant protein.

5.2.6 Localisation of RS mutants: S84A and S86A

Expression levels of LBR-GFP_5 fusion proteins with mutations at S84A or S86A were very low with only a few cells showing observable fluorescence. Cells transformed with LBR-GFP_5 S84A mutant protein showed weak NE labelling (Figure 5.10A, NE marked with arrow). No discernible ER labelling was observed, but in some instances small mobile punctate structures were observed (Figure 5.10B,

punctate structure marked with arrow). Cells expressing LBR-GFP$_5$ S86A mutant protein showed WT LBR-GFP$_5$-like NE and ER labelling (Figure 5.10C and D respectively). A variety of infiltration concentrations were used to increase labelling, but resulted in no appreciable change in expression or transformation level.

5.3 DISCUSSION

The incorporation of a range of amino acid changes in the LBR-GFP$_5$ protein and subsequent localisation of the proteins *in vivo* has provided information on the nature of protein retention at the plant NE, and possibly protein over-expression in plant cells. A summary of the mutant protein locations is included in Table 5.1.

Table 5.1 Summary of LBR-GFP$_5$ mutant location.

Mutant	*Putative binding region*	*Location/effect*
Δ1-60LBR-GFP$_5$	Lamin binding region	Nucleoplasmic labelling, altered cortical ER morphology
S80A	Chromatin binding region	Nuclear inclusions and NE labelling
S82A	Chromatin binding region	WT-like NE labelling
S84A	Chromatin binding region	Low expression, WT-like NE labelling, some small punctate structures
S86A	Chromatin binding region	Low expression, WT-like NE labelling

5.3.1 Lamin binding domain deletion Δ1-60LBR-GFP$_5$

Cells expressing the lamin binding domain deletion Δ1-60LBR-GFP$_5$ mutant showed two locations. A subset of cells exhibited WT LBR-GFP$_5$-like NE labelling,

with apparent distension of the NE lumen in many cells (Figure 5.2). This enlargement of the NE may be a result of protein over-expression and such enlargement has been observed in the ER of cells over-expressing an unlabelled protein (Crofts *et al.* 1999). A significant number of cells showed labelling of the nucleoplasm as well as the NE.

Nucleoplasmic labelling has been observed in cells where the ERAD (ER associated degradation) pathway is active (Brandizzi *et al.* 2003). The possibility of ERAD activity is supported by the presence of ER labelling, which in ERAD is due to association of the over-expressed protein with BiP (Brandizzi *et al.* 2003). The labelling may also be due to proteasome activity. Proteasomes break down misfolded, ubiquitinated proteins. In plant cells they have been located at the nuclear rim and within the cytoplasm (Yanagawa *et al.* 2002). Whether the labelling is due to ERAD or proteasomal activity the different labelling is likely to be due to protein degradation as a result of protein over-expression or misfolding as a result of the truncation. The labelling may be a result of altered location due to the truncation, however the presence of a subset of cells in which WT labelling is seen may contradict this idea.

The ER tubule structure formation may be a form of stress reaction to over-expression of the protein. The tubular pattern may also be a cellular change associated with the cell ceasing to function correctly possibly preceding cell death or necrosis. Structural changes symptomatic of apoptosis include disappearance of the nuclear condensation and plasma membrane blebbing (Greenberg 1996), changes in ER formation are not indicated in the literature.

The punctate structures observed in the cytoplasm of cells showing fluorescence of the tubular ER were not as large as Golgi bodies, and attempts at dual labelling provided little clarification as the detection channel for GFP had a large signal to noise ratio that made the small punctate structures difficult to identify. The structures may be vesicles transporting protein to the nucleoplasm, vacuole or other destination for degradation.

5.3.2 Mutation in the chromatin binding region of LBR: S80A

The nuclear inclusions observed in a significant subset of cells expressing S80A bear striking similarity to tubular nuclear bodies observed in mammalian cells over-expressing the nuclear pore protein POM121 (Söderqvist *et al.* 1996). The POM121 structures were proposed to be a result of protein over-expression. Over-expression of LBR-EGFP in mammalian cells also showed changes in NE structure, with invaginations extending into the nucleoplasm (Ellenberg *et al.* 1997). Hence the structures seen in cells expressing the S80A mutant protein may be a result of protein over-expression. The formation of the inclusions within the nucleus may be a method of sequestering excess membrane protein in order to prevent accumulation elsewhere in the cell. The presence of the membrane structures within the nucleus and the subset of transformed cells showing WT labelling suggests that NE targeting and retention is still occuring with the S80A point mutation. If the protein's chromatin binding ability was perturbed this would be likely to manifest itself in a lack of association with the NE, effectively turning the protein into an ER membrane protein. However the formation of inclusions within the nuclei would suggest that the protein reaches its NE destination, with the over-expression leading to the expansion of INE surface area to cope with the excess protein. The constraint of the size of the

nucleus would force the extra membrane to form compact structures such as the observed membrane stacks, to minimise cellular disruption of nuclear contents. As the inclusions were only observed in cells expressing the S80A mutant protein it is possible that the amino acid change alters the protein's interactions, maybe increasing its ability to bind substrate, hence the increase in NE area within the inclusions. However this does not account for the close membrane stacks, with no substrate in between the layers. Possibly the protein self-associates, which may explain these stacks. When nuclear inclusions were photobleached they did not show recovery of fluorescence (Figure 5.7). This may indicate a lack of membrane continuity between the NE and the inclusions, thus preventing exchange of bleached and fluorescent protein. Alternatively the membrane stack arrangement may impair protein movement, preventing recovery of fluorescence.

The nuclear inclusions observed on expression of the S80A mutant bear some resemblance to images captured by light micrscopy of aggresomes in mammalian cells. Aggresomes are aggregates of misfolded ubiquitinated proteins, which are thought to form when the proteasome is saturated with proteins destined for degradation (Johnston *et al.* 1998), their presence has not been reported in plant cells. These aggregates are usually juxta-nuclear and are associated with MTOCs, with MT mediated transport of proteins to the structure (Johnston *et al.* 1998, García-Mata *et al.* 1999). As aggresomes have been shown to form as a result of protein over-expression their formation in plant cells could theoretically occur. Plant cells are generally acentriolar, with the surface of the nucleus acting as a site for MT nucleation (although nucleation also occurs at the cell cortex). The association of aggresomes with MTOCs would mean that such an aggregate in a plant cell could

occur anywhere, but is likely to be membrane-adjacent as the complexes that form nucleation sites assemble on membranes. The ultrastructural composition of the S80A inclusions, consisting of structures formed from multiple membrane layers, sometimes encircling chromatin, bears no similarity to the ultrastructure of aggresomes, which consist of a protein mass surrounded by a MT cage, with a few vesicles as the only membrane present.

A range of *Agrobacterium* infiltration concentrations were used to determine if the appearance of inclusions was dosage dependent. The inclusions appeared with similar frequency at each concentration. As such this may suggest that the inclusions are the result of a property of the mutant protein. In addition, use of the same concentration range for the WT and other mutant proteins did not give rise to inclusions, even at the highest concentration level.

5.3.3 Mutation in the chromatin binding region of LBR: S82A

The incorporation of the S82A point mutation resulted in no obvious change in labelling from the WT protein. This result suggests that S82 does not seem to be crucial for retention of LBR at the plant NE, as altering this amino acid has no effect on location of the protein. Nucleoplasmic labelling observed in a small number of cells may be due to protein over-expression (as discussed in lamin binding deletion section 5.3.1).

5.3.4 Mutation in the chromatin binding region of LBR: S84A and S86A

The lack of discernible fluorescence with mutants S84A and S86A, even at high infiltration concentration levels may indicate that these serine residues are crucial for

LBR targeting and retention at the NE as altering these amino acids dramatically alters fluorescence levels. In the few cells that did show labelling a weak signal was observed at the NE. Possibly the alteration these amino acids act as a signal to increase breakdown of the proteins, explaining why minimal fluorescence is observed even at high concentrations of infiltration. The punctate structures observed in cells expressing S84A (Figure 5.10) may be vesicles transporting protein for degradation. The mutations could alter the folding of the protein leading to a decrease in fluorescence, maybe causing the LBR protein to associate with the GFP preventing correct formation of the fluorophore.

5.3.5 Other factors that may contribute to LBR targeting and retention at the plant nuclear envelope

In mammalian cells and *in vitro* assays, binding of LBR to HP1 has been demonstrated. Plants contain HP1 homologues (Gaudin *et al.* 2001), so the association of LBR and HP1-like proteins may contribute to anchoring of LBR at the plant NE. Disruption or deletion of the proposed HP1 binding region would be a valuable future avenue of investigation for factors that play a part in LBR binding. There are reports of LBR interacting with histones 3/4 (Polioudaki *et al.* 2001), as such histones could act as a binding site for LBR in plant cells. TM domain length has been shown to play a role in protein targetting at later stages of the endomembrane system in plants (Brandizzi *et al.* 2002a) and has been linked to LBR targeting to the NE in animal cells. Therefore TM domain size may be a contributing factor to LBR retention at the plant NE.

It is apparent from published research that retention of LBR at the NE is due to a variety of interactions (chromatin; Pyrpasopoulou *et al.* 1996; Lamin B; Ye and Worman 1994, Dreger *et al.* 2002; HP1; Ye *et al.* 1997). Introducing single mutations may not significantly effect retention as other binding mechanisms could be sufficient to retain the protein at the NE. If this is the case however, it suggests that the LBR in plants is retained by at least two interactions, suggesting a high degree of conservation of binding mechanisms. This is all the more interesting given the absence of lamin and LBR homologues in plants.

In summary, mutations were introduced into the LBR-GFP_5 construct in order to gain information on the factors that function to target and retain the protein at the plant NE. Deletion of the protein's lamin binding region produced a combination of WT location and others showing clear nucleoplasmic labelling, with some changes in ER morphology. The altered location maybe due to protein over-expression leading to degradation, as the ERAD pathway shows nucleoplasmic labelling. Point mutations incorporated into the RS region of the protein produced a range of fluorescence locations. S80A produced nuclear inclusions, such structures have been observed in mammalian cells and have been ascribed as a strategy to cope with protein over-expression. WT-like labelling was also seen in a subset of S80A cells, hence the amino acid doesn't appear to be crucial for the LBR retention at the NE. S82A gave only WT-like NE labelling, as such this amino acid doesn't seem to affect the protein's retention. Mutations S84A and S86A showed very weak labelling, this absence may be due to changes in retention as a result of the amino acid alterations.

Figure 5.1 Amino acid sequence of LBR chromatin binding region.

68			71							78	80		82		84		86	
T	S	S	**S**	**P**	**S**	**R**	R	R	G	**S**	**R**	**S**	**R**	**S**	**R**	**S**	**R**	**S**

Figure 5.2 Location of fluorescence of Δ1-60LBR-GFP$_5$ lamin binding domain deletion mutant.

A. Multiple cells expressing Δ1-60LBR-GFP$_5$ lamin binding deletion mutant, located at NE (marked by white arrow).

B. Same cells as A, view of cell cortex.

C. Single cell expressing Δ1-60LBR-GFP$_5$ lamin binding deletion mutant.

D. Same cell and C, view of cell cortex showing ER labelling.

E. Multiple cells expressing Δ1-60LBR-GFP$_5$ lamin binding deletion mutant showing nucleoplasmic labelling.

F. Same cells as E, view of cell cortex showing tubule-like ER.

G. Single cell expressing Δ1-60LBR-GFP$_5$ lamin binding deletion mutant showing nucleoplasmic labelling.

H. Same cell as G, view of cell cortex showing tubule-like ER labelling. Punctate mobile structure marked by arrow.

Scale bars = A, B, E, F 20 μm, C, D, G, H 10 μm.

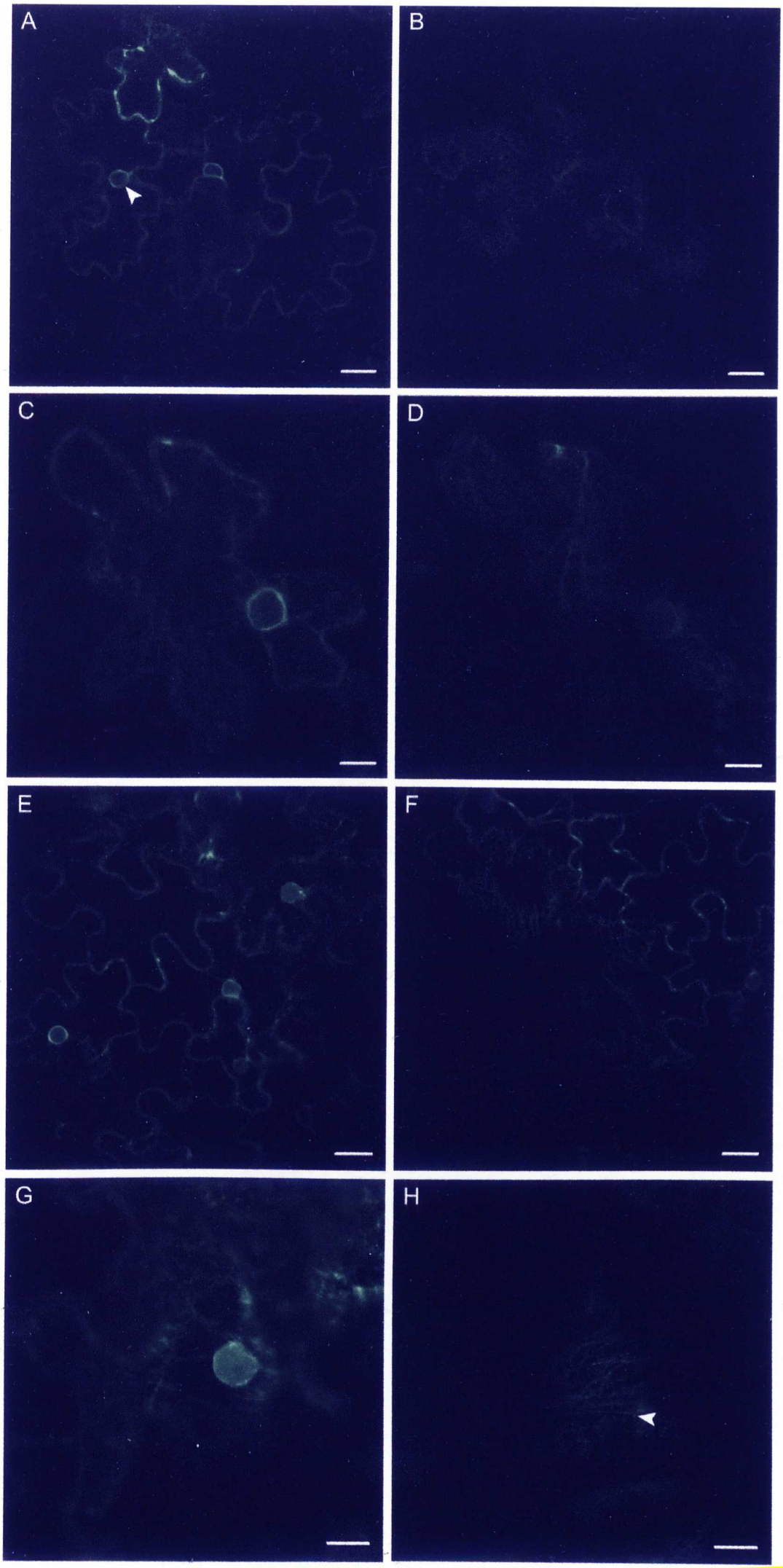
A
B
C
D
E
F
G
H

Figure 5.3 Amino acid (*a.a.*) and nucleotide (*nt*) sequences of the wild type RS motif of LBR and directed point mutations (nucleotides altered to produce amino acid change and mutated amino acids, highlighted in red).

a.a. no.		78		80		82		84		86
WT	*a.a.*	S	R	S	R	S	R	S	R	S
	nt	agt	cga	tca	agg	tca	cgc	tcc	cga	tcc
S80A	*a.a.*	S	R	**A**	R	S	R	S	R	S
	nt	agt	cga	gca	agg	tca	cgc	tcc	cga	tcc
S82A	*a.a.*	S	R	S	R	**A**	R	S	R	S
	nt	agt	cga	tca	agg	gca	cgc	tcc	cga	tcc
S84A	*a.a.*	S	R	S	R	S	R	**A**	R	S
	nt	agt	cga	tca	agg	tca	cgc	gcc	cga	tcc
S86A	*a.a.*	S	R	S	R	S	R	S	R	**A**
	nt	agt	cga	tca	agg	tca	cgc	tcc	cga	gcc

Figure 5.4 Schematic representation of overlapping PCR used to produce the RS mutants.

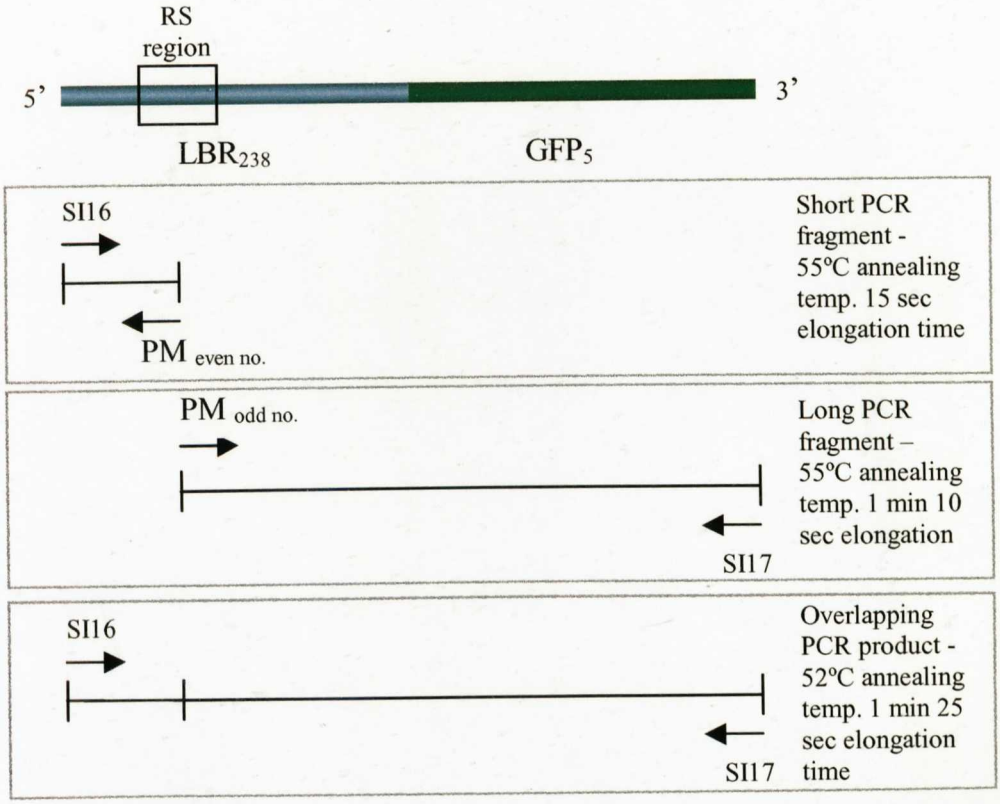
RS
region
5'
3'
LBR238
GFP5
SI16
PM even no.
Short PCR fragment - 55°C annealing temp. 15 sec elongation time
PM odd no.
SI17
Long PCR fragment – 55°C annealing temp. 1 min 10 sec elongation
SI16
SI17
Overlapping PCR product - 52°C annealing temp. 1 min 25 sec elongation time

Figure 5.5 Transient expression of the LBR-GFP_5 S80A mutant protein in tobacco leaf epidermal cells.

A. Multiple cells expressing LBR-GFP_5 S80A mutant protein. Cells contain brightly fluorescent nuclear inclusions and WT-like NE labelling (marked with white arrow).

B. WT-like NE labelling with LBR-GFP_5 S80A mutant protein.

C. LBR-GFP_5 S80A mutant protein labelled nuclear inclusions.

D. Same cell as C, stained with ethidium bromide. Chromatin enclosed within fluorescent structure marked with white arrow.

E. Same cell as C/D, merged GFP and ethidium bromide labelling.

F. LBR-GFP_5 S80A mutant protein labelled nuclear inclusions.

G. Same cell as F, stained with ethidium bromide. Chromatin enclosed within fluorescent structure marked with white arrow.

H. Same cell as F/G, merged GFP and ethidium bromide labelling.

Scale bars = A 20 µm, B 10 µm, C-H 2 µm.

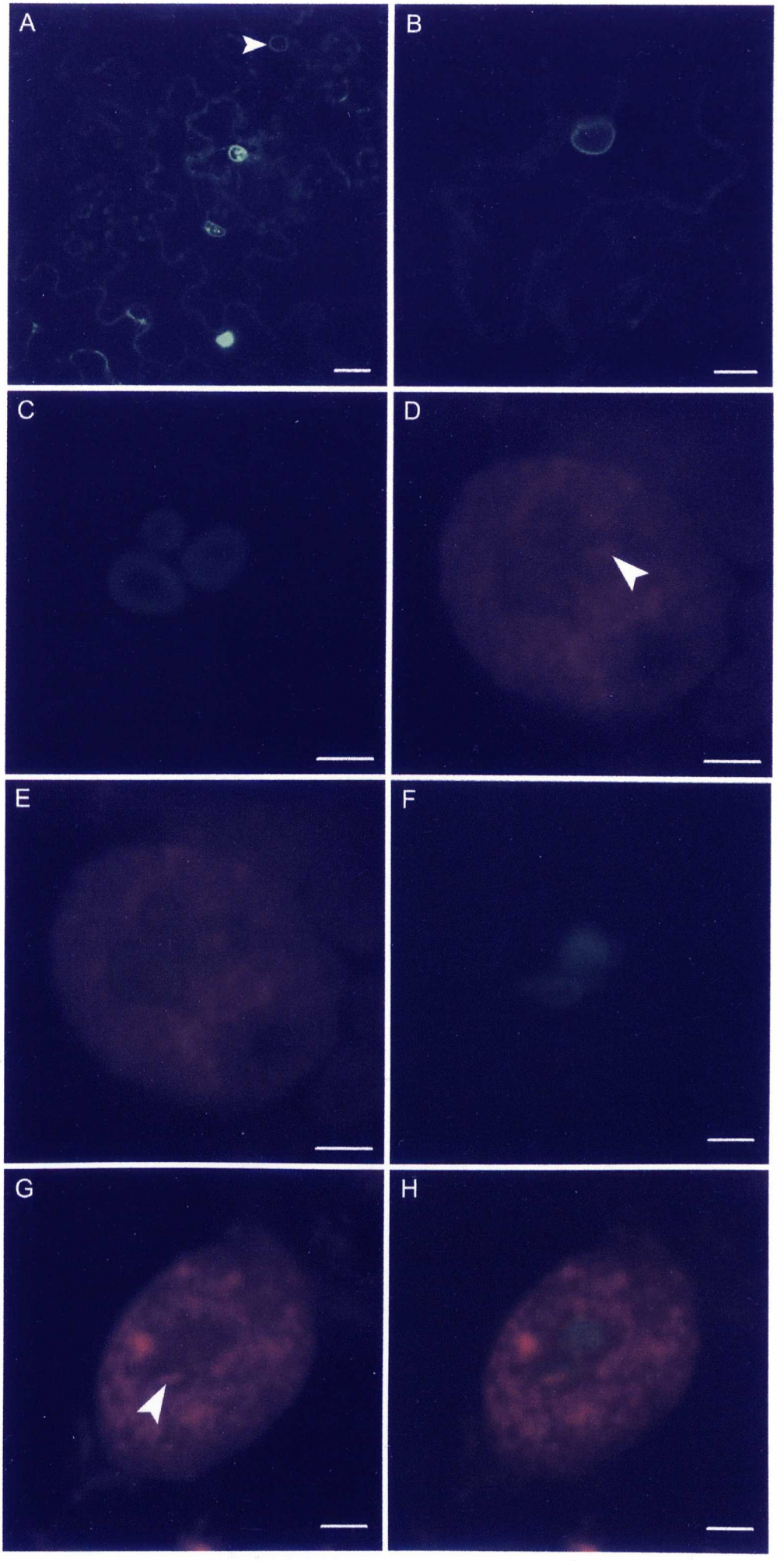
A
B
C
D
E
F
G
H

Figure 5.6 Reconstructed Z-stack of nuclear inclusions in a nucleus transiently expressing the LBR-GFP$_5$ S80A mutant protein in tobacco leaf epidermal cells.

A. Single cell expressing LBR-GFP$_5$ S80A mutant protein, with brightly fluorescent nuclear inclusions

B. Z-stack reconstruction of nucleus in A, showing tubular structure of the inclusions.

Scale bars = 5 µm.

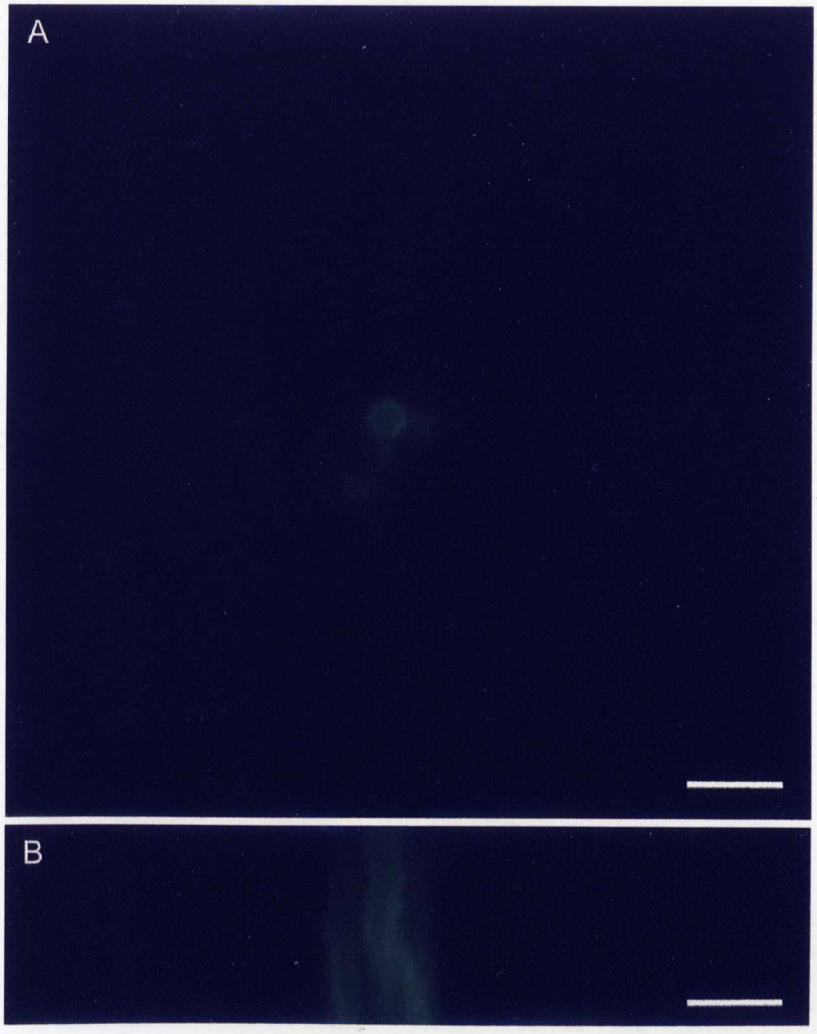
A
B

Figure 5.7 Fluorescence recovery after photobleaching of nuclear inclusions LBR-GFP$_5$ S80A mutant protein.

Graph showing fluorescence recovery after photobleaching of a LBR-GFP$_5$ S80A mutant protein labelled nuclear inclusion in transiently transformed tobacco leaf epidermal cell (green line). Fluorescence of an unbleached inclusion (red line).

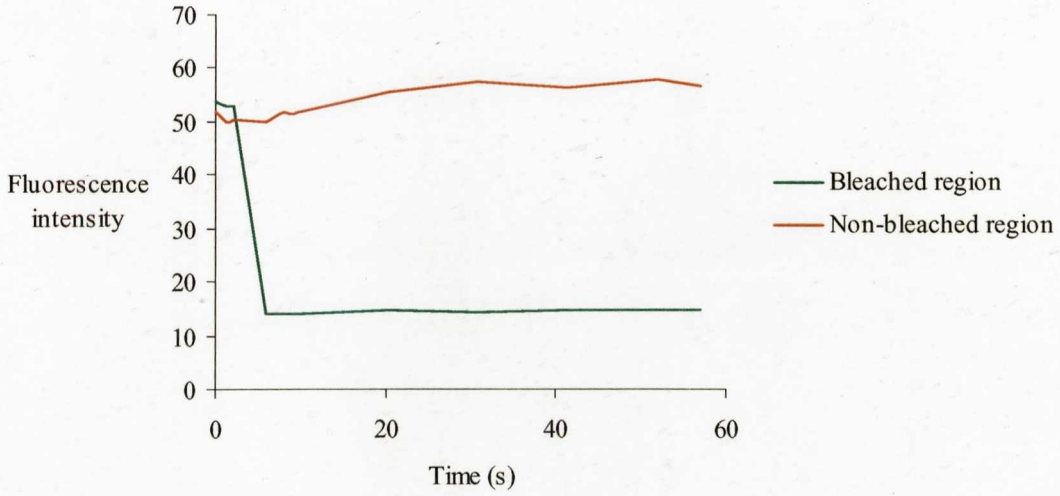
70
60
50
40
30
20
10
0
Fluorescence intensity
0
20
40
60
Time (s)
Bleached region
Non-bleached region

Figure 5.8 Electron micrographs of ultrastructural features of LBR-GFP_5 S80A mutant protein transiently expressed in tobacco leaf epidermal cells.

A. Nucleus expressing LBR-GFP_5 S80A mutant protein with nuclear inclusions.

B. Higher magnification image of inclusion marked with cross in image A, the structure encloses chromatin (marked with arrow).

C. Higher magnification image of inclusion marked with star in image A, the structure encloses chromatin (marked with arrow).

D. Higher magnification image of C, showing membrane layers.

E. Higher magnification image of B, showing membrane layers.

F. Nucleus expressing LBR-GFP_5 S80A mutant protein with invagination of NE.

G. Higher magnification image of F.

Scale bars = A, F 1 μm; B, G 200 nm; C 400 nm; D 50 nm; E 100 nm.

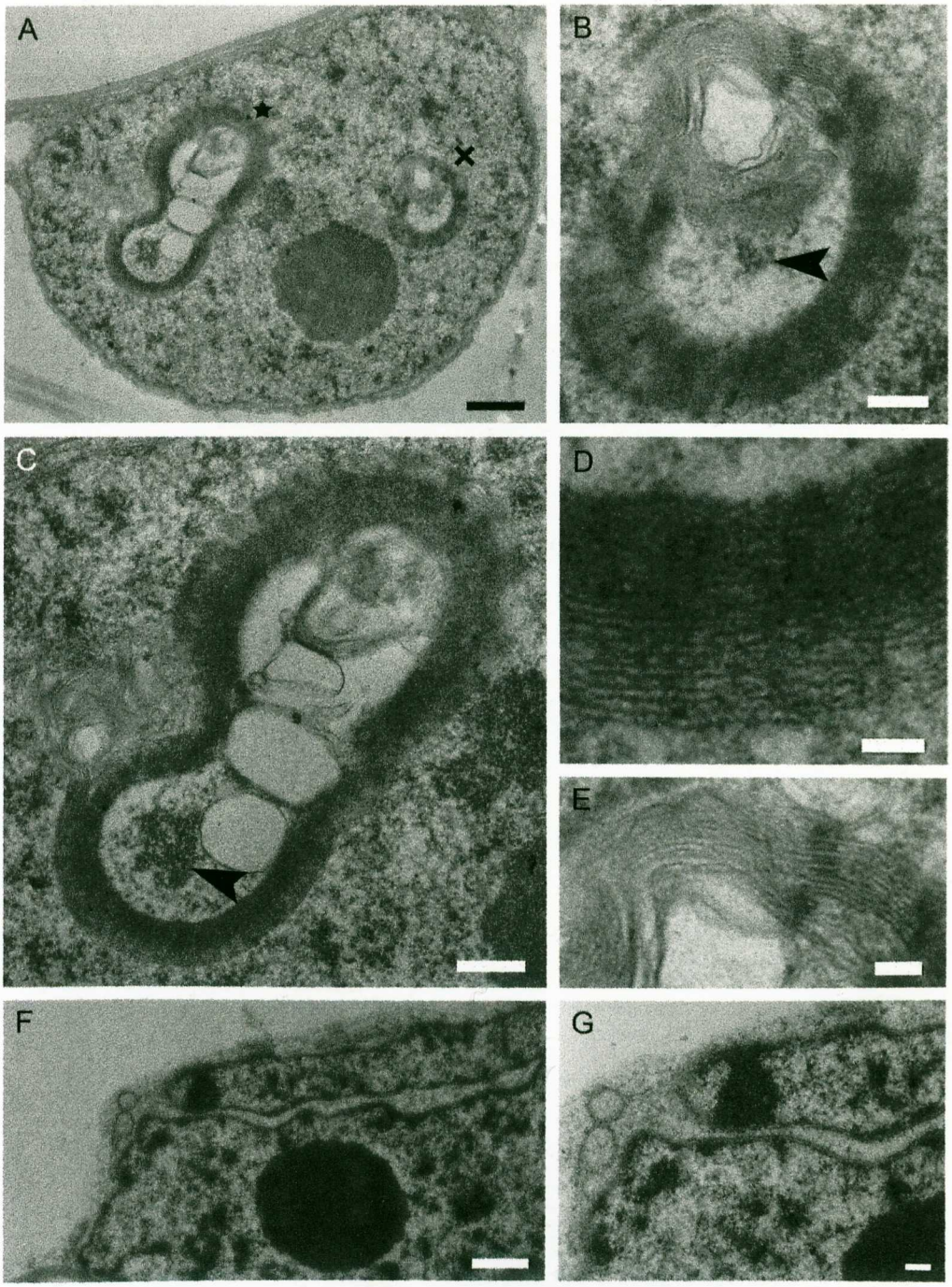
A
B
C
D
E
F
G

Figure 5.9 Transient expression of the LBR-GFP_5 S82A mutant protein in tobacco leaf epidermal cells.

A. Single cell expressing LBR-GFP_5 S82A mutant.

B. Same cell as A, view of cell cortex.

C. Single cell expressing LBR-GFP_5 S82A mutant.

D. Same cell as C, view of cell cortex.

E. Single cell expressing LBR-GFP_5 S82A mutant showing nucleoplasmic labelling.

F. Same cell as G, view of cell cortex.

Scale bars = 10 µm.

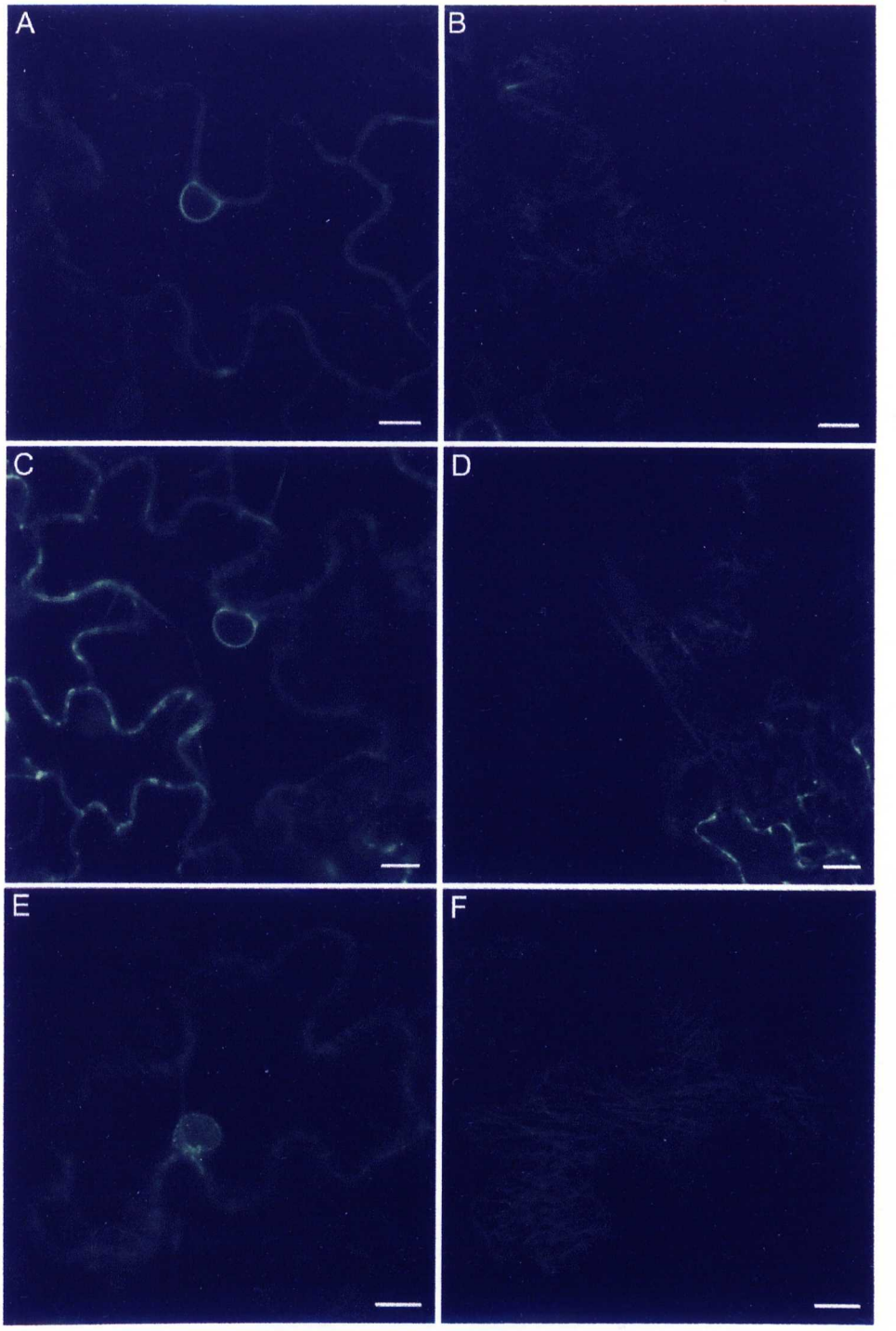
A
B
C
D
E
F

Figure 5.10 Transient expression of the LBR-GFP_5 S84A mutant protein in tobacco leaf epidermal cells.

A. Single cell expressing LBR-GFP_5 S84A mutant protein, NE marked with white arrow.

B. Same cells as A, view of cell cortex. Punctate structure marked with small white arrow.

C. Single cell expressing LBR-GFP_5 S86A mutant protein showing WT LBR-GFP_5-like NE labelling.

D. Same cell as C, view of cell cortex.

Scale bars = 10 µm.

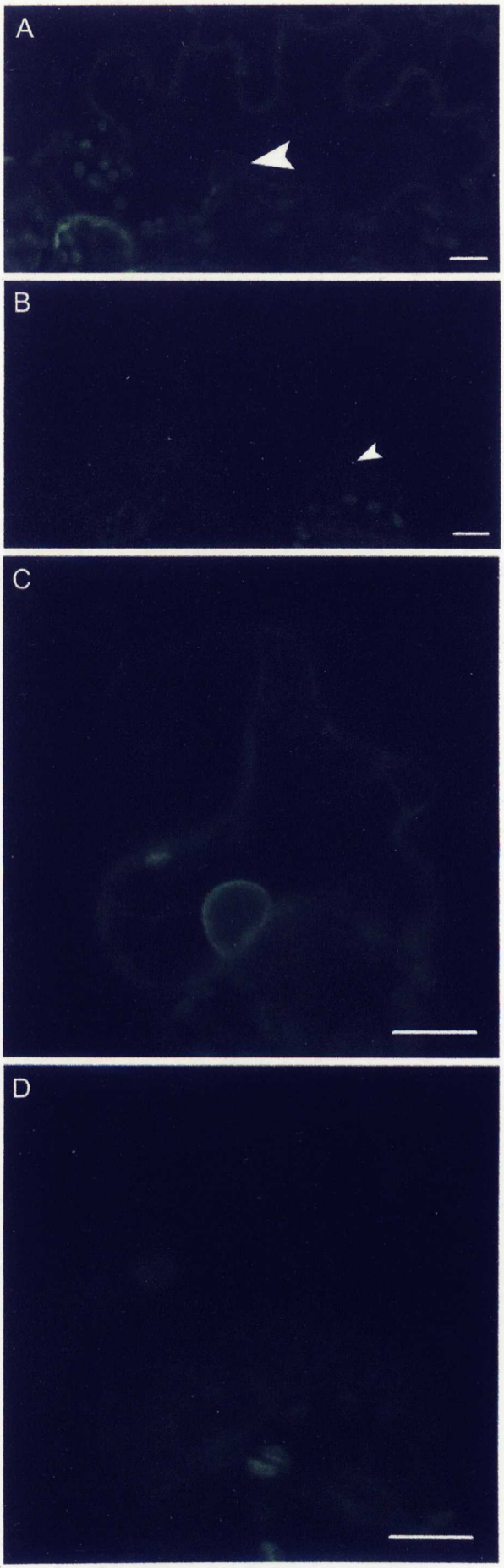
A
B
C
D

CHAPTER 6.

GENERAL DISCUSSION AND FUTURE WORK

6. GENERAL DISCUSSION AND FUTURE WORK

6.1 INTRODUCTION

When a truncated form of the mammalian INE protein LBR was fused to a modified form of GFP and expressed in tobacco cells it localised to the NE. This targeting was significant for a number of reasons. Firstly, the location of the LBR-GFP_5 protein at the plant NE is the first instance of a specific *in vivo* marker for this membrane in plant cells (see Chapter 3 and below). With this novel tool it was possible to study the movement of the NE protein during the cell cycle (see Chapter 4 and below). Secondly, plant genomes sequenced to date do not contain any homologues to LBR or one of its binding partners, the B-type lamins (Rose *et al.* 2004). As such, the targeting of LBR to the NE in plant cells raises questions about protein targeting and retention to the NE in plants, as well as wider issues regarding the structure of the plant nucleus compared to its mammalian counterparts.

6.2 LBR AS A PLANT NUCLEAR ENVELOPE MARKER

Visualisation of the LBR-GFP_5 protein expressed in tobacco leaf epidermal cells through transient and stable transformation methods, showed uniform fluorescence localised to the nuclear rim, consistent with labelling of the membranes of the NE (Chapter 3). Observation of a range of cell types stably expressing the protein also showed NE labelling, with the notable exception of cells in the root which showed high levels of GFP in the vacuole.

To examine labelling of the NE at a higher resolution, leaf tissue stably expressing LBR-GFP_5 was observed by transmission electron microscopy, with GFP labelled indirectly with gold conjugates (Chapter 3). Gold particles were found associated with the INE, NE lumen and ONE. With the secondary antibody labelling technique used there is a spatial separation between the gold particle and the epitope that it is labelling; as the INE, NE lumen and ONE are in close proximity it is not possible to distinguish between them with this technique. The technique does demonstrate that the construct is found associated with the NE and no other structures.

The LBR-GFP_5 protein was shown to be membrane-integral in a phase separation procedure using Triton X-114 (Chapter 3), thus demonstrating successful translation, folding and membrane insertion of the protein in plant cells. A population of free GFP was detected in the soluble protein fraction; this is likely to correlate with the fluorescence observed in the vacuole of root cells. Vacuolar fluorescence is ablated on exposure to light therefore free GFP was not seen in the vacuoles of leaf cells (Tamura *et al.* 2003).

Taken in combination, the location of the LBR-GFP_5 protein as demonstrated by confocal and electron microscopy and the protein's membrane-integral status confirms that LBR-GFP_5 can be considered a specific NE marker in plants.

Attempts to produce other *in vivo* NE markers are described in Appendices 1 and 2: Production of a fluorescently tagged ER calcium ATPase, ECA1, failed at the cloning stage as it did not grow in *E. coli* (see Appendix 1). A construct that gave

speckle-like labelling similar to nuclear pore localisation seen in mammalian cells, identified from a random cDNA fusion approach (Escobar *et al.* 2003) did not give reproducible labelling using the binary vector/*Agrobacterium*-mediated transformation method (see Appendix 2) and was not investigated further.

6.2.1 What targets and retains LBR in the plant nuclear envelope?

Current hypotheses suggest that in order for a protein to be retained at the NE, it needs to bind to a nucleoplasmic constituent like chromatin, lamins, HP1, histones, other nucleoplasmic proteins or to be retained by virtue of TM domain length or formation of large multimeric complexes, either with different proteins or by self-association (Mattaj 2004). The targeting and retention of LBR-GFP_5 at the plant NE indicates that INE targeting can occur in plant cells; this suggests conservation between animal and plant NE protein targeting and retention mechanisms.

In vitro and *in vivo* studies have shown that LBR binds to chromatin (Pyrpasopoulou *et al.* 1996, Duband-Goulet and Courvalin 2000, Takano *et al.* 2002), B-type lamins (Ye and Worman 1994, Wu *et al.* 2002, Dreger *et al.* 2002), HP1 (Polioudaki *et al.* 2001, Wu *et al.* 2002) and other proteins within the nucleus (Polioudaki *et al.* 2001). The plant genomes sequenced to date lack lamin-B homologues (Mewes *et al.* 2002, Rose *et al.* 2004); hence one factor which contributes to LBR retention in animal nuclei is apparently not present in plant cells.

Plants do contain long filament-like plant proteins (FPPs; Rose *et al.* 2003) with similar structural domains to lamins. Early immunolabelling studies of plant nuclei

using anti-lamin antibodies gave positive labelling suggesting a common epitope to lamins may be present in the plant nuclei (McNulty and Saunders 1992). Recently, peptide fragments isolated from *Pisum sativum* L. have been demonstrated to have a degree of similarity to lamins and the proteins that gave rise to the fragments showed positive labelling with anti-lamin antibodies (Blumenthal *et al.* 2004). These results do not constitute sufficient evidence for the presence of lamins in plants. The apparent lack of lamins in plants would imply that retention of LBR at the plant NE is due to interactions with chromatin, HP1 or some other nuclear protein.

To investigate whether the lamin binding domain (amino acids 1-60) was involved in LBR retention at the plant NE the domain was deleted from the LBR-GFP_5 chimaera (Chapter 5). Expression of the truncated protein showed altered distribution to that of the WT protein, with labelling of the nucleoplasm and changes in cortical ER morphology. This altered location suggests that the domain does play a part in the retention of LBR at the plant NE. This could be due to binding to the presence of lamin-like epitopes within the nucleus, like those which have been recognised by anti-lamin immunolabelling of plant cells (McNulty and Saunders 1992). The short regions within plant nuclear intermediate filaments (IF) that bear similar amino acid composition to animal lamins and keratins (Blumenthal *et al.* 2004) may mediate interaction with the lamin binding domain of LBR. Alternatively, the domain may be interacting with a non-IF type protein, or proteins, in a manner different to that previously described for the domain in animal cells.

The binding of LBR to chromatin is important for a number of reasons; in recruitment of LBR to re-forming NEs, in retaining the protein at the NE in interphase thus contributing to the overall structural integrity of the nucleus and chromatin organisation, with cessation of binding at the onset of mitosis contributing to NE breakdown. The RS region of LBR has been shown to bind chromatin in *in vitro* studies, with binding dependent on phosphorylation status (Takano *et al.* 2002, 2004). To determine whether interactions within the RS region were mediating LBR retention at the plant NE a set of point mutations were introduced into the protein and its location observed in plant cells (Chapter 5). The mutations produced a range of protein locations, from NE labelling similar to WT-LBR labelling, to nucleoplasmic labelling, nuclear inclusions and altered ER morphology. These alterations strongly suggest that chromatin interactions are involved in LBR retention as extreme phenotypes were produced by single point mutations. As DNA is present in all organisms and previous work which suggests that LBR binds to DNA secondary structures (Duband-Goulet and Courvalin 2000), chromatin is an obvious candidate for LBR interaction within the plant nucleus. The perturbed localisation of some of the RS mutants suggests that specific chromatin interactions, which the point mutations disrupted, are occurring in the RS region.

Whilst the mutation work shown here has provided an initial insight into the possible mechanisms of LBR retention at the plant NE, other interactions e.g. with HP1 or histones, may be contributing to the protein's retention which have not been addressed here. Indeed, the multiple associations that LBR maintains in animal cells may mean that removing a single interaction may not overtly affect

protein location. For each of the mutants the possibility of mis-targeting of the protein as a result of protein misfolding cannot be discounted. How such issues could be addressed is considered in 'Future work' (6.4).

In summary, it appears that LBR-GFP_5 is retained in the plant NE by a variety of mechanisms including chromatin binding, though further work is required to confirm this and to explore other factors that contribute to retention.

6.2.2 Mitosis as visualised with LBR in plant cells

The expression of LBR-GFP_5 in tobacco BY-2 cells allowed the fate of a NE constituent to be examined. It was found that LBR-GFP_5 co-localised with an ER marker during mitosis (Chapter 4), such ER absorption has been demonstrated for a number of NE proteins in animal cells (Ellenberg *et al.* 1997, Haraguchi *et al.* 2000). This provides evidence against the theory that the NE breakdown is due to vesiculation and supports the ER absorption theory (Introduction 1.2). As both mammalian cells and the suspension cultured plant cells observed here show ER absorption at mitosis it may mean that the mechanism of NEBD is conserved between kingdoms. Thus LBR-GFP_5 suggests that plant, like animal NE are absorbed into mitotic ER, from which new NE reforms at late anaphase/telophase.

The data obtained in this study (Chapter 4) suggests that LBR appears to assemble around newly reforming daughter nuclei in a uniform fashion in plant cells during anaphase/telophase. In animal cells, recruitment has been shown to be more localised, with LBR found at the top of chromosomes, and emerin tending to associate with the central regions of the chromosomes (Haraguchi *et al.* 2000).

Such differences are thought to be due to differing concentrations of binding partners, which become uniform as the nucleus matures (Haraguchi *et al.* 2000). This may have an effect on the localisation pattern of LBR in plant cells, which lack at least some of LBR's binding partners e.g. lamins. Remarkably, immunolabelling of a Ca^{2+}-ATPase, LCA1, in tomato root cells undergoing division showed labelling of specific regions of the mitotic apparatus (MA), as well as clear NE labelling during interphase (Downie *et al.* 1998). This specificity of location during division is in contrast to the uniform distribution of fluorescence throughout the membranes of the MA observed with LBR-GFP_5. Such specificity of location could be due to the requirement of fine control of calcium levels during mitosis (Hepler 1992, 1994), which could require specific localisation of Ca^{2+}-ATPases to produce such Ca^{2+} fluxes. As LBR has no specific role in the plant cell, perhaps a uniform distribution within the MA should be expected. The finer events of NE reformation will only be uncovered as knowledge of the components of the plant NE increases. Identifying native plant NE markers may be expected to be central to this.

The lack of lamins or analogous IF proteins in yeast, in combination with the fact that yeast undergo closed mitosis (NE breakdown does not occur during cell division), unlike the animal and plant open mitosis, suggests that lamins, or proteins analogous to lamins, are necessary for open mitosis to occur. On expression of LBR in yeast the protein targeted the NE, suggesting that a nuclear lamina (or equivalent) is not necessary for retention of LBR at the NE.

6.3 THE MISSING PROTEINS OF THE PLANT NUCLEAR ENVELOPE

A synopsis of current descriptions of animal, plant and yeast nuclear structure is shown in Table 6.1. The table highlights the lack of knowledge of nuclear architecture in plants and yeast. It also emphasises some fundamental differences between organisms, e.g. animal cells contain lamins that form the nuclear lamina, plants have intermediate filaments that appear to form a structure morphologically similar to the animal lamina, but lack sequence homologues to the lamins and yeast appear to lack such a filamentous network. There are also similarities in the organisation of chromatin between plants, animals and yeast, which all contain histones, HP1 and high mobility group (HMG) proteins. The organisms also all have NPCs, with animal and yeast examples showing similarity in protein composition. A few homologues to NPC proteins have been identified in the plant genomes, but they have yet to be characterised (Rose *et al.* 2004). In view of the similarities and differences in nuclear structure it appears there has been evolutionary divergence resulting in evolution of different nuclear structures as seen in plants, animals and yeast, whilst all retain proteins involved in chromatin organisation. It appears that the complexity of the NE may have been underestimated, as recent work has identified at least 8 previously unknown NE integral membrane proteins isolated from animal cells (Schirmer *et al.* 2003).

What is the reason for the current failure to identify NE proteins in plants? One explanantion is that plants contain a set of functionally homologous NE proteins that lack sequence homology to their animal counterparts. A second possibility is that discrepancies in, and lack of completeness of, the sequence data available for plants means that their genes have yet to be identified. A final possibility is an

inherent lack of NE proteins encoded in the plant genome. If the latter is the case, however, a subsequent question is: how is the structure of the nucleus maintained in plant cells?

Nuclear pores have been visualised in plant cells by electron microscopy (Heese-Peck and Raikhel 1998). A proteomic approach to the characterisation of yeast (Rout *et al.* 2000) and mammalian (Cronshaw *et al.* 2002) NPCs has led to the current proposal that the NPC consists of multiple copies of 30 proteins, rather than 100-200 different proteins as was previously thought (Melchior and Gerace 1995). Three *Arabidopsis* proteins, which bear partial similarity to mammalian nucleoporins, have recently been identified by database mining (Rose *et al.* 2004).

Increasing numbers of animal NE proteins are being identified (Schirmer *et al.* 2003). As such, homologous proteins may be present in animal and plant genomes, which are as yet undescribed. The first example of a yeast NE membrane integral protein has recently been described (Beilharz *et al.* 2003). The protein, Prm3, was found to be involved in membrane fusion, a requirement for karyogamy (Beilharz *et al.* 2003). Whilst the *Arabidopsis* genome is fully sequenced and apparently lacks NE proteins, it may not be fully anotated, hence genes may be present but are unidentified.

The third possibility – that plants lack unique INE proteins seems unlikely. If so, it might be speculated that their unique structure (being walled cells) means that nuclear structure can be maintained by a combination of cytoskeletal proteins and their interactions with membrane proteins not unique to the INE. This would,

however, lead to a number of further questions, including the mechanism of NE breakdown and re-formation.

6.3.1 Laminopathies

Rapid progress in identifying animal NE proteins has been as a result of the characterisation of proteins involved in human diseases linked to mutations within nuclear membrane proteins and lamins (so called 'laminopathies'). A mutation in the C-terminal domain of LBR is linked to Greenberg skeletal dysplasia due to altered sterol reductase activity (Waterham *et al.* 2003). Pelger-Huet anomaly, which has a phenotype of abnormal nuclear shape and chromatin organisation in blood granulocytes, has been linked to reduced LBR expression and mutations within the LBR gene (Hoffman *et al.* 2002). Mutations or absence of the INE protein, emerin results in Emery-Dreifuss muscular dystrophy (EDMD; Manilal *et al.* 1996, Nagano *et al.* 1996), a similar phenotype to EDMD is also observed in cells with mutations in the lamin A/C gene (Bonne *et al.* 1999). The production of extreme phenotypes as a result of the loss of a single protein emphasises the importance that the nuclear proteins play in maintaining the structural integrity of the nucleus – which can in turn affect the cell and ultimately the whole organism. In many instances, it has not been clear why the disease phenotype results from mutation of NE or nuclear proteins and the discovery of NE proteins by this means has therefore been suprising. It is not clear what phenotype a plant laminopathy or INE protein mutant would show; as the number of known plant nuclear proteins is currently limited and an appreciation of their functions even more so, it is difficult to extrapolate the effects of 'laminopathies' to plant cells. In the only example, mutations in the plant HP1 homologue, LHP1, leads to alteration of plant structure

and flowering time (Gaudin *et al.* 2001), showing that mutation of a plant nuclear protein results in an altered phenotype. As plant nuclear protein research is in relative infancy, mutants that can be traced back to altered INE proteins or IF proteins have not been described, but if and when identified are likely to offer valuable information into protein function. The mechanical stress that animal cells are exposed to differ to those experienced by plant cells, as such impaired nuclear integrity may not produce such severe effects as the plant nuclei may be afforded protection from mechanical damage by the cell wall. Plant nuclei show high mobility within certain cells (Chytilova *et al.* 2000, Van Bruaene *et al.* 2003) such movement is not seen in animal cells, and as such may indicate different structural and functional features which allow mobility and a certain degree of elasticity in plant nuclei compared to animal nuclei.

6.4 SUGGESTIONS FOR FUTURE WORK

Comparison of various aspects of animal, yeast and plant nuclear research (see Table 6.1) indicates that characterisation of the plant nucleus, including the NE is some way behind that of other organisms. As such this field is a relatively blank canvas, with great potential for future research.

6.4.1 Further investigation using the LBR-GFP$_5$ fusion and derivatives

As has been demonstrated in the preceeding chapters, LBR-GFP$_5$ can serve as a specific marker for the plant NE. The construct has been used to highlight the distribution of the marker during cell division and through the use of dual labelling, to demonstrate co-localisation with an ER marker. Further multiple protein expression studies would allow the visualisation of different cell constituents to

examine their interaction with the NE (as labelled with LBR) during different stages of the cell cycle. Candidates for co-expression include H2B-YFP (Boisnard-Lorig *et al.* 2001), microtubule units e.g. TUA6 (Ueda *et al.* 1996), γ-tubulin (Kumagai et al. 2003) or microtubule binding protein (MBD; Dixit and Cyr 2002), filament-like plant proteins (Rose *et al.* 2003) and putative nucleoporins (Rose *et al.* 2004).

Labelling of H2B allows *in vivo* visualisation of DNA without the application of stains (like ethidium bromide) that perturb cell function, and as such would allow accurate evaluation of cell cycle stage. Co-expression of MTs would allow further investigation into the MT-induced tearing of the NE as demonstrated in animal cells (Beaudouin *et al.* 2002) and preliminarily described in plant cells (Dixit and Cyr 2002). The possibility of FPPs (Gindullis *et al.* 2002) or other IF-type proteins (nuclear IF-protein; Blumenthal *et al.* 2004, NMCP1; Masuda *et al.* 1997, MFP1; Samaniego *et al.* 2001, nuclear matrix proteins [NMPs]; Rose *et al.* 2003) found in the plant nuclear matrix being analogous to mammalian lamins and their relative localisation to the NE during mitosis would be an interesting study to undertake. This work could provide information about the fate of IF proteins during division in plants, and when compared to animal proteins, may allow an insight into similarity or lack thereof, in nuclear IF protein function between the two kingdoms. The localisation of putative nucleoporins to the NE using LBR as a marker could also be used to highlight the fate of NPCs during mitosis in plant cells.

The combination of a range of fluorescent protein variants and advances in microscopy is beginning to permit the labelling of 3 or more constructs in unison.

As this technology becomes more readily available, the relative location of different proteins at the NE and within the nucleus should become easier to determine.

Chromatin immunoprecipitation (ChIP) is a technique that preserves the interactions of chromatin and proteins through biochemical isolation procedures (Wang *et al.* 2002). By using this method on plant tissue expressing LBR-GFP_5, and using anti-GFP antibody for immunoprecipitation, it may be possible to demonstrate whether LBR interacts with chromatin in the plant cell. In addition, the procedure may show if LBR associates with other proteins, which may be precipitated in complexes with LBR and as such may be a way to identify proteins found at the plant NE.

In relation to the factors that contribute to targeting and retention of LBR-GFP_5 at the NE much further work can be accomplished with the mutants described in Chapter 5. Analysis of the mutant protein's diffusional mobility using photobleaching methods (see Introduction section 1.2) could provide information on changes in protein retention. Ultrastructural observation of the cells expressing the mutant proteins would provide an insight into alterations in cellular architecture produced on expression of the mutants e.g. the altered ER morphology (showing a tubular formation) and nucleoplasmic labelling observed in the lamin binding domain deletion mutant. The production of further mutants, for example, deletion of the HP1 binding domain and directed mutations within the lamin binding domain, would allow further elucidation of the regions involved in LBR retention at the NE in plants. Production of plants or suspension culture cells stably

expressing the mutant proteins may show if the mutations alter plant growth, and would provide a consistent level of expression to compare cells in the same plant (unlike the variety of expression levels that transient expression provides).

6.4.2 Identification of plant NE proteins

The identification of native plant INE proteins would be an ideal way forward in the study of the NE. Recent technical advances have added new tools that may aid in this discovery. A process termed 'subtractive proteomics' has been used as a way to comprehensively describe the complement of nuclear proteins isolated from liver cells (Schirmer *et al.* 2003). This method identified all previously described INE proteins and a multitude of, as yet undescribed membrane proteins (Schirmer *et al.* 2003). This technique applied to plant cell extracts would provide a good method for identifying proteins that have evaded prior isolation attempts. The ChIP method (see section 6.4.1) could be used in combination with the subtractive proteomics approch to identify membrane proteins that associate with chromatin. In addition, the characterisation of aberrant plant phenotypes may lead to the identification and elucidation of function of NE proteins.

Table 6.1 Comparison of current characterised structural components of nuclei in animal plant and yeast cells.

Component	*Animal*	*Plant*	*Yeast*
INE proteins	13 characterised, more recently identified (Schirmer *et al.* 2003).	None identified to date (Rose *et al.* 2004).	1 protein described: Prm3 (Beilharz *et al.* 2003).
Lamina	Lamins A, B and C, form lattice adjacent to INE.	Filamentous matrix present (Samaniego *et al.* 2001, Calikowski *et al.* 2003) (Filament-like plant proteins (FPPs; Gindullis *et al.* 2002, Rose *et al.* 2003). Fragments similar to lamins (Blumenthal *et al.* 2004).	No lamin homologues identified, no ultrastructural evidence of lamina/matrix (Rose *et al.* 2004).
Histones	H1/2A/2B/3/4/5.	H1-4 homologues.	H1-4 homologues.
Non-histone chromatin associated proteins	HP1 homologues, High mobility group (HMG) proteins.	HP1 homologue, HMG protein homologues.	HP1 homologue, HMG protein homologues.
NPCs	Complex consists of multiple copies of ~30 proteins. Several proteins characterised.	Visualised in plant cells by EM, few putative homologues present, yet to be characterised (Rose *et al.* 2004).	Complex consists of multiple copies of ~30 proteins (Rout *et al.* 2000).

APPENDIX 1.

PRODUCTION OF AN ECA1-GFP_5 FUSION

APPENDIX 1. PRODUCTION OF AN ECA1-GFP$_5$ FUSION

Immunolabelling of the tomato Ca^{2+}-ATPase LCA1 showed localisation at the nuclear rim (Chapter 1 and 6, and Downie *et al.* 1998). A homologue of the protein, ECA1, was cloned from Arabidopsis (Liang *et al.* 1997). In an attempt to use this plant protein as a possible NE marker the cDNA encoding the full length ECA1 was fused to GFP$_5$ using overlapping PCR and the fusion ligated into the binary vector pVKH18En6. The ligation reactions were used to transform *E. coli*, in order to produce colonies to be screened for clones carrying the construct, which could then be sequenced and used for *in planta* expression. However over several attempts, the ECA1 ligations produced no positive clones despite varying the transformation method, *E. coli* stocks and strains, ligation reaction conditions and reagents and DNA preparation prior to ligation.

On communication with other research groups trying to clone Ca^{2+}-ATPases it was found that the proteins can be lethal to *E. coli* strains unless under the control of a chemical promoter (reviewed by Gatz 1997, Gatz and Lenk 1998) or by using a truncated form of the Ca^{2+}-ATPase. An alternative method using a truncated version of the ECA1, which would theoretically render the protein non-functional was produced, and again yielded no positive clones.

APPENDIX 2.

ADAPTION OF A PUTATIVE NUCLEAR PORE MARKER

APPENDIX 2. ADAPTION OF A PUTATIVE NUCLEAR PORE MARKER

Libraries of random cDNA sequences fused to GFP were produced at the Scottish Crop Research Institute and expressed using a viral vector system, which allowed a high throughput approach for localization of unknown proteins (Escobar *et al.* 2003). A clone designated 5'-026 was found to localise in discrete punctate structures at the nuclear rim, suggestive of nuclear pore complex association. Using the sequence of the open reading frame that contained the cDNA fragment start and stop codons were identified which corresponded to the sequence of the 5'-026 fragment. Oligonucleotide primers (see table A2.1 below, restriction sites 5' *Xba*I in SI38 and 3' *Sac*I in SI41, included for cloning in to pVKH18En6 vector shown in red) were designed to amplify this sequence and in a subsequent PCR reaction fuse it to EYFP for use in dual expression studies with GFP-fused proteins.

Table A2.1 Sequence of oligonucleotides used for production of nuclear pore-YFP fusion by PCR.

Nuclear pore-YFP	SI38	GGCTGCTCTAGAATGGGCAACCAACATAGCA GC
	SI39b	GAGGAAGAAGATGCGATCCGAGCGGCCGCT GGGTCGACTGTG
	SI40b	CTCCTCGCCCTTGCTCACAGTCGACCCAGCG GCCGC
	SI41	CGACTGGAGCTCTTACCAATCCTCCTCAGAG ATAAG

Several positive clones were produced from the ligation, 2 of which were sequenced and contained no mutations. The two sequenced clones were used to transform *Agrobacterium* which was used to transiently transform tobacco leaf

epidermal cells. Expression of the YFP fused putative nuclear pore marker showed nucleoplasmic labelling (see Figure A2.1).

Figure A2.1 Location of a putative nucleoporin, after fusion to YFP and ligation in to pVKH18En6.

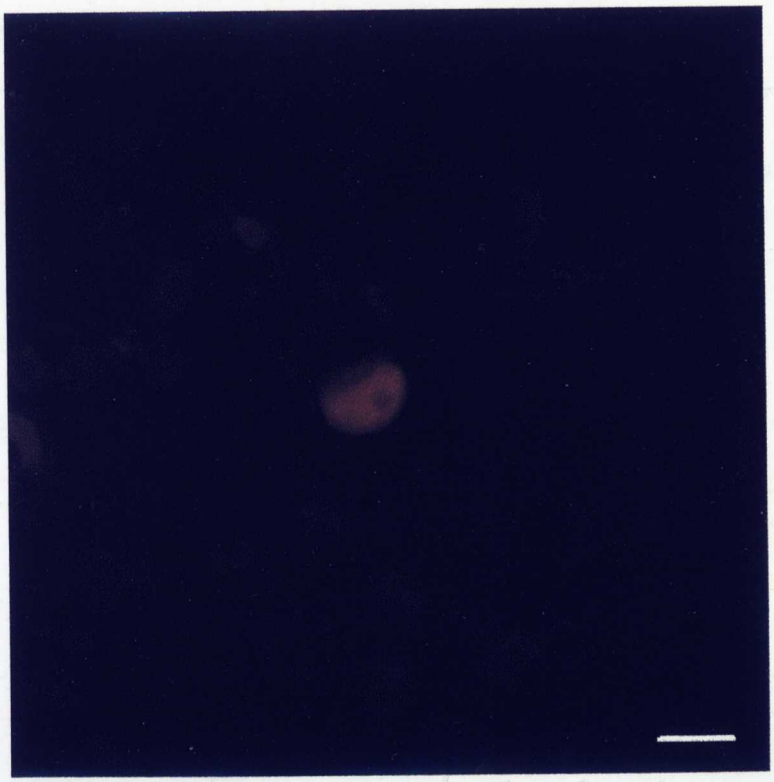

APPENDIX 3.

DIVIDING TOBACCO BY-2 CELL MOVIE

(ON C.D.)

APPENDIX 4.

STRAINS TABLE

APPENDIX 4. STRAINS TABLE

	Strain	*Description*	*Source*
PLANT	*Nicotiana tabacum* sp.	Family *Solanaceae*, thought to have been produced from artificial crossing of *N. sylvestris* with *N. tomentosiformis*	
	Nicotiana tabacum plant stable LBR-GFP_5 transformed	Plant constitutively expressing LBR-GFP_5 protein	This study, Irons *et al.* (2003)
	Nicotiana tabacum L. cv. Bright Yellow 2 (BY2) cells	Sterile suspension cultured cells with high growth rate and amenability to synchronisation by aphidicolin (Nagata and Kumagai 1999)	Kato *et al.* (1972)
	Nicotiana tabacum L. cv. BY2 cells stable LBR-GFP_5 transformed	Suspension cells constitutively expressing LBR-GFP_5 protein	This study, Irons *et al.* (2003)
	Nicotiana tabacum L. cv. BY2 cells stable LBR-GFP_5 and spYFP-HDEL transformed	Suspension cells constitutively expressing LBR-GFP_5 and spYFP-HDEL proteins	This study, Irons *et al.* (2003)
BACTERIA	*Escherichia coli* DH5α	Attenuated strain of *E. coli*.	Hanahan (1983)
	Agrobacterium tumefaciens GV3101::pMP90	Disarmed Ti plasmid, gentamycin resistant. When transformed with pVKH18En6 plasmids used for transient and stable transformation protocols	Koncz and Schell (1986)

	Strain	*Description*	*Source*
VECTORS	pVKH18En6 plasmid	CaMV 35S constitutive promoter, 6X enhancer region, kanamycin resistant in bacteria, hygromycin resistant in plants	Moore *et al.* (1998)
	pVKH18En6 LBR-GFP_5	First 238 amino acids of LBR fused to N-glycosylation peptide at the N-terminus of GFP_5. Inserted in *Bam*HI/*Sac*I site of pVKH18En6	This study, Irons *et al.* (2003)
	pVKH18En6-sp-EYFP-HDEL	C-myc tagged EYFP (Clontech) inserted downstream of a sporamin signal peptide at *Sal*I/*Sac*I site of an existing sporamin signal peptide-GFP_5-HDEL pVKH18En6	Federica Brandizzi
	pVKH18En6-sp-GFP_5-Calnexin	GFP_5 fused at the 5' end to a sporamin signal peptide and glycosylatable region (Batoko *et al.* 2000) was fused to the last 236 base pairs of *Arabidopsis* calnexin (Huang *et al.* 1993). 7 aa spacer inserted between the GFP_5 and calnexin sequence. In *Bam*HI/*Sac*I site of pVKH18En6	Federica Brandizzi
	pVKH18En6-Δ1-60LBR-GFP_5	Amino acids 61-238 of LBR fused to N-glycosylation peptide and GFP_5. Inserted in *Bam*HI/*Sac*I site of pVKH18En6	This study
	pVKH18En6- S80A LBR-GFP_5	Point mutation (tca → gca) producing Ser→Ala change at residue 80. Inserted in *Bam*HI/*Sac*I site of pVKH18En6	This study

	Strain	*Description*	*Source*
VECTORS	pVKH18En6- S82A LBR-GFP_5	Point mutation (tca → gca) producing Ser→Ala change at residue 82. Inserted in *Bam*HI/*Sac*I site of pVKH18En6	This study
	pVKH18En6- S84A LBR-GFP_5	Point mutation (tcc → gcc) producing Ser→Ala change at residue 84. Inserted in *Bam*HI/*Sac*I site of pVKH18En6	This study
	pVKH18En6- S86A LBR-GFP_5	Point mutation (tcc → gcc) producing Ser→Ala change at residue 86. Inserted in *Bam*HI/*Sac*I site of pVKH18En6	This study

APPENDIX 5.

PRODUCTION AND VALIDATION OF LBR-GFP$_5$ AND RELATED CONSTRUCTS

APPENDIX 5. PRODUCTION AND VALIDATION OF LBR-GFP$_5$ AND RELATED CONSTRUCTS

A5.1 Production of the LBR-GFP$_5$ constructs

Images of agarose gels showing LBR-GFP$_5$ and mutants bands are shown in Figure A5.1. The LBR-GFP$_5$ and RS mutants (S80A, S82A, S84A, S86A), shown in Figure A5.1. A and B, all show bands of ~1500 bp on *Bam*HI/*Sac*I restriction enzyme digest of plasmids. The Δ1-60LBR-GFP$_5$ *Bam*HI/*Sac*I fragment, shown in Figure A5.1. C, is ~1300 bp long. Examples of cut and uncut pVKH18En6 are also shown in Figure A5.1. C.

A5.2 Sequencing

Sequencing was undertaken using the conditions prescribed by the Univeristy of Oxford sequencing lab. The reaction samples were prepared as follows: 0.5 µg plasmid, 1 µl primer (oligonucleotide concentration 3.2 pmol/µl), 4 µl BigDye, 4µl sequencing buffer (200mM Tris 5mM $MgCl_2$ pH 9.8), water to final volume of 20 µl in 0.2 ml tubes. Reaction mix was vortexed, briefly centrifuged and placed in thermal cycler for the following programme:

Table A5.1 Thermal cycler programme for ABI BigDye terminator sequencing reactions

Temperature (°C)	*Time (min:sec)*	*Number of cycles*
95	**2:00**	**1**
95	**0:30**	
50	**0:15**	**25**
60	**4:00**	
4	**hold**	**-**

Once the programme reached the 4°C hold stage samples were removed and precipitated. For each reaction 2 µl 1.5M sodium acetate 250mM EDTA, pH 8 and 50 µl 100% ethanol were added, briefly vortexed and incubated at room temperature for 15 minutes. Samples were then centrifuged at 16°C at maximum speed in a microcentrifuge for 20 minutes and supernatant carefully removed and discarded. The pellet was washed with 200 µl 70% ethanol, briefly vortexed and centrifuged for 10 minutes, all supernatant was removed to waste and the pellet dried gently (30 minutes at 37°C). Dried samples were delivered to the Oxford University Sequencing lab for analysis.

The oligonucleotides used for the sequencing reactions are detailed in Table A5.2 and Figure A5.2. Sequencing results are shown in Figure A5.3.

Table A5.2 Oliogonucleotides used for DNA sequencing of LBR-GFP_5 and related mutant constructs.

Oligonucleotide	***Direction***	***Anticipated sequence coverage***
SI13[+]	3'	Large part of LBR, including the start of the protein
SI16[+]	5'	The majority of LBR and the fusion area between LBR and GFP_5
FB92*	3'	The fusion region and most, if not all of the LBR sequence

[+] See Table 2.2 for oligo sequence.
* FB92 oligonucleotide sequence: 5' GTGTTGGCGATGGAACAGGTAG

A5.3 Domain information and sequences

Anotated nucleotide and amino acid sequences for LBR-GFP_5 are shown in Figures A5.4 and A5.5, respectively.

Figure A5.1 Images of agarose gels showing *Bam*HI/*Sac*I restriction enzyme digests of LBR-GFP$_5$ and mutant plasmids.

A. LBR-GFP$_5$ and RS mutants (S80A, S82A, S84A), all show bands of ~1500 bp on *Bam*HI/*Sac*I restriction enzyme digest of plasmids, against 100 bp ladder. Lane 1, 100 bp ladder; Lanes 2 and 3, *Bam*HI/*Sac*I cut LBR-GFP$_5$; Lanes 4 and 5, *Bam*HI/*Sac*I cut S80A LBR-GFP$_5$; Lanes 6 and 7, *Bam*HI/*Sac*I cut S82A LBR-GFP$_5$; Lanes 8 and 9, *Bam*HI/*Sac*I cut S84A LBR-GFP$_5$.

B. LBR-GFP$_5$ S86A, bands of ~1500 bp on *Bam*HI/*Sac*I restriction enzyme digest of plasmids, against 100 bp ladder. Lane 1, 100 bp ladder; Lanes 2 and 3, *Bam*HI/*Sac*I cut S86A LBR-GFP$_5$.

C. Δ1-60LBR-GFP$_5$ *Bam*HI/*Sac*I fragment, ~1300 bp long (lane 4). Examples of cut (lane 2) and uncut (lane 3) pVKH18En6 are also shown, against 1 kb ladder.

A

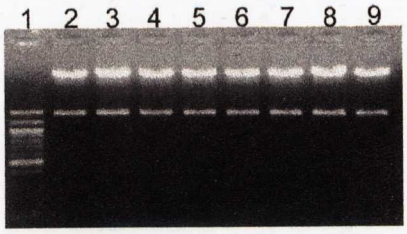

B

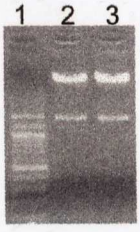

C

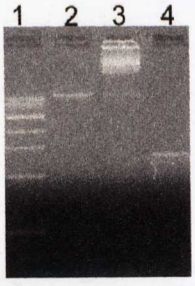

Figure A5.2 Schematic representation of regions to be sequenced in LBR-GFP$_5$ and related mutants.

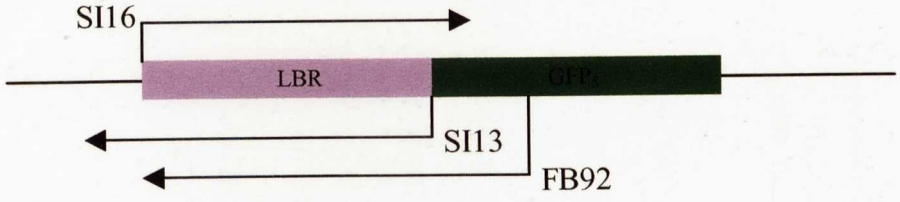
SI16
LBR
GFP
SI13
FB92

Figure A5.3 LBR-GFP$_5$ and related mutants sequencing results (nucleotide sequence translated to amino acid sequence).

```
T-COFFEE, Version_1.41(Fri Jun 28 14:24:48 MDT 2002)
Notredame, Higgins, Heringa, JMB(302)pp205-217,2000
CPU TIME:393 sec.
SCORE=45

20/2/2003

LBRGFP   ---MPSRKFADGEVVRGRWPGSSLYYEVEILSHDSTSQLYTVKYKDGTELELKENDIKPLTSF
LBR238   ---MPSRKFADGEVVRGRWPGSSLYYEVEILSHDSTSQLYTVKYKDGTELELKENDIKPLTSF
M1A13    ---MPSRKFADGEVVRGRWPGSSLYYEVEILSHDSTSQLYTVKYKDGTELELKENDIKPLTSF
M1A16    ------------------------------------TSQLYTVKYKDGTELELKENDIKPLTSF
M1A92    -------------------------------SHDSTSQLYTVKYKDGTELELKENDIKPLTSF
M1C16    ------------------------------------TSQLYTVKYKDGTELELKENDIKPLTSF
M1C92    ---MPSRKFADGEVVRGRWPGSSLYYEVEILSHDSTSQLYTVKYKDGTELELKENDIKPLTSF
M2A16    ------------------------------------STSQLYTVKYKDGTELELKENDIKPLTSF
M2A92    ------------------------------------SQLYTVKYKDGTELELKENDIKPLTSF
M2H13    -------------------------------SHDSTSQLYTVKYKDGTELELKENDIKPLTSF
M2H16    ------------------------------------------------GTELELKENDIKPLTSF
M2H92    -------KFADGEVVRGRWPGSSLYYEVEILSHDSTSQLYTVKYKDGTELELKENDIKPLTSF
M3D13    ---MPSRKFADGEVVRGRWPGSSLYYEVEILSHDSTSQLYTVKYKDGTELELKENDIKPLTSF
M3D16    ------------------------------------TSQLYTVKYKDGTELELKENDIKPLTSF
M3D92    -------------------------------SHDSTSQLYTVKYKDGTELELKENDIKPLTSF
M3E16    ------------------------------------TSQLYTVKYKDGTELELKENDIKPLTSF
M3E92    ---MPSRKFADGEVVRGRWPGSSLYYEVEILSHDSTSQLYTVKYKDGTELELKENDIKPLTSF
M4A16    ------------------------------------STSQLYTVKYKDGTELELKENDIKPLTSF
M4A92    ---MPSRKFADGEVVRGRWPGSSLYYEVEILSHDSTSQLYTVKYKDGTELELKENDIKPLTSF
M4B16    ------------------------------------STSQLYTVKYKDGTELELKENDIKPLTSF
M4B92    --------------------PGSSLYYEVEILSHDSTSQLYTVKYKDGTELELKENDIKPLTSF

Cons                                                 ******************
```

```
LBRGFP    RQRKGGSTSSSPSRRRGSRSRSRSRSPGRPPKSARRSASASHQADIKEARREVEVKLTPLILK
LBR238    RQRKGGSTSSSPSRRRGSRSRSRSRSPGRPPKSARRSASASHQADIKEARREVEVKLTPLILK
M1A13     RQRKGGSTSSSPSRRRGSRARSRSRSPGRPPKSARRSASASHQADIKEARREVEVKLTPLILK
M1A16     RQRKGGSTSSSPSRRRGSRARSRSRSPGRPPKSARRSASASHQADIKEARREVEVKLTPLILK
M1A92     RQRKGGSTSSSPSRRRGSRARSRSRSPGRPPKSARRSASASHQADIKEARREVEVKLTPLILK
M1C16     RQRKGGSTSSSPSRRRGSRARSRSRSPGRPPKSARRSASASHQADIKEARREVEVKLTPLILK
M1C92     RQRKGGSTSSSPSRRRGSRARSRSRSPGRPPKSARRSASASHQADIKEARREVEVKLTPLILK
M2A16     RQRKGGSTSSSPSRRRGSRSRARSRSPGRPPKSARRSASASHQADIKEARREVEVKLTPLILK
M2A92     RQRKGGSTSSSPSRRRGSRSRARSRSPGRPPKSARRSASASHQADIKEARREVEVKLTPLILK
M2H13     RQRKGGSTSSSPSRRRGSRSRARSRSPGRPPKSARRSASASHQADIKEARREVEVKLTPLILK
M2H16     RQRKGGSTSSSPSRRRGSRSRARSRSPGRPPKSARRSASASHQADIKEARREVEVKLTPLILK
M2H92     RQRKGGSTSSSPSRRRGSRSRARSRSPGRPPKSARRSASASHQADIKEARREVEVKLTPLILK
M3D13     RQRKGGSTSSSPSRRRGSRSRSRARSPGRPPKSARRSASASHQADIKEARREVEVKLTPLILK
M3D16     RQRKGGSTSSSPSRRRGSRSRSRARSPGRPPKSARRSASASHQADIKEARREVEVKLTPLILK
M3D92     RQRKGGSTSSSPSRRRGSRSRSRARSPGRPPKSARRSASASHQADIKEARREVEVKLTPLILK
M3E16     RQRKGGSTSSSPSRRRGSRSRSRARSPGRPPKSARRSASASHQADIKEARREVEVKLTPLILK
M3E92     RQRKGGSTSSSPSRRRGSRSRSRARSPGRPPKSARRSASASHQADIKEARREVEVKLTPLILK
M4A16     RQRKGGSTSSSPSRRRGSRSRSRSRAPGRPPKSARRSASASHQADIKEARREVEVKLTPLILK
M4A92     RQRKGGSTSSSPSRRRGSRSRSRSRAPGRPPKSARRSASASHQADIKEARREVEVKLTPLILK
M4B16     RQRKGGSTSSSPSRRRGSRSRSRSRAPGRPPKSARRSASASHQADIKEARREVEVKLTPLILK
M4B92     RQRKGGSTSSSPSRRRGSRSRSRSRAPGRPPKSARRSASASHQADIKEARREVEVKLTPLILK

Cons      ********************:*:*:*:************************************
```

```
LBRGFP    PFGNSISRYNGEPEHIERNDAPHKNTQEKFSLSQESSYIATQYSLRPRREEVKLKEIDSKEEK
LBR238    PFGNSISRYNGEPEHIERNDAPHKNTQEKFSLSQESSYIATQYSLRPRREEVKLKEIDSKEEK
M1A13     PFGNSISRYNGEPEHIERNDAPHKNTQEKFSLSQESSYIATQYSLRPRREEVKLKEIDSKEEK
M1A16     PFGNSISRYNGEPEHIERNDAPHKNTQEKFSLSQESSYIATQYSLRPRREEVKLKEIDSKEEK
M1A92     PFGNSISRYNGEPEHIERNDAPHKNTQEKFSLSQESSYIATQYSLRPRREEVKLKEIDSKEEK
M1C16     PFGNSISRYNGEPEHIERNDAPHKNTQEKFSLSQESSYIATQYSLRPRREEVKLKEIDSKEEK
M1C92     PFGNSISRYNGEPEHIERNDAPHKNTQEKFSLSQESSYIATQYSLRPRREEVKLKEIDSKEEK
M2A16     PFGNSISRYNGEPEHIERNDAPHKNTQEKFSLSQESSYIATQYSLRPRREEVKLKEIDSKEEK
M2A92     PFGNSISRYNGEPEHIERNDAPHKNTQEKFSLSQESSYIATQYSLRPRREEVKLKEIDSKEEK
M2H13     PFGNSISRYNGEPEHIERNDAPHKNTQEKFSLSQESSYIATQYSLRPRREEVKLKEIDSKEEK
M2H16     PFGNSISRYNGEPEHIERNDAPHKNTQEKFSLSQESSYIATQYSLRPRREEVKLKEIDSKEEK
M2H92     PFGNSISRYNGEPEHIERNDAPHKNTQEKFSLSQESSYIATQYSLRPRREEVKLKEIDSKEEK
M3D13     PFGNSISRYNGEPEHIERNDAPHKNTQEKFSLSQESSYIATQYSLRPRREEVKLKEIDSKEEK
M3D16     PFGNSISRYNGEPEHIERNDAPHKNTQEKFSLSQESSYIATQYSLRPRREEVKLKEIDSKEEK
M3D92     PFGNSISRYNGEPEHIERNDAPHKNTQEKFSLSQESSYIATQYSLRPRREEVKLKEIDSKEEK
M3E16     PFGNSISRYNGEPEHIERNDAPHKNTQEKFSLSQESSYIATQYSLRPRREEVKLKEIDSKEEK
M3E92     PFGNSISRYNGEPEHIERNDAPHKNTQEKFSLSQESSYIATQYSLRPRREEVKLKEIDSKEEK
M4A16     PFGNSISRYNGEPEHIERNDAPHKNTQEKFSLSQESSYIATQYSLRPRREEVKLKEIDSKEEK
M4A92     PFGNSISRYNGEPEHIERNDAPHKNTQEKFSLSQESSYIATQYSLRPRREEVKLKEIDSKEEK
M4B16     PFGNSISRYNGEPEHIERNDAPHKNTQEKFSLSQESSYIATQYSLRPRREEVKLKEIDSKEEK
M4B92     PFGNSISRYNGEPEHIERNDAPHKNTQEKFSLSQESSYIATQYSLRPRREEVKLKEIDSKEEK

Cons      ************************************************************
```

```
LBRGFP   YVAKELAVRTFEVTPIRAKDLEFGGVPGVFLIMFGLPVFLFLLLLMCKQKDPTSTGELVSNGT
LBR238   YVAKELAVRTFEVTPIRAKDLEFGGVPGVFLIMFGLPVFLFLLLLMCKQKDP-----------
M1A13    YVAKELA-----------------------------------------------------
M1A16    YVAKELAVRTFEVTPIRAKDLEFGGVPGVFLIMFGLPVFLFLLLLMCKQKDPTSTGELVSNGT
M1A92    YVAKELAVRTFEVTPIRAKDLEFGGVPGVFLIMFGLPVFLFLLLLMCKQKDPTSTGELVSNGT
M1C16    YVAKELAVRTFEVTPIRAKDLEFGGVPGVFLIMFGLPVFLFLLLLMCKQKDPTSTGELVSNGT
M1C92    YVAKELAVRTFEVTPIRAKDLEFGGVPGVFLIMFGLPVFLFLLLLMCKQKDPTSTGELVSNGT
M2A16    YVAKELAVRTFEVTPIRAKDLEFGGVPGVFLIMFGLPVFLFLLLLMCKQKDPTSTGELVSNGT
M2A92    YVAKELAVRTFEVTPIRAKDLEFGGVPGVFLIMFGLPVFLFLLLLMCKQKDPTSTGELVSNGT
M2H13    YVAKELAVRTFEVTPIRAK-------------------------------------------
M2H16    YVAKELAVRTFEVTPIRAKDLEFGGVPGVFLIMFGLPVFLFLLLLMCKQKDPTSTGELVSNGT
M2H92    YVAKELAVRTFEVTPIRAKDLEFGGVPGVFLIMFGLPVFLFLLLLMCKQKDPTSTGELVSNGT
M3D13    YVAKELAVRTFEVTPIRAK-------------------------------------------
M3D16    YVAKELAVRTFEVTPIRAKDLEFGGVPGVFLIMFGLPVFLFLLLLMCKQKDPTSTGELVSNGT
M3D92    YVAKELAVRTFEVTPIRAKDLEFGGVPGVFLIMFGLPVFLFLLLLMCKQKDPTSTGELVSNGT
M3E16    YVAKELAVRTFEVTPIRAKDLEFGGVPGVFLIMFGLPVFLFLLLLMCKQKDPTSTGELVSNGT
M3E92    YVAKELAVRTFEVTPIRAKDLEFGGVPGVFLIMFGLPVFLFLLLLMCKQKDPTSTGELVSNGT
M4A16    YVAKELAVRTFEVTPIRAKDLEFGGVPGVFLIMFGLPVFLFLLLLMCKQKDPTSTGELVSNGT
M4A92    YVAKELAVRTFEVTPIRAKDLEFGGVPGVFLIMFGLPVFLFLLLLMCKQKDPTSTGELVSNGT
M4B16    YVAKELAVRTFEVTPIRAKDLEFGGVPGVFLIMFGLPVSLFLLLLMCKQKDPTSTGELVSNGT
M4B92    YVAKELAVRTFEVTPIRAKDLEFGGVPGVFLIMFGLPVSLFLLLLMCKQKDPTSTGELVSNGT

Cons     *******
```

```
LBRGFP   VTGSTFSKGEELFTGVVPILVELDGDVNGHKFSVSGEGEGDATYGKLTLKFICTTGKLPVPWP (312)
LBR238   ------------------------------------------------------------
M1A13    ------------------------------------------------------------
M1A16    VTGSTFSKGEELFTGVVPILVELDGDVNGHKFSVSGEGEGDATYGKLT--------------
M1A92    VTGSTFSKGEELFTGVV-------------------------------------------
M1C16    VTGSTFSKGEELFTGVVPILVELDGDVNGHKFSVSGEGEGDATYGKLTLKFICTTGKLPVPW-
M1C92    VTGSTFSKGEELFTGVVPILVELDGDVNG-------------------------------
M2A16    VTGSTFSKGEELFTGVVPILVELDGDVNGHKFSVSGEGEGDATYGKLTLKFICTTGKLPVPW-
M2A92    VTGSTFSKGEELFTGVVPILVEL--------------------------------------
M2H13    ------------------------------------------------------------
M2H16    VTGSTFSKGEELFTGVVPILVELD-------------------------------------
M2H92    VTGSTFSKGEELFTGVVPILVELDGD-----------------------------------
M3D13    ------------------------------------------------------------
M3D16    VTGSTFSKGEELFTGVVPILVELDGDVNGHKFSV---------------------------
M3D92    VTGSTFSKGEELFTGVVPILVELDGDVNG--------------------------------
M3E16    VTGSTFSKGEELFTGVVPILVELDGDVNGHKFSVSGEGEGDATYGKLTLKFICTTGKLPV---
M3E92    VTGSTFSKGEELFTGVVP------------------------------------------
M4A16    VTGSTFSKGEELFTGVVPILVELDGDVNGHKFSVSGEGEGDATYGKLTLKFICTTGKLPVPW-
M4A92    VTGSTFSKGEELFTGVVPILVELDGDVNG--------------------------------
M4B16    VTGSTFSKGEELFTGVVPILVELDGDVNGHKFSVSGEGEGDATYGKLTLKFICTTGKLPV---
M4B92    VTGSTFSKGEELFTGVV-------------------------------------------

Cons
```

Figure A5.4 LBR-GFP$_5$ nucleotide sequence.

Colour code:

LBR (N-terminal 238 amino acids)

N-glycosylation site

GFP$_5$

TM domain

Restriction sites

RS region

LBR-GFP$_5$ NUCLEOTIDE SEQUENCE

ggatccatgccaagtaggaaatttgccgatggtgaagtggtaagaggtcgatggcctgggagttcactttattatgaagtagaaattctgagcc
acgacagcacctcccagctttacactgtgaagtataaagatggaacagagcttgaattgaaagagaatgatattaagcctttaacttcctttag
gcaaaggaaaggtggctcaacttccagttccccttccagacgccgaggg**agtcgatcaaggtcacgctcccgatcc**cctggtcgaccacctaaa
agtgcccgccgatctgcttctgcttcccaccaggccgacattaaggaagcaaggagggaagtggaagttaaattgactccgctgattctgaagc
catttggaaatagcatcagcagatataatggggagcctgagcatattgagagaaatgacgcacctcataaaaatacacaggaaaaattcagttt
gtcacaagaaagcagttacatagcaacacagtatagccttcgtccaagaagagaagaagtcaaattaaaagaaatagattctaaggaagaaaaa
tacgttgcaaaagaactggcagtgagaacctttgaagtgacccccatccgggcaaaggacttggagtttggaggagtacctggtgtgtttctca
tcatgtttggcctgcctgtgttcctcttcctgttgctgttgatgtgtaaacagaaagatcccacgtcgactggagaacttgtttcaaatggaac
cgttaccggctcgacttcagtaaaggagaagaacttttcactggagttgtcccaattcttgttgaattagatggtgatgttaatgggcacaaa
ttttctgtcagtggagagggtgaaggtgatgcaacatacggaaaacttacccttaaatttatttgcactactggaaaactacctgttccatggc
caacacttgtcactactttctcttatggtgttcaatgcttttcaagatacccagatcatatgaagcggcacgacttcttcaagagcgccatgcc
tgagggatacgtgcaggagaggaccatcttcttcaaggacgacgggaactacaagacacgtgctgaagtcaagtttgagggagacaccctcgtc
aacaggatcgagcttaagggaatcgatttcaaggaggacggaaacatcctcggccacaagttggaatacaactacaactcccacaacgtataca
tcatggccgacaagcaaaagaacggcatcaaagccaacttcaagacccgccacaacatcgaagacggcggcgtgcaactcgctgatcattatca
acaaaatactccaattggcgatggccctgtccttttaccagacaaccattacctgtccacacaatctgccctttcgaaagatcccaacgaaaag
agagaccacatggtccttcttgagtttgtaacagctgctgggattacacatggcatggatgaactatacaaataagagctc

(1479 base pairs)

Figure A5.5 LBR-GFP_5 amino acid sequence.

Colour code:

LBR (N-terminal 238 amino acids)

N-glycosylation site

GFP_5

TM domain

Lamin binding domain

chromatin binding domain

HP-1 binding domain

RS region

LBR-GFP$_5$ AMINO ACID SEQUENCE

MPSRKFADGEVVRGRWPGSSLYYEVEILSHDSTSQLYTVKYKDGTELELKENDIKPLTSFRQRKGGSTSSSPSRRRGSRSR
SRSRSPGRPPKSARRSASASHQADIKEARREVEVKLTPLILKPFGNSISRYNGEPEHIERNDAPHKNTQEKFSLSQESSYI
ATQYSLRPRREEVKLKEIDSKEEKYVAKELAVRTFEVTPIRAKDLEFGGVPGVFLIMFGLPVFLFLLLLMCKQKDPTSTGE
LVSNGTVTGSTFSKGEELFTGVVPILVELDGDVNGHKFSVSGEGEGDATYGKLTLKFICTTGKLPVPWPTLVTTFSYGVQC
FSRYPDHMKRHDFFKSAMPEGYVQERTIFFKDDGNYKTRAEVKFEGDTLVNRIELKGIDFKEDGNILGHKLEYNYNSHNVY
IMADKQKNGIKANFKTRHNIEDGGVQLADHYQQNTPIGDGPVLLPDNHYLSTQSALSKDPNEKRDHMVLLEFVTAAGITHG
MDELYK

(492 amino acids)

REFERENCES

REFERENCES

Andreeva, A.V., Zheng, H., Saint-Jore, C.M., Kutuzov, M.A., Evans, D.E. and Hawes, C.R. (2000) Organization of transport from endoplasmic reticulum to Golgi in higher plants. *Biochemical Society Transactions* **28**: 505-512.

Batoko, H., Zheng, H.Q., Hawes, C. and Moore, I. (2000) A Rab1 GTPase is required for transport between the endoplasmic reticulum and Golgi apparatus and for normal Golgi movement in plants. *Plant Cell* **12**: 2201-2217.

Beaudouin, J., Gerlich, D., Daigle, N., Eils, R. and Ellenberg, J. (2002) Nuclear envelope breakdown proceeds by microtubule-induced tearing of the lamina. *Cell* **108**: 83-96.

Beilharz, T., Egan B., Silver, P.A., Hofmann, K. and Lithgow, T. (2003) Bipartite signals mediate subcellular targeting of tail anchored membrane proteins in *Saccharomyces cerevisiae*. *Journal of Biological Chemistry* **273**: 8219-8223.

Beven, A., Guan, Y., Peart, J., Cooper, C. and Shaw, P. (1991) Monoclonal-antibodies to plant nuclear matrix reveal intermediate filament-related components within the nucleus. *Journal of Cell Science* **98**: 293-302.

Blumenthal, S.S., Clark, G.B. and Roux, S.J. (in press) Biochemical and immunological characterization of pea nuclear intermediate filament proteins. *Planta*.

Boevink, P., Oparka, K., Santa Cruz, S., Martin, B., Betteridge, A. and Hawes, C. (1998) Stacks on Tracks: the plant Golgi Apparatus traffics on an actin/ER network. *Plant Journal* **15**: 441-447.

Boevink, P., Martin, B., Oparka, K., Santa Cruz, S. and Hawes, C. (1999) Transport of virally expressed green fluorescent protein through the secretory pathway in tobacco leaves is inhibited by cold shock and brefeldin A. *Planta* **208**: 392-400.

Boisnard-Lorig, C., Colon-Carmona, A., Bauch, M., Hodge, S., Doerner, P., Bancharel, E., Dumas, C., Haseloff, J. and Berger, F. (2001) Dynamic analyses of the expression of the HISTONE::YFP fusion protein in arabidopsis show that syncytial endosperm is divided in mitotic domains. *Plant Cell* **13**: 495-509.

Bonne, G., Raffaele di Barletta, M., Varnous, S., Bécane, H.-M., Hammounda, E.-H., Merlini, L., Muntoni, F., Greenberg, C.R., Gary, F., Urtizberea, J.-A., Duboc, D., Fardeau, M., Toniolo, D. and Schwartz, K. (1999) Mutations in the gene encoding lamin A/C cause autosomal dominant Emery-Driefuss muscular dystrophy. *Nature Genetics* **21**: 285-288.

Bordier, C. (1981) Phase separation of integral membrane proteins in Triton X-114 solution. *Journal of Biological Chemistry* **256**: 1604-1607.

Boucher, L., Ouzounis, C.A., Enright, A.J. and Blencowe, B.J. (2001) A genome-wide survey of RS domain proteins. *RNA* **7**: 1693-1701.

Brandizzi, F. and Caiola, M.G. (1998) Flow cytometric analysis of nuclear DNA in *Crocus sativus* and allies (Iridaceae). *Plant Systematics And Evolution* **211**: 149-154.

Brandizzi, F., Frangne, N., Marc-Martin, S., Hawes, C., Neuhaus, J.M. and Paris, N. (2002a) The destination for single-pass membrane proteins is influenced markedly by the length of the hydrophobic domain. *Plant Cell* **14**: 1077-1092.

Brandizzi, F., Fricker, M. and Hawes, C. (2002b) A Greener World: The Revolution in Plant Bioimaging. *Nature Reviews Molecular Cell Biology* **3**: 520-530.

Brandizzi, F., Snapp, E.L., Roberts, A.G., Lippincott-Schwartz, J. and Hawes, C. (2002c) Membrane Protein Transport between the Endoplasmic Reticulum and the Golgi in Tobacco Leaves Is Energy Dependent but Cytoskeleton Independent: Evidence from Selective Photobleaching. *Plant Cell* **14**:1293-1309.

Brandizzi, F., Hanton, S., Pinto daSilva, L.L., Boevink, P., Evans, D., Oparka, K., Denecke, J. and Hawes, C. (2003) ER quality control can lead to retrograde transport from the ER lumen to the cytosol and the nucleoplasm in plants. *Plant Journal* **34**: 269-281.

Bretscher, M.S. and Munro, S. (1993) Cholesterol and the Golgi apparatus. *Science* **261**: 1280-1.

Breyne, P., Dreesen, R., Vandepoele, K., De Veylder, L., Van Breusegem, F., Callewaert, L., Rombauts, S., Raes, J., Cannoot, B., Engler, G., Inzé, D. and Zabeau, M. (2002) Transcriptome analysis during cell division in plants.

Proceedings of the National Academy of Sciences of the United States of America **99**: 14825-14830.

Buendia, B. and Courvalin, J.-C. (1997) Domain specific disassembly and reassembly of nuclear membranes during mitosis. *Experimental Cell Research* **230**: 133-144.

Buendia, B., Courvalin, J.-C. and Collas, P. (2001) Dynamics of the nuclear envelope at mitosis and during apoptosis. *Cellular and Molecular Life Sciences* **58**: 1781-1789.

Burke, B. and Ellenberg, J. (2002) Remodelling the walls of the nucleus. *Nature Reviews Molecular Cell Biology* **3**: 487-497.

Bustamante, J.O., Hanover, J.A. and Liepins, A. (1995) The Ion Channel Behaviour of the Nuclear Pore Complex. *The Journal of Membrane Biology* **146**: 239-251.

Calikowski, T.T., Meulia, T. and Meier, I. (2003) A proteomic study of the Arabidopsis nuclear matrix. *Journal of Cellular Biochemistry* **90**: 361-378.

Chalfie, M., Tu, Y., Euskirchen, G., Ward, W.W. and Prasher, D.C. (1994) Green Fluorescent Protein as a Marker for Gene Expression. *Science* **263**: 802-805.

Chaudhary, N. and Courvalin, J.-C. (1993) Stepwise reassembly of the nuclear envelope at the end of mitosis. *Journal of Cell Biology* **122**: 295-306.

Chytilova, E., Macas, J., Sliwinska, E., Rafelski, S.M., Lambert, G.M. and Galbraith, D.W. (2000) Nuclear dynamics in *Arabidopsis thaliana*. *Molecular Biology of the Cell* **11**: 2733-2741.

Collas, P. and Courvalin, J.-C. (2000) Sorting nuclear membrane proteins at mitosis. *Trends in Cell Biology* **10**: 5-8.

Courvalin, J.-C., Segil, N., Blobel, G. and Worman, H.J. (1992) The lamin B receptor of the inner nuclear membrane undergoes mitosis-specific phosphorylation and is a substrate for p34cdc2-type protein kinase. *Journal of Biological Chemistry* **267**: 19035-19038.

Crofts, A.J., Leborgne-Castel, N., Hillmer, S., Robinson, D.G., Phillipson, B., Carlsson, L.E., Ashford, D.A. Denecke, J. (1999) Saturation of the endoplasmic reticulum machinery reveals anterograde bulk flow. *Plant Cell* **11**: 2233-2247.

Cronshaw, J.M., Krutchinsky, A.N., Zhang, W., Chait, B.T. and Mátunis, M.J. (2002) Proteomic analysis of the mammalian nuclear pore complex. *Journal of Cell Biology* **158**: 915-927.

Daigle, N., Beaudouin, J., Hartnell, L., Imreh, G., Hallberg, E., Lippincott-Schwartz, J., Ellenberg, J. (2001) Nuclear pore complexes form immobile networks and have a very low turnover in live mammalian cells. *Journal of Cell Biology* **154**: 71-84.

Dambrauskas, G., Aves, S.J., Bryant, J.A., Francis, D. and Rogers, H.J. (2003) Genes encoding two essential DNA replication activation proteins, Cdc6 and Mcm3, exhibit very different patterns of expression in the tobacco BY-2 cell cycle. *Journal of Experimental Botany* **54**: 699-706.

De la Torre, C., Sacristán-Gárate, A. and Navarette, M.H. (1979) Dynamics of the nuclear envelope during cell cycle in plants. *Cytobios* **24**: 25-31.

Denecke, J., Carlsson, L.E., Vidal, S., Höglund, A.-S., Ek, B., van Zeijl, M.J., Sinjorgo, K.M.C. and Palva, E.T. (1995) The Tobacco homolog of mammalian calreticulin is present in protein complexes in vivo. *Plant Cell* **7**: 391-406.

Dingwall, C. and Laskey, R. (1992) The Nuclear Membrane. *Science* **258**: 942-947.

Dingwall, C., Robbins, J., Dilworth, S.M., Roberts, B. and Richardson, W.D. (1988) The nucleoplasmin nuclear location sequence is larger and more complex than that of SV40 large T antigen. *Journal of Cell Biology* **107**: 841-849.

Dixit, R. and Cyr, R.J. (2002) Spatio-temporal relationship between nuclear-envelope breakdown and preprophase band disappearance in cultured tobacco cells. *Protoplasma* **219**: 116-21.

Downie, L., Priddle, J., Hawes, C. and Evans, D.E. (1998) A calcium pump at the higher plant nuclear envelope? *FEBS Letters* **429**: 44-48.

Dreger, C.K., König, A.P., Spring, H., Lichter, P. and Herrmann, H. (2002) Investigation of nuclear architecture with a domain-presenting expression system. *Journal of Structural Biology* **140**: 100-115.

Duband-Goulet, I. and Courvalin, J.-C. (2000) Inner nuclear membrane protein LBR preferentially interacts with DNA secondary structures and nucleosomal linker. *Biochemistry* **39**: 6483-6488.

Ellenberg, J. and Lippincott-Schwartz, J. (1999) Dynamics and Mobility of Nuclear Envelope Proteins in Interphase and Mitotic Cells Revealed by Green

Fluorescent Protein Chimeras. *Methods: A companion to Methods in Enzymology* **19**: 362-372.

Ellenberg, J., Siggia, E.D., Moreira, J.E., Smith, C.L., Presley, J.F., Worman, H.J. and Lippincott-Schwartz, J. (1997) Nuclear membrane dynamics and reassembly in living cells: Targeting of an inner nuclear membrane protein in interphase and mitosis. *Journal of Cell Biology* **138**: 1193-1206.

Ellis, D.J., Jenkins, H., Whitfield, W.G.F. and Hutchison, C.J. (1997) GST-lamin fusion proteins act as dominant negative mutants in Xenopus egg extract and reveal the function of the lamina in DNA replication. *Journal of Cell Science* **110**: 2507-2518.

Escobar, N.M., Haupt, S., Thow, G., Boevink, P., Chapman, S. and Oparka, K. (2003) High-throughput viral expression of cDNA-green fluorescent protein fusions reveals novel subcellular addresses and identifies unique proteins that interact with plasmodesamata. *Plant Cell* **15**: 1507-1523.

Evans, D.E. and Williams, L.E. (1998) P-type calcium ATPases in higher plants - biochemical, molecular and functional properties. *Biochimica et Biophysica Acta* **1376**: 1-25.

Fass, E., Shahar, S., Zhao, J., Zemach, A., Avivi, Y. and Graft, G. (2002) Phosphorylation of histone H3 at serine 10 cannot account directly for the detachment of human heterochromatin protein 1γ from mitotic chromosomes in plant cells. *Journal of Biological Chemistry* **277**: 30921-30927.

Foisner, R. and Gerace, L. (1993) Integral membrane proteins of the nuclear envelope interact with lamins and chromosomes, and binding is modulated by mitotic phosphorylation. *Cell* **73**: 1267-1279.

García-Mata, R., Bebök, Z., Sorscher, E.J. and Sztul, E.S. (1999) Characterization and dynamics of aggresome formation by a cytosolic GFP-chimera. *Journal of Cell Biology* **146**: 1239-1254.

Gatz, C. (1997) Chemical control of gene expression. *Annual Review of Plant Physiology and Plant Molecular Biology* **48**: 89-108.

Gatz, C. and Lenk, I. (1998) Promoters that respond to chemical enducers. *Trends in Plant Science* **3**: 352-358.

Gaudin, V., Libault, M., Pouteau, S., Juui, T., Zhao, G., Lefebvre, D and Grandjean, O. (2001) Mutations in *LIKE HETEROCHROMATIN PROTEIN 1*

affect flowering time and plant architecture in *Arabidopsis*. *Development* **128**: 4847-4858.

Geelen, D.N.V. and Inzé, D.G. (2001) A bright future for the Bright Yellow-2 culture. *Plant Physiology* **127**: 1375-1379.

Gerace, L. and Burke, B. (1988) Functional Organization of the Nuclear Envelope. *Annual Review of Cell Biology* **4**: 335-374.

Gerace, L. and Foisner, R. (1994) Integral membrane proteins and dynamic organisation of the nuclear envelope. *Trends in Cell Biology* **4**:127-131.

Gerlich, D., Beaudouin, J., Gebhard, M., Ellenberg, J. and Eils, R. (2001) Four-dimensional imaging and quantitative reconstruction to analyse complex spatiotemporal processes in live cells. *Nature Cell Biology* **3**: 852-855.

Gindullis, F. and Meier, I. (1999) Matrix Attachment Region Binding Protein MFP1 Is Localized in Discrete Domains at the Nuclear Envelope. *Plant Cell* **11**: 1117-1128.

Gindullis, F., Peffer, N.J. and Meier, I. (1999) MAF1, a Novel Plant Protein Interacting with Matrix Attachment Region Binding Protein MFP1, Is Located at the Nuclear Envelope. *Plant Cell* **11**: 1755-1767.

Gindullis, F., Rose, A., Patel, S. and Meier, I. (2002) Four signature motifs define the first class of structurally related large coiled-coil proteins in plants. *BMC Genomics* **3**: 9 (http://www.biomedcentral.com/1471-2164/3/9).

Goldberg, M., Nili, E., Cojocaru, G., Tzur, Y.B., Berger, R., Brandies, M., Rechavi, G., Gruenbaum, Y and Simon, A.J. (1999) Functional organization of the nuclear lamina. *Gene Therapy and Molecular Biology* **4**: 143-158.

Greenberg, J.T. (1996) Programmed cell death: A way of life for plants. *Proceedings of the National Academy of Sciences of the United States of America* **93**: 12094-12097.

Gunawardena, A.H.L.A.N., Pearce, D.M., Jackson, M.B., Hawes, C.R. and Evans, D.E. (2001) Rapid changes in cell wall pectic polysaccharides are closely associated with early stages of aerenchyma formation, a spatially localized form of programmed cell death in roots of maize (*Zea mays* L.) promoted by ethylene. *Plant Cell and Environment* **24**: 1369-1375.

Hadlington, J.L. and Denecke, J. (2001) Transient expression, a tool to address questions in plant cell biology. In: Hawes, C. and Satiat-Jeunemaitre, B., Eds.

Plant Cell Biology A Practical Approach 2nd edition, Oxford University Press, Oxford, 107-126.

Hanahan, D. (1983) Studies in transformation of *Escherichia coli* with plasmids. *Journal of Molecular Biology* **166**: 557-580.

Haraguchi, T., Koujin, T., Hayakawa, T., Kaneda, T., Tsutsumi, C., Imamoto, N., Akazawa, C., Sukegawa, J., Yoneda, Y. and Hiraoka, Y. (2000) Live fluorescence imaging reveals early recruitment of emerin, LBR, RanBP2 and Nup153 to reforming functional nuclear envelopes. *Journal of Cell Science* **113**: 779-794.

Harder, P.A., Silverstein, R.A. and Meier, I. (2000) Conservation of matrix attachment region-binding filament-like protein 1 among higher plants. *Plant Physiology* **122**: 225-234.

Haseloff, J., Siemering, K.R., Prasher, D.C. and Hodge, S. (1997) Removal of a cryptic intron and subcellular localization of green fluorescent protein are required to mark transgenic Arabidopsis plants brightly. *Proceedings of the National Academy of Sciences of the United States of America* **94**: 2122-2127.

Hasezawa, S., Ueda, K. and Kumagai, F. (2000) Time-sequence observations of microtubule dynamics throughout mitosis in living cell suspensions of stable transgenic Arabidopsis - direct evidence for the origin of cortical microtubules at M/G1 interface. *Plant and Cell Physiology* **41**: 244-50.

Hawes, C.R., Juniper, B.E. and Horne, J.C. (1981) Low and high voltage electron microscopy of mitosis and cytokinesis in maize roots. *Planta* **152**: 397-407.

Heese-Peck, A. and Raikhel, N.V. (1998) The nuclear pore complex. *Plant Molecular Biology* **38**: 145-62.

Hepler, P.K. (1980) Membranes of the mitotic apparatus of barley cells. *Journal of Cell Biology* **86**: 490-499.

Hepler, P.K. (1985) Calcium restriction prolongs metaphase in dividing *Tradescantia* stamen hair cells. *Journal of Cell Biology* **100**: 1363-1368.

Hepler, P.K. (1992) Calcium and Mitosis. *International Review of Cytology* **138**: 239-268.

Hepler, P.K. (1994) The role of calcium in cell division. *Cell Calcium* **16**: 322-330.

Herbert, R.J., Vilhar, B., Evett, C., Orchard, C.B., Rogers, H.J., Davies, M.S. and Francis, D. (2001) Ethylene induces cell death at particular phases of the cell

cycle in the tobacco TBY-2 cell line. *Journal of Experimental Botany* **52**: 1615-1623.

Hicks, G.R. and Raikhel, N.V. (1995) Protein Import into the Nucleus: An Integrated View. *Annual Review of Cell Biology* **11**: 155-188.

Hinshaw, J.E., Carragher, B.O. and Milligan, R.A. (1992) Architecture and design of the nuclear pore complex. *Cell* **69**: 1133-1141.

Hoffman, K., Dreger, C.K., Olins, A.L., Olins, D.E., Shultz, L.D., Lucke, B., Karl, H., Kaps, R., Muller, D., Vaya, A., Aznar, J., Ware, R.E., Cruz, N.S., Lindner, T.H., Herrmann, H., Reis, A. and Sperling, K. (2002) Mutations in the gene encoding the lamin B receptor produce an altered nuclear morphology in granulocytes (Pelger-Huet anomaly). *Nature Genetics* **31**: 410-414.

Holaska, J.M., Wilson, K.L. and Mansharamani, M. (2002) The nuclear envelope, lamins and nuclear assembly. *Current Opinion in Cell Biology* **14**: 357-364.

Holmer, L. and Worman, H.J. (2001) Inner nuclear membrane proteins: functions and targeting. *Cellular and Molecular Life Sciences* **58**: 1741-1747.

Holmer, L., Pezhman, A. and Worman, H.J. (1998) The Human Lamin B Receptor/Sterol Reductase Multigene Family. *Genomics* **54**: 469-476.

Hooykaas, P.J.J. and Beijersbergen, A.G.M. (1994) The virulence system of *Agrobacterium tumefaciens*. *Annual Review of Phytopathology* **32**: 157-179.

Huang, L.Q., Franklin, A.E. and Hoffman, N.E. (1993) Primary structure and characterization of an *Arabidopsis thaliana* calnexin-like protein. *Journal of Biological Chemistry* **268**: 6560-6566.

Humbert, J.P., Matter, N., Artault, J.C., Koppler, P. and Malviya, A.N. (1996) Inositol 1,4,5-trisphosphate receptor is located to the inner nuclear membrane vindicating regulation of nuclear calcium signalling by inositol 1,4,5-trisphosphate. Discrete distribution of inositol phosphate receptors to inner and outer nuclear membranes. *Journal of Biological Chemistry* **271**: 478-85.

Ikegami, S., Taguchi, T., Ohashi, M., Oguro, M., Nagano, H. and Mano, Y. (1978) Aphidicolin prevents mitotic cell division by interfering with the activity of DNA polymerase-alpha. *Nature* **275**: 458-460.

Irons, S.L., Evans, D.E. and Brandizzi, F. (2003) The first 238 amino acids of the human lamin B receptor are targeted to the nuclear envelope in plants. *Journal of Experimental Botany* **54**: 943-950.

Jeong, S.Y., Rose, A. and Meier, I. (2003) MFP1 is a thylakoid-associated, nucleoid-binding protein with a coiled-coil structure. *Nucleic Acids Research* **31**: 5175-5185.

Johnson, J.A., Ward, C.L. and Kopito, R.R. (1998) Aggresomes: A cellular response to misfolded proteins. *Journal of Cell Biology* **143**: 1883-1898.

Kalderon, D., Richardson, W.D., Markham, A.F. and Smith, A.E. (1984) Sequence requirements for nuclear location of simian virus 40 large-T antigen. *Nature* **311**: 33-38.

Kasbekar, D.P. (1999) Ascribing functions to the lamin B receptor. *Journal of Biosciences* **24**: 401-408.

Kato, K., Matsumoto, T., Koiwai, A., Mizusaki, S., Nishida, K., Noguchi, M. and Tamaki, E. (1972) *Fermentation Technology Today*. Terui, G., ed. Society of Fermentation Technology, Osaka, Japan.

Koncz, C. and Schell, J. (1986) The promoter of T_L-DNA gene 5 controls the tissue specific expression of chimaeric genes carried by a novel type of *Agrobacterium* binary vector. *Molecular and General Genetics* **204:** 383-396.

Kourmouli, N., Theodoropoulos, P.A., Dialynas, G., Bakou, A., Politou, A.S., Cowell, I.G., Singh, P.B. and Georgatos, S.D. (2000) Dynamic associations of heterochromatin protein 1 with the nuclear envelope. *EMBO Journal* **19**: 6558-68.

Kumagai, F., Nagata, T., Yahara, N., Moriyama, Y., Horio, T., Naio, K., Hashimoto, T., Murata, T. and Hasezawa, S. (2003) γ-Tubulin distribution during cortical microtubule reorganization at the M/G_1 interface in tobacco BY-2 cells. *European Journal of Cell Biology* **82**: 43-51.

Laemmli, U.K. (1970) Cleavage of structural proteins during the assembly of the head of bacteriophage T4. *Nature* **227**: 680-685.

Lazar, G., Schaal, T., Maniatis, T. and Goodman, H.M. (1995) Identification of a plant serine-arginine-rich protein similar to the mammalian splicing factor SF2/ASF. *Proceedings of the National Academy of Sciences of the United States of America* **92**: 7672-7676.

Lenz-Bohme, B., Wismar, J., Fuchs, S., Reifegerste, R., Buchner, E., Betz, H. and Schmitt, B. (1997) Insertional mutation of the Drosophila nuclear lamin Dm0 gene results in defective nuclear envelopes, clustering of nuclear pore

complexes, and accumulation of annulate lamellae. *Journal of Cell Biology* **137**: 1001-1016.

Liang, F., Cunningham, K.W., Harper, J.F. and Sze, H. (1997) ECA1 complements yeast mutants defective in Ca^{2+} pumps and encodes an endoplasmic reticulum-type Ca^{2+}-ATPase in *Arabidopsis thaliana*. *Proceedings of the National Academy of Sciences of the United States of America* **94**: 8579-8584.

Lippincott-Schwartz, J., Yuan, L.C., Bonifacino, J.S. and Klausner, R.D. (1989) Rapid redistribution of Golgi proteins into the ER in cells treated with brefeldin A: evidence for membrane cycling from Golgi to ER. *Cell* **56**: 801-813.

Lippincott-Schwartz, J., Snapp, E. and Kenworthy, A. (2001) Studying protein dynamics in living cells. *Nature Reviews Molecular Cell Biology* **2**: 444-456.

Lloyd, C. and Hussey, P. (2001) Microtubule-associated proteins in plants - why we need a MAP. *Nature Reviews Molecular Cell Biology* **2**: 40-7.

Lu, P. and Zhai, Z.H. (2001) Nuclear reassembly of demembranated *Xenopus* sperm in plant cell-free extracts from *Nicotiana* ovules. *Experimental Cell Research* **15**: 96-101.

Lyman, S.K. and Gerace, L. (2001) Nuclear pore complexes: dynamics in unexpected places. *Journal of Cell Biology* **154**: 17-20.

Malviya, A.N. and Rogue, P.J. (1998) "Tell Me Where Is Calcium Bred": Clarifying the Roles of Nuclear Calcium. *Cell* **92**: 17-23.

Manilal, S., Nguyen thi Man, Sewery, C.A. and Morris, G.E. (1996) The Emery-Dreifuss muscular dystrophy protein, emerin, is a nuclear membrane protein. *Human Molecular Genetics* **5**: 801-808.

Masuda, K., Xu, Z.-J., Takahashi, S., Ito, A., Ono, A., Nomura, K. and Inoue, M. (1997) Peripheral framework of carrot cell nucleus contains a novel protein predicted to exhibit a long α-helical domain. *Experimental Cell Research* **232**: 173-181.

Mattaj, I.W. (2004) Sorting out the nuclear envelope from the endoplasmic reticulum. *Nature Reviews Molecular Cell Biology* **5**: 65-69.

McNulty, A.K. and Saunders, M.J. (1992) Purification and immunological detection of pea nuclear intermediate filaments: evidence for plant nuclear lamins. *Journal of Cell Science* **103**: 407-414.

Meier, I., Phelan, T., Gruissem, T., Spiker, S. and Schneider, D. (1996) MFP1, a novel plant filament-like protein with affinity for matrix attachment region DNA. *Plant Cell* **8**: 2105-2115.

Meier, I. (2000) A novel link between ran signal transduction and nuclear envelope proteins in plants. *Plant Physiology* **124**: 1507-1510.

Meier, I. (2001) The plant nuclear envelope. *Cellular and Molecular Life Sciences* **58**: 1774-1780.

Meier, J. and Georgatos, S.D. (1994) Type B lamins remain associated with the integral nuclear envelope protein p58 during mitosis: implications for nuclear reassembly. *EMBO Journal* **13**: 1888-1898.

Melchior, F. and Gerace, L. (1995) Mechanisms of nuclear protein import. *Current Opinion in Cell Biology* **7**: 310-318.

Mewes, H.W., Frishman, D., Guldener, U., Mannhaupt, G., Mayer, K., Mokrejs, M., Morgenstern, B., Munsterkotter, M., Rudd, S. and Weil, B. (2002) MIPS: a database for genomes and protein sequences. *Nucleic Acids Research* **30**: 31-34.

Meyer G, Gicklhorn D, Strive T, Radsak K, Eickmann M. (2002) A three-residue signal confers localization of a reporter protein in the inner nuclear membrane. *Biochemical and Biophysical Research Communications* **291**: 966-71.

Mical, T.I. and Monteiro, M.J. (1998) The role of sequences unique to nuclear intermediate filaments in the targeting and assembly of hunam lamin B: evidence for lack of interaction of lamin B and its putative receptor. *Journal of Cell Science* **111**: 3471-3485.

Minguez, A. and Moreno Diaz de la Espina, S. (1993) Immunological characterization of lamins in the nuclear matrix of onion cells. *Journal of Cell Science* **106**: 431-439.

Moore, I., Galweiler, L., Grosskopf, D., Schell, J. and Palme, K. (1998) A transcription activation system for regulated gene expression in transgenic plants. *Proceedings of the National Academy of Sciences of the United States of America* **95**: 376-81.

Moreno Diaz de la Espina, S. (1995) Nuclear Matrix Isolated from Plant Cells. *International Review of Cytology* **162B**: 75-139.

Nagano, A., Koga, R., Ogawa, M., Kurano, Y., Kawada, J., Okada, R., Hayashi, Y.K., Tsukahara, T. and Arahata, K. (1996) Emerin deficiency at the nuclear

membrane in patients with Emery-Dreifuss muscular dystrophy. *Nature Genetics* **12**: 254-259.

Nagata, T. and Kumagai, F. (1999) Plant cell biology through the window of the highly synchronizsed tobacco BY-2 cell line. *Methods in Cell Science* **21**: 123-127.

Nagata, T., Nemoto, Y. and Hasezawa, S. (1992) Tobacco BY-2 cell line as the 'HeLa' cell in the cell biology of higher plants. *International Review of Cytology* **132**: 1-30.

Nebenführ, A., Frohlick, J.A. and Staehelin, L.A. (2000) Redistribution of Golgi stacks and other organelles during mitosis and cytokinesis in plant cells. *Plant Physiology* **124**: 135-151.

Nikolakaki, E., Simos, G., Georgatos, S.D. and Giannakouros, T. (1996) A nuclear envelope-associated kinase phosphorylates arginine-serine motifs and modulates interactions between the lamin B receptor and other nuclear proteins. *Journal of Biological Chemistry* **271**: 8365-8372.

Nikolakaki, E., Meier, J., Simos, G., Georgatos, S.D. and Giannakouros, T. (1997) Mitotic phosphorylation of the lamin B receptor by a serine/arginine kinase and $p34^{cdc2}$. *Journal of Biological Chemistry* **272**: 6208-6213.

Nilsson, T. and Warren, G. (1994) Retention and retrieval in the endoplasmic reticulum and the Golgi apparatus. *Current Opinion in Cell Biology* **6**: 517-521.

Östlund, C., Ellenberg, J., Hallberg, E., Lippincott-Schwartz, J. and Worman, H.J. (1999) Intracellular trafficking of emerin, the Emery-Dreifuss muscular dystrophy protein. *Journal of Cell Science* **112**: 1709-1719.

Otto, H., Dreger, M., Bengtsson, L. and Hucho, F. (2001) Identification of tyrosine-phosphorylated proteins associated with the nuclear envelope. *European Journal of Biochemistry* **268**: 420-428.

Panté, N. and Aebi, U. (1994) Towards understanding the 3-dimensional structure of the nuclear pore complex at the molecular level. *Current Opinion in Structural Biology* **4**: 187-196.

Pay, A., Resch, K., Frohnmeyer, H., Fejes, E., Nagy, F. and Nick, P. (2002) Plant RanGAPs are localized at the nuclear envelope in interphase and associated with microtubules in mitotic cells. *Plant Journal* **30**: 699-709.

Polioudaki, H., Kourmouli, N., Drosou, V., Bakou, A., Theodoropoulos, P.A., Singh, P.B., Giannakouros, T. and Georgatos, S.D. (2001) Histones H3/H4 form a tight complex with the inner nuclear membrane protein LBR and heterochromatin protein 1. *EMBO Reports* **21**: 920-925.

Pyrpasopoulou, A., Meier, J., Maison, C., Simos, G. and Georgatos, S.D. (1996) The lamin B receptor (LBR) provides essential chromatin docking sites at the nuclear envelope. *EMBO Journal* **15**: 7108-7119.

Reynolds, E.S. (1963) The use of lead citrate at high pH as an electron opaque stain in electron microscopy. *Journal of Cell Biology* **17**: 208-212.

Roderick, H.L., Campbell, A.K. and Llewellyn, D.H. (1997) Nuclear localization of calreticulin in vivo is enhanced by its interaction with glucocorticoid receptors. *FEBS Letters* **405**: 181-185.

Rolls, M.M., Stein, P.A., Taylor, S.S., Ha, E., McKeon, F. and Rapoport, T.A. (1999) A visual screen of a GFP-fusion library identifies a new type of nuclear envelope membrane protein. *Journal of Cell Biology* **146**: 29-43.

Rose, A. and Meier, I. (2001) A domain unique to plant RanGAP is responsible for its targeting to the plant nuclear rim. *Proceedings of the National Academy of Sciences of the United States of America* **98**: 15377-15382.

Rose, A., Gindullis, F. and Meier, I. (2003) A novel alpha helical protein, specific to and highly conserved in plants, is associated with the nuclear matrix fraction. *Journal of Experimental Botany* **385**: 1133-1141.

Rose, A., Patel, S. and Meier, I. (2004) The plant nuclear envelope. *Planta* **218**: 327-36.

Rout, M.P., Aitchison, J.D., Suprapto, A., Hjertaas, K., Zhao, Y. and Chait, B.T. (2000) The yeast nuclear pore complex: Composition, architecture, and transport mechanism. *Journal of Cell Biology* **148**: 635-651.

Saint-Jore, C.M., Evins, J., Brandizzi, F., Batoko, H., Moore, I. and Hawes, C. (2002) Redistribution of membrane proteins between the Golgi apparatus and endoplasmic reticulum in plants is reversible and not dependent on cytoskeletal networks. *Plant Journal* **29**: 661-679.

Samaniego, R., Yu, W., Meier, I. and Moreno Diaz de la Espina, S. (2001) Characterisation and high-resolution distribution of a matrix attachment region-binding protein (MFP1) in proliferating cells of onion. *Planta* **212**: 535-546.

Sambrook, J. and Russell, D.W. (2001) *Molecular Cloning. A laboratory manual* 3rd edition. Cold Spring Harbor Laboratory Press, Cold Spring Harbor, New York.

Samuels, A.L., Giddings Jr, T.H., Staehelin, L.A. (1995) Cytokinesis in tobacco BY-2 and root tip cells: A new model of cell plate formation in higher plants. *Journal of Cell Biology* **130**: 1345-1357.

Schirmer, E.C., Florens, L., Guan, T., Yates, J.R. 3rd, Gerace, L. (2003) Nuclear membrane proteins with potential disease links found by subtractive proteomics. *Science* **301**: 1380-1382.

Schrick, K., Mayer, U., Horrichs, A., Kuhnt, C., Bellini, C., Dangl, J., Schmidt, J. and Jurgens, G. (2000) FACKEL is a sterol C-14 reductase required for organised cell division and expansion in *Arabidopsis* embryogenesis. *Genes and Development* **14**: 1471-1484.

Schuler, E., Lin, F. and Worman, H.J. (1994) Characterization of the human gene encoding LBR, an integral protein of the nuclear envelope inner membrane. *Journal of Biological Chemistry* **269**: 11312-11317.

Scofield, G.N., Beven, A.F., Shaw, P.J and Doonan, J.H. (1992) Identification and localization of a nucleoporin-like protein-component of the plant nuclear matrix. *Planta* **187**: 414-420.

Smith, S. and Blobel, G. (1993) The First Membrane Spanning Region of the Lamin B Receptor Is Sufficient for Sorting to the Inner Nuclear Membrane. *Journal of Cell Biology* **120**: 631-637.

Smith, S. and Blobel, G. (1994) Colocalization of vertebrate lamin B and lamin B receptor (LBR) in nuclear envelopes and in LBR-induced membrane stacks of the yeast *Saccharomyces cerevisiae. Proceedings of the National Academy of Sciences of the United States of America* **91**: 10124-10128.

Söderqvist, H., Jiang, W.Q., Ringertz, N. and Hallberg, E. (1996) Formation of nuclear bodies in cells overexpressing the nuclear pore protein POM121. *Experimental Cell Research* **225**: 75-84.

Soullam, B. and Worman, H. (1993) The Amino-Terminal Domain of the Lamin B Receptor Is a Nuclear Envelope Targeting Signal. *Journal of Cell Biology* **120**: 1093-1100.

Soullam, B. and Worman, H.J. (1995) Signals and Structural Features Involved in Integral Membrane Protein Targeting to the Inner Nuclear Membrane. *Journal of Cell Biology* **130**: 15-27.

Staehelin, L.A. (1997) The plant ER: a dynamic organelle composed of a large number of discrete functional domains. *Plant Journal* **11**: 1151-1165.

Stehno-Bittel, L., Perez-Terzic, C. and Clapham, D.E. (1995) Diffusion Across the Nuclear Envelope Inhibited by Depletion of the Nuclear Ca2+ store. *Science* **270**: 1835-1838.

Stoffler, D., Fahrenkrog, B. and Aebi, U. (1999) The nuclear pore complex: from molecular architecture to functional dynamics. *Current Opinion in Cell Biology* **11**: 391-401.

Suzuki, M. (1989) SPXX, a frequent sequence motif in gene regulatory proteins. *Journal of Molecular Biology* **207**: 61-84.

Takano, M., Takeuchi, M., Ito, H., Furukawa, K. Sugimoto, K., Omata, S. and Horigome, T. (2002) The binding of lamin B receptor to chromatin is regulated by phosphorylation in the RS region. *European Journal of Biochemistry* **269**: 943-953.

Takano, M., Koyama, Y., Ito, H., Hoshino, S., Onogi, H., Hagiwara, M., Furukawa, K. and Horigome, T. (in press) Regulation of binding of lamin B receptor to chromatin by SR protein kinase and cdc2 kinase in Xenopus egg extracts. *Journal of Biological Chemistry.*

Tamura, K., Shimada, T., Ono, E., Tanaka, Y., Nagatini, A., Higashi, S., Watanabe, M., Nishimura, M. and Hara-Nishimura, I. (2003) Why green fluorescent fusion proteins have not been observed in the vacuoles of higher plants. *The Plant Journal* **35**: 545-555.

Terasaki, M. Campagnola, P., Rolls, M.M., Stein, P.A., Ellenberg, J., Hinkle, B. and Slepchenko, B. (2001) A New Model for Nuclear Envelope Breakdown. *Molecular Biology of the Cell* **12**: 503-510.

Tsien, R. (1998) The Green Fluorescent Protein. *Annual Review of Biochemistry* **67**: 509-544.

Ueda, K., Matsuyama, T. and Hashimoto, T. (1999) Visualization of microtubules in living cells of transgenic *Arabidopsis thaliana. Protoplasma* **206**: 201-206.

Ulitzur, N., Harel, A., Goldberg, M., Feinstein, N. and Gruenbaum, Y. (1997) Nuclear membrane vesicle targeting to chromatin in a *Drosophila* embryo cell-free system. *Molecular Biology of the Cell* **8**:1439-48.

Van Bruaene, N., Joss, G., Thas, O. and Van Oostveldt, P. (2003) Four-dimensional imaging and computer-assisted track analysis of nuclear migration in root hairs of *Arabidopsis thaliana*. *Journal of Microscopy* **211**: 167-178.

Van Haaren, M.J., Sedee, N.J., de Boer, H.A., Schilperoort, R.A. and Hooykaas, P.J. (1988) Bidirectional transfer from a 24 bp border repeat of Agrobacterium tumefaciens. *Nucleic Acids Research* **16**: 10225-10236.

Vaughan, O.A., Whitfield, W.G.F. and Hutchison, C.J. (2000) Functions of the nuclear lamins. *Protoplasma* **211**: 1-7.

Vigers, G.P. and Lohka, M.J. (1991) A distinct vesicle population targets membranes and pore complexes to the nuclear envelope in *Xenopus* eggs. *Journal of Cell Biology* **112**: 545-556.

Vos, J.W., Valster, A.H. and Hepler, P.K. (1999) Methods for studying cell division in higher plants. *Methods in Cell Biology* **61**: 413-437.

Vos, J.W., Safadi, F., Reddy, A.S.N. and Hepler, P.K. (2000) The kinesin-like calmodulin binding protein is differentially involved in cell division. *Plant Cell* **12**: 979-990.

Wang, H., Tang, W., Zhu, C. and Perry, S.E. (2002) A chromatin immunoprecipitation (ChIP) approach to isolate genes regulated by AGL15, a MADS domain protein that preferentially accumulates in embryos. *Plant Journal* **32**: 831-843.

Ward, B.M. and Lazarowitz, S.G. (1999) Nuclear export in plants: Use of Geminivirus movement proteins for a cell-based export assay. *The Plant Cell* **11**: 1267-1276.

Waterham, H.R., Koster, J., Mooyer, P., Van Noort, G., Kelley, R.I., Wilcox, W.R., Wanders, R.J.A., Hennekam, R.C.M. and Oosterwijk, J.C. (2003) Autosomal recessive HEM/Greenberg Skeletal Dysplasia is caused by 3β-hydroxysterol Δ^{14}-reductase deficiency due to mutations in the lamin B receptor gene. *American Journal of Human Genetics* **72**: 1013-1017.

Worman, H.J., Yuan, J., Blobel, G. and Georgatos, S.G. (1988) A lamin B receptor in the nuclear envelope. *Proceedings of the National Academy of Sciences of the United States of America* **85**: 8531-8534.

Worman, H.J., Evans, C.D. and Blobel, G. (1990) The Lamin B Receptor of the Nuclear Envelope Inner Membrane: A Polytopic Protein with Eight Potential Transmembrane Domains. *Journal of Cell Biology* **111**: 1535-1542.

Worman, H.J. and Courvalin, J.-C. (2000) The inner nuclear membrane. *Journal of Membrane Biology* **177**: 1-11.

Wu, W., Lin, F and Worman, H.J. (2002) Intracellular trafficking of MAN1, an integral protein of the nuclear envelope inner membrane. *Journal of Cell Science* **115**: 1361-1372.

Yanagawa, Y., Hasezawa, S., Kumagai, F., Oka, M., Fujimuro, M., Naito, T., Makino, T., Yokosawa, H., Tanaka, K., Komamine, A., Hashimoto, J., Sato, T. and Nakagawa, H. (2002) Cell-cycle dependent dynamic change of 26S proteasome distribution in Tobacco BY-2 cells. *Plant and Cell Physiology* **43**: 604-613.

Yang, L., Guan, T. and Gerace, L. (1997) Integral Membrane Proteins of the Nuclear Envelope are Dispersed throughout the Endoplasmic Reticulum during Mitosis. *Journal of Cell Biology* **137**: 1199-1210.

Ye, Q. and Worman, H. (1994) Primary Structure Analysis and Lamin B and DNA Binding of Human LBR, an Integral Protein of the Nuclear Envelope Inner Membrane. *Journal of Biological Chemistry* **269**: 11306-11311.

Ye, Q. and Worman, H.J. (1996) Interaction between an integral protein of the nuclear envelope inner membrane and human chromodomain proteins homologous to Drosophila HP1. *Journal of Biological Chemistry* **271**: 14653-14656.

Ye, Q., Callebaut, I., Pezhman, A., Courvalin, J.-C. and Worman, H.J. (1997) Domain-specific interactions of human HP1-type chromodomain proteins and inner nuclear membrane protein LBR. *Journal of Biological Chemistry* **272**: 14983-14989.

Zhao, Y., Liu, X., Wu, M., Tao, W. and Zhai, Z. (2000) In vitro nuclear reconstitution could be induced in a plant cell-free system. *FEBS Letters* **480**: 208-212.

COPY OF PUBLISHED WORK

PUBLISHED PAPERS NOT COPIED AT THE REQUEST OF THE UNIVERSITY

THESIS CONTAINS CD/DVD